AD/A-001 456

THE MEASUREMENT OF THE MC DONNELL-DOUGLAS DC9 TRAILING VORTEX SYSTEM USING THE TOWER FLY-BY TECHNIQUE

Leo J. Garodz, et al

National Aviation Facilities Experimental Center

Prepared for:

Federal Aviation Administration

November 1974

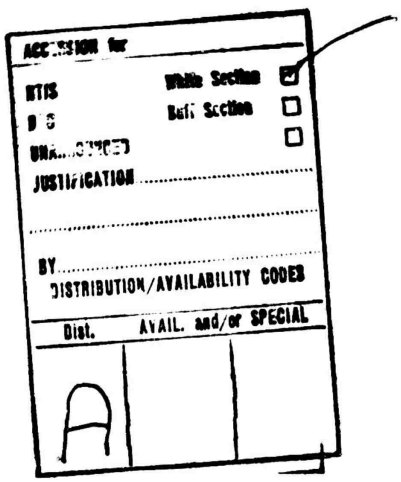

NOTICE

This document is disseminated under the sponsorship of the Department of Transportation in the interest of information exchange. The United States Government assumes no liability for its contents or use thereof.

Technical Report Documentation Page

1. Report No.	2. Government Accession No.	3. Recipient's Catalog No.
FAA-RD-74-173		AD/A-001456

4. Title and Subtitle	5. Report Date
THE MEASUREMENT OF THE McDONNELL-DOUGLAS DC9 TRAILING VORTEX SYSTEM USING THE TOWER FLY-BY TECHNIQUE	November 1974
	6. Performing Organization Code
7. Author(s)	8. Performing Organization Report No.
Leo J. Garodz, David Lawrence, and Nelson Miller	FAA-NA-74-28
9. Performing Organization Name and Address	10. Work Unit No. (TRAIS)
Federal Aviation Administration National Aviation Facilities Experimental Center Atlantic City, New Jersey 08405	11. Contract or Grant No. 214-531-070
	13. Type of Report and Period Covered
12. Sponsoring Agency Name and Address	Final May 11, 1972 - May 12, 1974
U.S. Department of Transportation Federal Aviation Administration Systems Research and Development Service Washington D.C. 20590	14. Sponsoring Agency Code

15. Supplementary Notes

16. Abstract

The results are presented of a series of low-altitude (approximately 200 feet above ground level) flight tests performed at the National Aviation Facilities Experimental Center (NAFEC), Atlantic City, New Jersey, in which the trailing vortices of the McDonnell-Douglas DC9 airplane were investigated, using a 140-foot instrumented tower. Flow visualization (colored smoke streams) was employed and film records made. The airplane was tracked by the NAFEC photo-theodolite facility. Data presented consists of plots of vortex tangential velocity distribution, peak velocity as a function of time, airplane configuration and windspeed, vortex descent rates, and lateral transport rates. Principal findings were that: (1) Within the time period 30 - 100 seconds after vortex generation, the peak velocities within the vortices were bounded by the function $V_\theta = 396\exp(-.0347t)$, with a half-life of 20 seconds; (2) Vortex cores were uniformly small (1 - 2 feet) in both configurations tested (takeoff and landing), and little or no growth with time was found; (3) Vortex lateral transport velocities correlated well with the crosswind measured at 140 feet; and (4) The presence of a temperature inversion markedly retarded the vortex descent rates. The highest peak recorded tangential velocity was 120 - 130 feet per second, found to occur in both configurations tested.

17. Key Words	18. Distribution Statement
Wake Turbulence Hot-Film Anemometry Trailing Vortices Full-Scale Flight Tests	Document is available to the public through the National Technical Information Service, Springfield, Virginia 22151

19. Security Classif. (of this report)	20. Security Classif. (of this page)	21. No. of Pages	22. Price
Unclassified	Unclassified	100	$4.75-2.25

Form DOT F 1700.7 (8-72) Reproduction of completed page authorized

TABLE OF CONTENTS

LIST OF ILLUSTRATIONS

LIST OF ILLUSTRATIONS (continued)

LIST OF SYMBOLS

s	=	Semi-distance between members of a vortex pair at time of generation, feet.
t	=	Time elapsed since vortex generation, seconds.
V	=	True airspeed, feet per second.
V_θ	=	Tangential velocity within vortex, feet per second.
$\hat{V}$	=	Peak recorded velocity within vortex, uncorrected for wind, feet per second.
y	=	Lateral distance of vortex from reference plane, feet.
z	=	Distance of vortex above ground, feet.
Γ	=	Vortex strength (circulation), feet squared per second.
Φ	=	Arcsec z/s.

INTRODUCTION

PURPOSE.

The work described in this report was performed to gain information on the wake-vortex characteristics of the McDonnell-Douglas DC9 airplane, and to aid in the development of improved air traffic control procedures in terminal area operations.

BACKGROUND.

It became apparent early in 1970 that there was a need to investigate further the wake characteristics (i.e., peak velocities, velocity distributions, dissipation rates, and transport velocities) of large jet transport airplanes, particularly under conditions representative of terminal area operations. A preliminary investigation was conducted in February 1970 as a joint operation involving the National Aviation Facilities Experimental Center (NAFEC), the National Aeronautics and Space Administration (NASA), the Boeing Company, and the United States Air Force. This work has been reported on in references 1, 2, and 3. NAFEC's part in the investigation included the acquisition of quantitative data on the wakes of the Boeing 707, 727, and 747; the McDonnell-Douglas DC8 and DC9; and the Lockheed C5A, using the tower fly-by technique. These early tests, while yielding some useful information, were later shown to be incomplete, by reason of the low resolution afforded by the anemometry (25 feet spacing between sensors) and the limited number of data runs made.

Of the airplanes in the above group, four (B707, B747, DC8, and C5A) have four wing-mounted engines, and three (B727, DC9, and C5A) are T-tail designs. Of the second group, the B727 and DC9 have rear-mounted engines and essentially aerodynamically "clean" wings. The low-wing, T-tail design is believed to provide sufficient vertical separation between the wing and horizontal tail that the trailing vortices generated by the negative lift normally required from the horizontal tail do not greatly interact with the trailing vortices produced by the wing. This is just a result of the design-configuration chosen, not a design objective, and is mentioned here because this type of interaction conceivably plays a part in the downstream development of the wake of airplanes using a different general layout. An essential difference between airplanes with four wing-mounted engines and those having fuselage-mounted engines can be seen when flight conditions lead to the production of condensation trails. In the former case, the four separate contrails rapidly merge into a pair of thicker contrails, which evidently become involved in, and render visible, the far-downstream development of the wing-tip vortices (figure 1). The white condensate remains near the core of each vortex, and within a few thousand feet behind the airplane, a condition arises in which the vortices develop a sinusoidal distortion, and ultimately, "pinch-off" into loops at regular intervals and then finally disintegrate. This process, which is well illustrated in reference 4, is only to be seen when the engines are mounted some

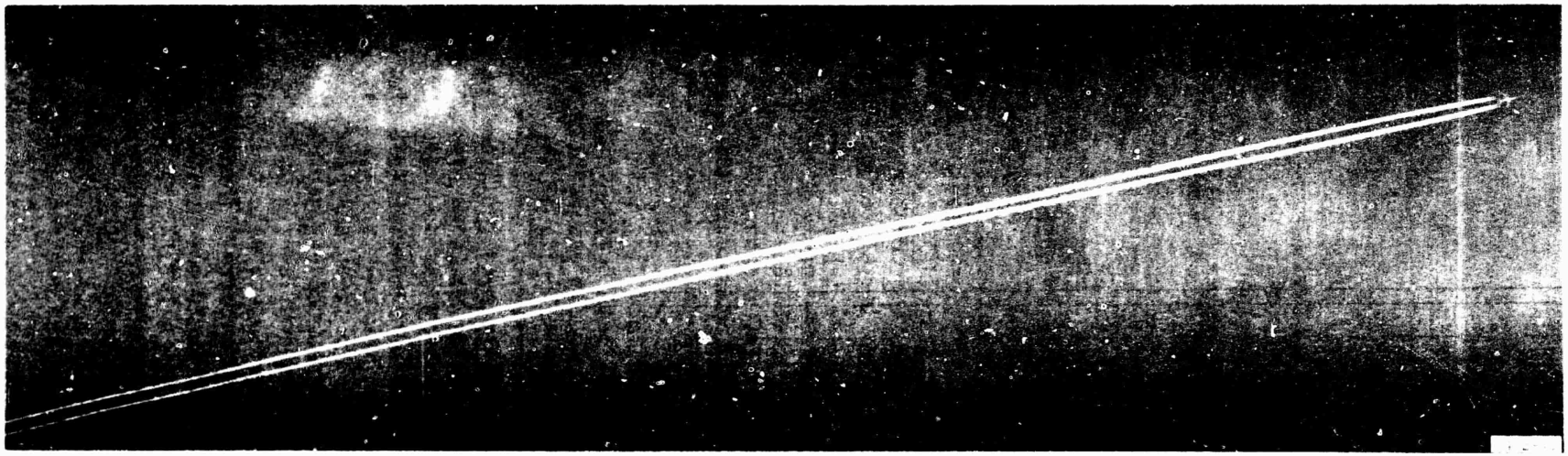

FIGURE 1. HIGH-ALTITUDE CONTRAILS, BOEING 707, SHOWING WING VORTEX ROLLUP BEFORE DEVELOPMENT OF SINUSOIDAL INSTABILITY

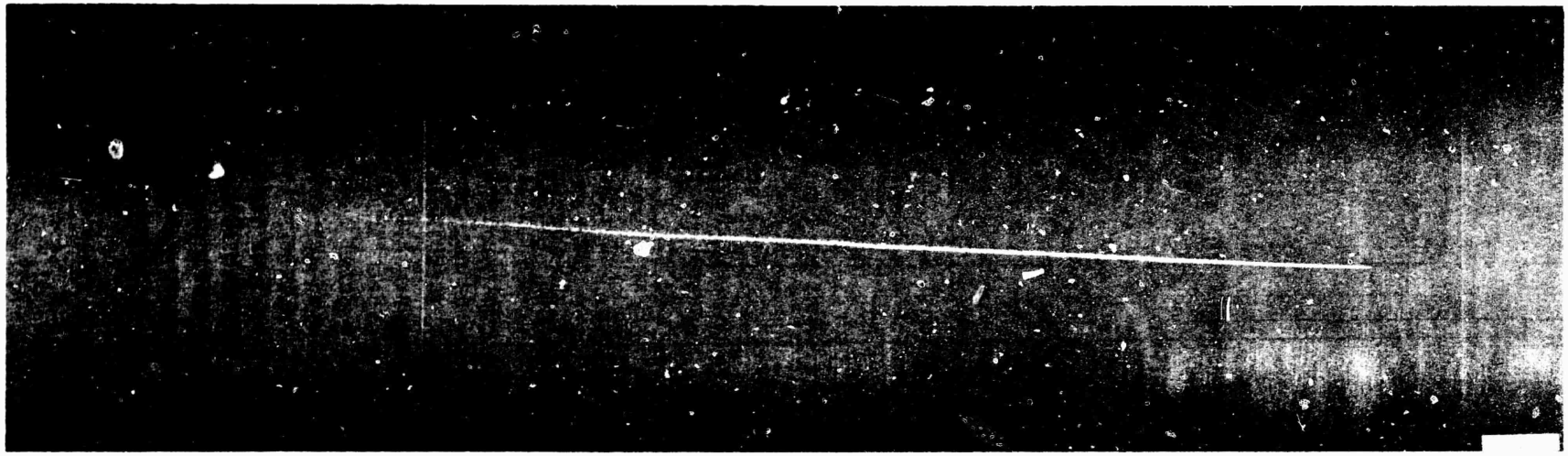

FIGURE 2. HIGH-ALTITUDE CONTRAILS, BOEING 727, SHOWING RELATIVE ABSENCE OF ENGINE EFFLUX PARTICIPATION IN WING VORTEX ROLLUP AND SUBSEQUENT WAKE DEVELOPMENT

distance out along the wing. When the engines are fuselage-mounted, the separate contrails merge into a single one almost at once, and do not appear to become involved in the wake development in any way. The large single contrail has been observed to remain virtually unchanged for minutes at a time. This is illustrated in figure 2.

The point of these observations is to indicate that airplane design-configuration is as important a variable, affecting the development and eventual disintegration of an airplane wake, as is the flight-configuration (degree of flap deployment, landing gear status, deployment of leading edge devices, etc.). It has been found, for example, that the Boeing 747 trailing vortices (reference 5) are strongly affected as to core size, maximum tangential velocity and velocity distribution by the flight-configuration of the airplane. On the other hand, in the case of the Boeing 727 airplane (reference 6), the trailing vortices appear to be constant in core size and velocity distribution, whatever the flap angle. Another finding concerning these two airplanes was that the B727 vortices produced higher peak tangential velocities than those of the B747, and that the decay envelope of the B727 peak velocities showed a slower rate of decay, despite the much lower gross weight and size of the latter airplane. This has been attributed, in a general way, to the different design-configuration of the B727. Therefore, it was of considerable interest to determine if a second airplane, of a generally similar configuration exhibited similar characteristics. The DC9 is such an airplane, though it obviously differs in several respects - notably, it does not have the third engine, and the wing design, especially the planform, reflects the short-field operational requirement and a lower design cruise Mach number.

In this series of tests, the required improvement in flow resolution was obtained by using a spacing of 1-foot between sensors on the test tower.

DISCUSSION

FLIGHT TEST PROGRAM.

Detailed discussion of the test procedure, test tower, instrumentation, photographic coverage, and time correlation is given in references 5 and 7 as indicated below.

TEST AIRPLANE. The McDonnell-Douglas DC9, series 10, airplane is shown in figures 3, 4, and 5. It is a two-engine commercial jet transport, powered by Pratt and Whitney JT8D-1 turbojet engines mounted on either side of the rear fuselage.

In cruising flight, the wing is essentially clean, except for minor fairings and excrescences. The wing design, which is well described in reference 8, features a fixed leading edge, conventional ailerons, and chord-extending flaps.

WING SPAN	= 89.4 FEET
LENGTH	= 104.4 FEET
HEIGHT	= 27.5 FEET
WING AREA	= 980 SQUARE FEET
ASPECT RATIO	= 8.5:1
TAPER RATIO	= 0.25:1
WING QUARTER-CHORD SWEEP ANGLE	= 24 DEGREES
MAXIMUM T.O. WEIGHT	= 98,700 POUNDS (MODEL 15)
MAXIMUM LANDING GROSS WEIGHT	= 81,760 POUNDS (MODEL 15)
POWERPLANT: PRATT & WHITNEY JT8D-1 (TWO)	

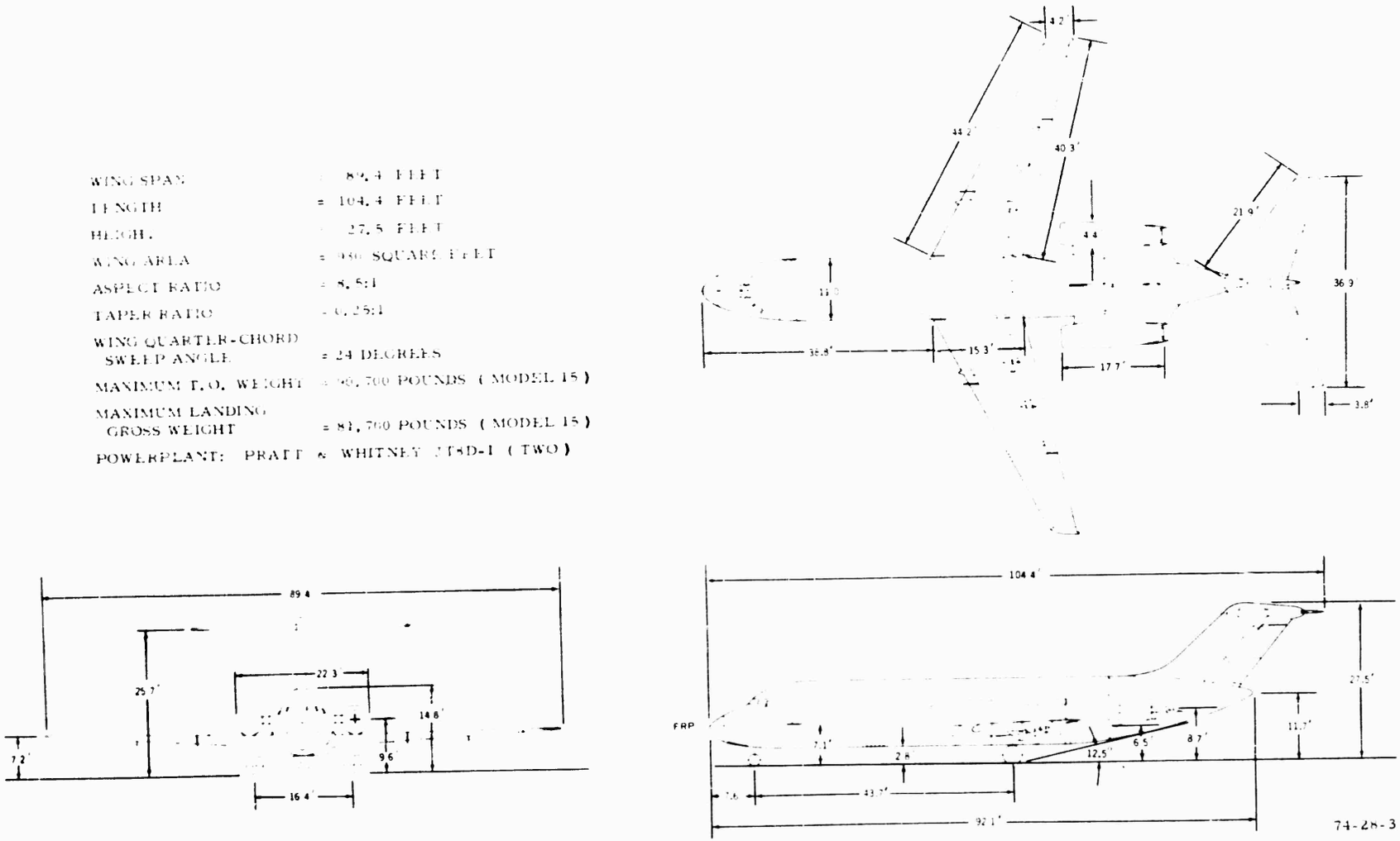

FIGURE 3. MCDONNELL-DOUGLAS DC9, SERIES 10, THREE-VIEW GENERAL ARRANGEMENT

74-28-4

FIGURE 4. MCDONNEL-DOUGLAS DC9, SERIES 10, THREE-QUARTER REAR VIEW

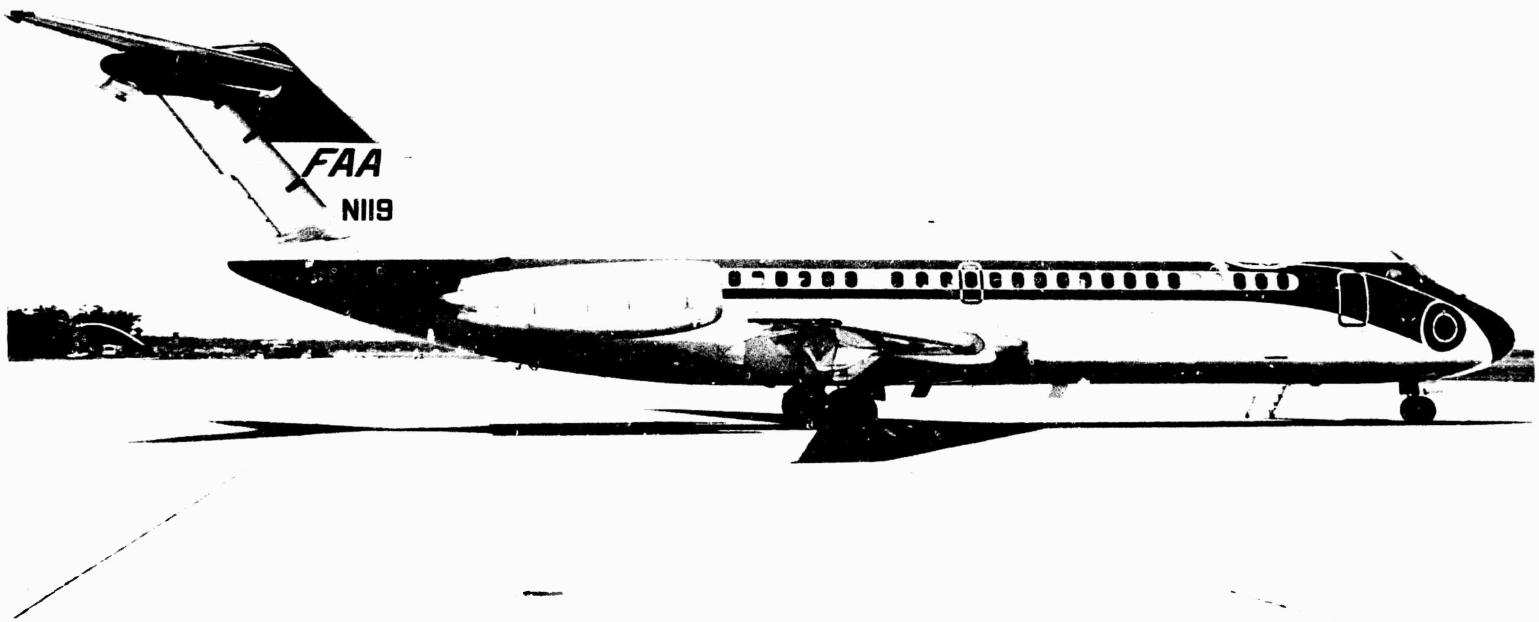

74-28-5

FIGURE 5. MCDONNEL-DOUGLAS DC9, SERIES 10, SIDE VIEW

The inboard flap sections, by use of a system of moveable vanes, function as single-slotted in the takeoff position and triple-slotted in the landing position. The outer flap sections function as single-slotted for takeoff and double-slotted for landing. Inboard and outboard sections operate as a single section, with no gap between them.

TEST PROCEDURE. See reference 7.

TEST TOWER. See reference 7.

INSTRUMENTATION.

AIRPLANE. The airplane required no special instrumentation. A pilot's log sheet was used to record the following information when the airplane was approximately abreast of the tower:

- Time
- Airplane Configuration
- Gross Weight (Estimated)
- Indicated Airspeed
- Radar Altitude
- Pressure Altitude
- Magnetic Track
- Clearance from Tower (From Ground Markings)
- Engine Performance
- Subjective Evaluation of Atmospheric Turbulence

For data reduction purposes, phototheodolite data on airplane altitude, groundspeed, track, and lateral offset of track from tower was used whenever available. Groundspeed was corrected to true airspeed using wind velocity data gathered at the top of the tower (140 feet above ground level (AGL)).

Since the test altitude was so low, it was not considered necessary to account for the difference between true airspeed and equivalent airspeed in any data reduction or calculations dependent on these quantities, such as the calculation of lift coefficient or estimation of the strength of the tip vortices.

TOWER VORTEX MEASUREMENT. See reference 5.

TOWER ATMOSPHERIC MEASUREMENTS. See reference 5.

PHOTOGRAPHY. See reference 7.

TIME CORRELATION. See reference 7.

TEST SITE. See reference 5.

DATA PROCESSING. See reference 5.

DATA PRESENTATION. The data output and presentation consist primarily of:

1. Computer tabular printout of peak recorded vortex tangential velocity and vortex ages, as recorded by the tower sensors.

2. Printout of atmospheric data (air temperature, wind direction and speed, and relative humidity) as recorded by sensors located at the 23-, 45-, 70-, 100-, and the 140-foot levels (appendix A).

3. Plots of tangential velocity scalar magnitude against time. Sample plots are shown in figures 6A and 6B.

4. Plots of tangential velocity scalar magnitude against time, using an expanded time scale for enhanced data resolution for more detailed analysis. A sample plot is shown in figure 7.

5. Vortex tangential velocity profiles (corrected for wind), as a function of height above the ground (appendix B).

DATA ANALYSIS.

A general discussion of the approach to the problem of analyzing the data is given in reference 7, under the same heading. The limitations and problems of the experimental technique are discussed - that is to say, the low height of the tower in relation to the airplane wingspan, aerodynamic interference effects, and ambiguities arising from the inability of the anemometry to yield directional information. Since the work in reference 7 was completed, resolution has been increased by mounting sensors at more frequent intervals (every 2 feet, from 8 feet above the base of the tower to 40 feet above the base, and at 1-foot intervals from 40 feet to the top of the tower), so that the chance of measuring a true peak velocity has been increased. The 1-foot spacing between sensors probably represents the limit of resolution, without introducing serious errors due to aerodynamic interference between the sensors and adjacent mounting hardware.

For the particular airplane under discussion, the tower height is nearly 60 percent greater than the airplane wingspan. When advantage is taken of this, by the vortex striking the tower high up, ground effect is minimized.

Figures 8 through 10 present peak recorded tangential velocity as a function of vortex age. A very small number of data runs were made in the takeoff configuration, and each of these only yielded a single vortex hit, the upwind vortex (figure 9). This is because the airplane altitude abreast of the tower was frequently too great, causing the downwind (first) vortex to pass over the top. Airplane altitude at this point in a data run was not entirely a matter of choice, but was determined by the following consideratons, in addition to the requirements of the experiment: location and height of another tower on the field, unconnected with present test series; wind strength and direction; and flight safety. It is significant that this small number of runs yielded a group of velocities that fall in the upper range of the data, despite the great scatter that is evident elsewhere. The complete set of peak velocities is presented in figure 8. This shows that between 30 and 50 seconds, there

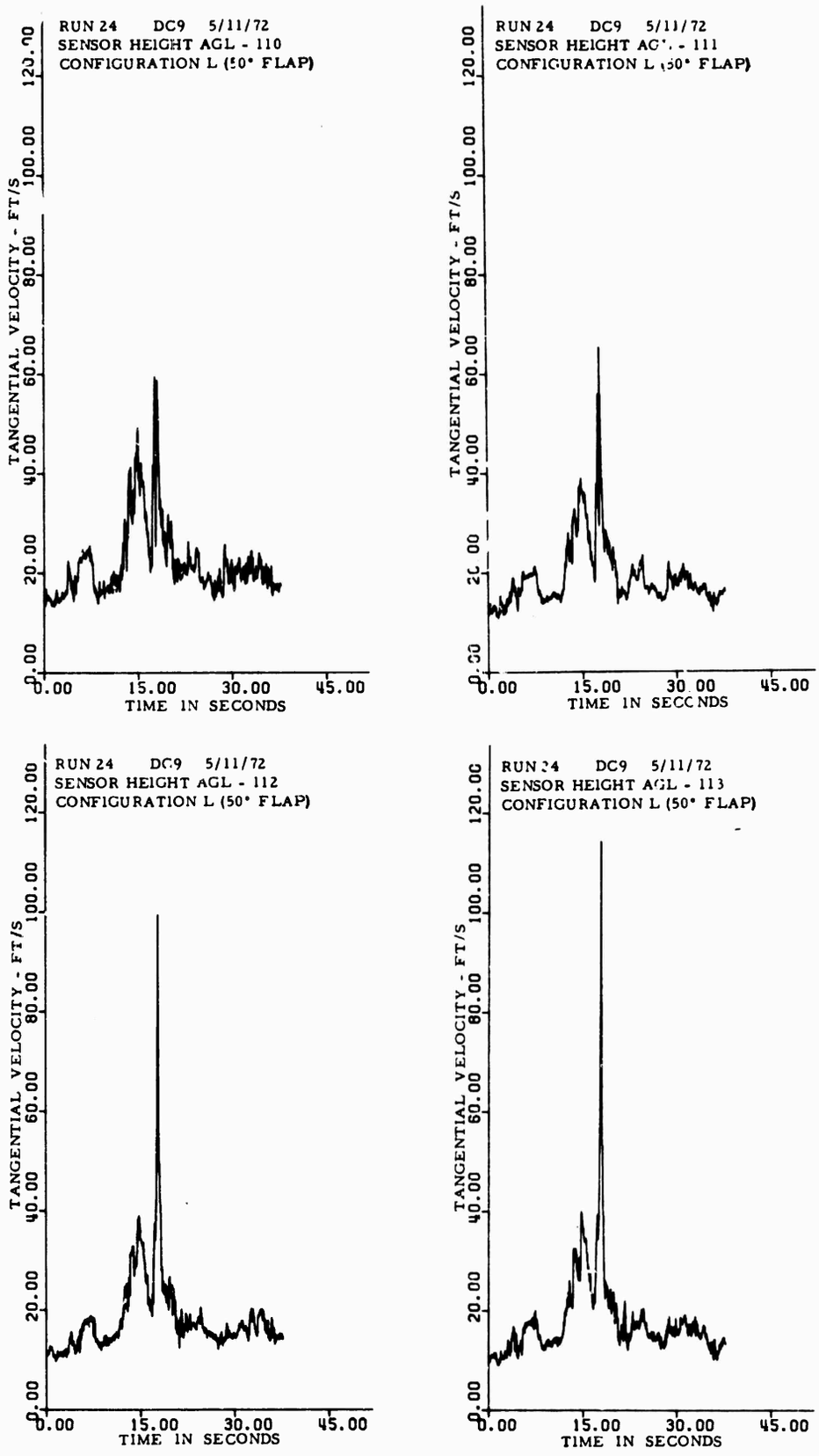

FIGURE 6A. SAMPLE PLOTS OF SENSOR VELOCITY TIME HISTORIES. RUN 24, LANDING CONFIGURATION, SENSORS 110-117, SHOWING SECOND VORTEX HIT AT SENSOR 113, T=18 SECONDS (Page 1 of 2)

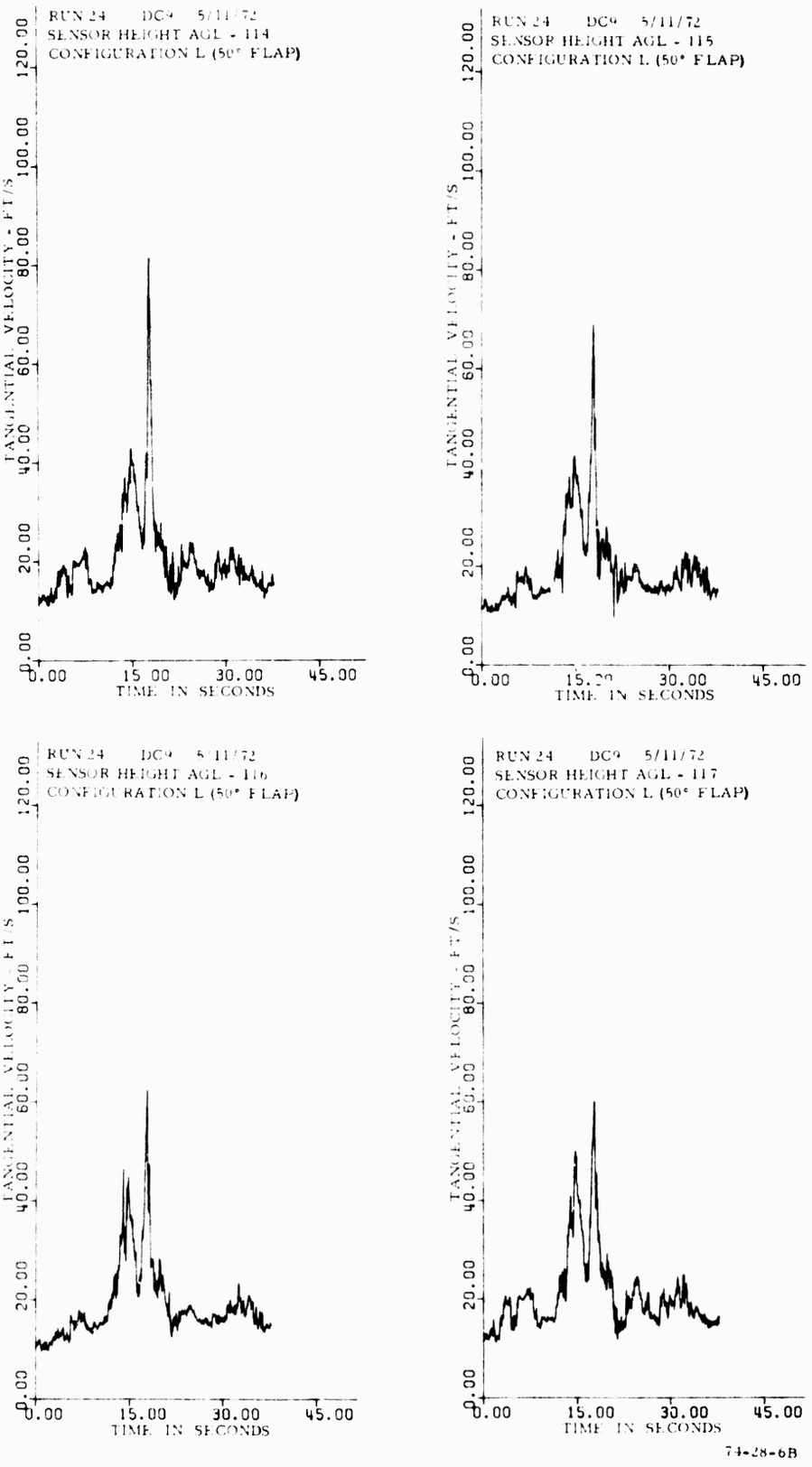

FIGURE 6B. SAMPLE PLOTS OF SENSOR VELOCITY TIME HISTORIES. RUN 24, LANDING CONFIGURATION, SENSORS 110-117, SHOWING SECOND VORTEX HIT AT SENSOR 113, T=18 SECONDS (Page 2 of 2)

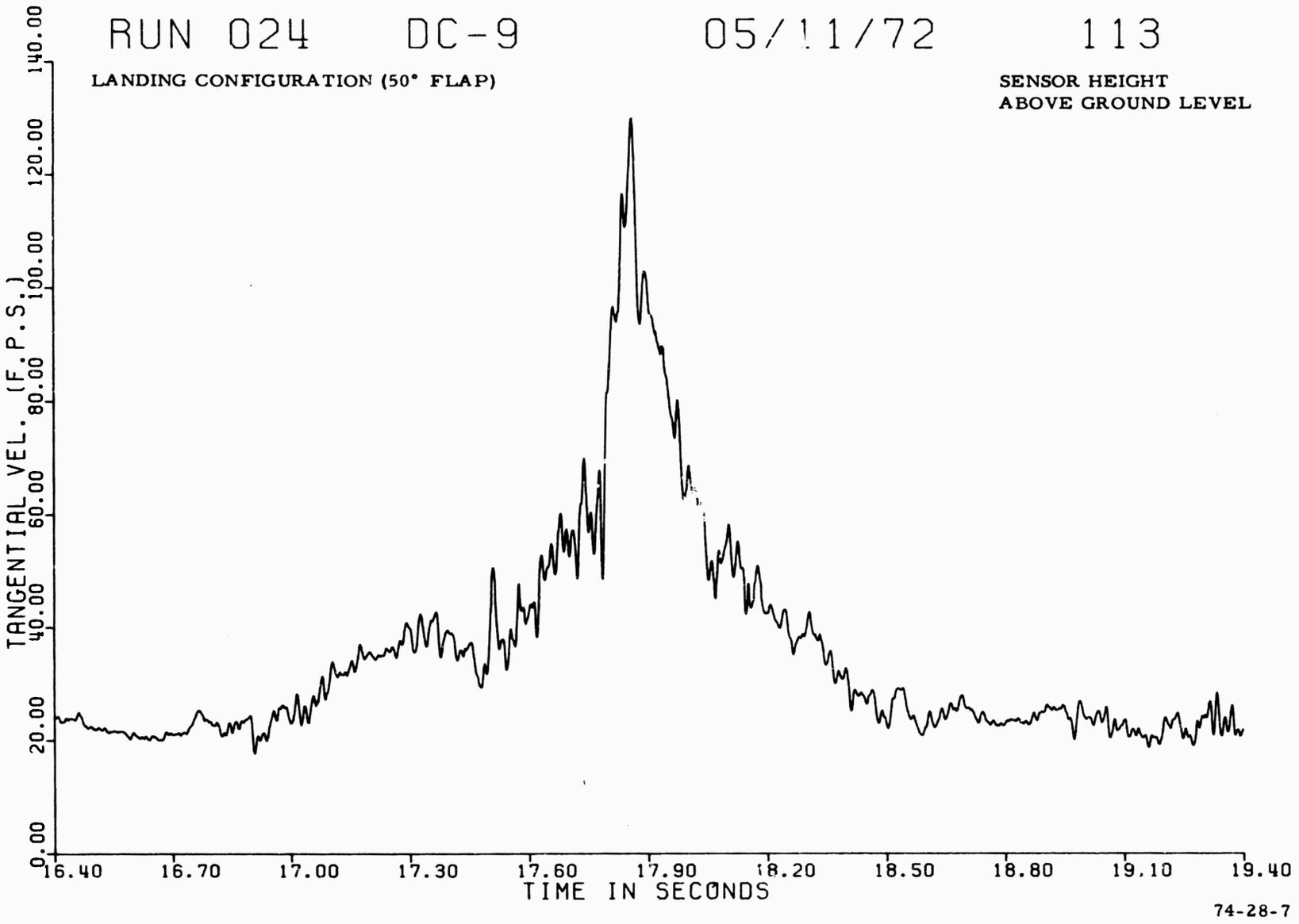

FIGURE 7. EXPANDED PLOT OF SENSOR 113 TIME HISTORY

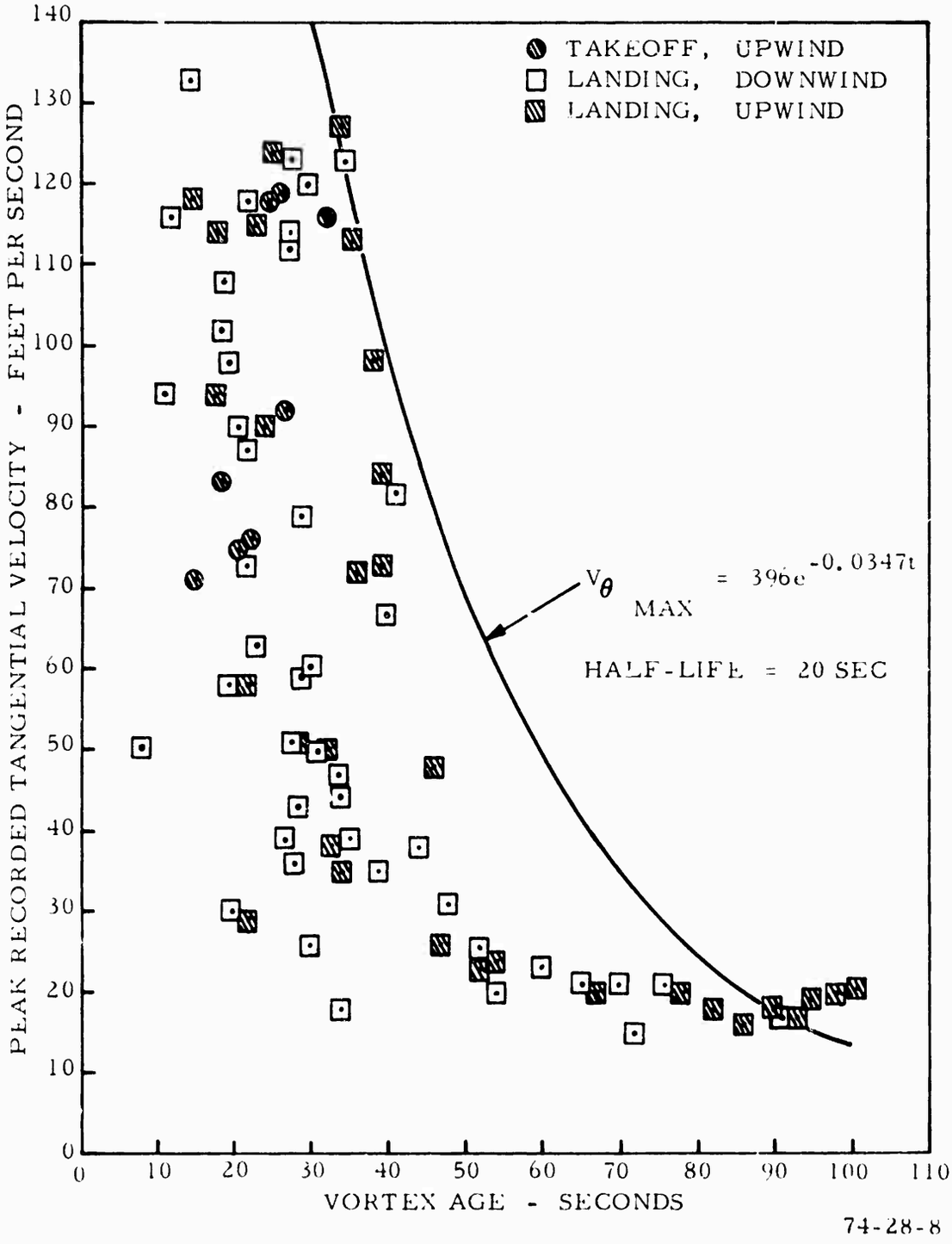

FIGURE 8. MCDONNELL-DOUGLAS DC9, SERIES 10, PEAK RECORDED TANGENTIAL VELOCITY VS. VORTEX AGE. ALL DATA POINTS (UNCORRECTED FOR WIND)

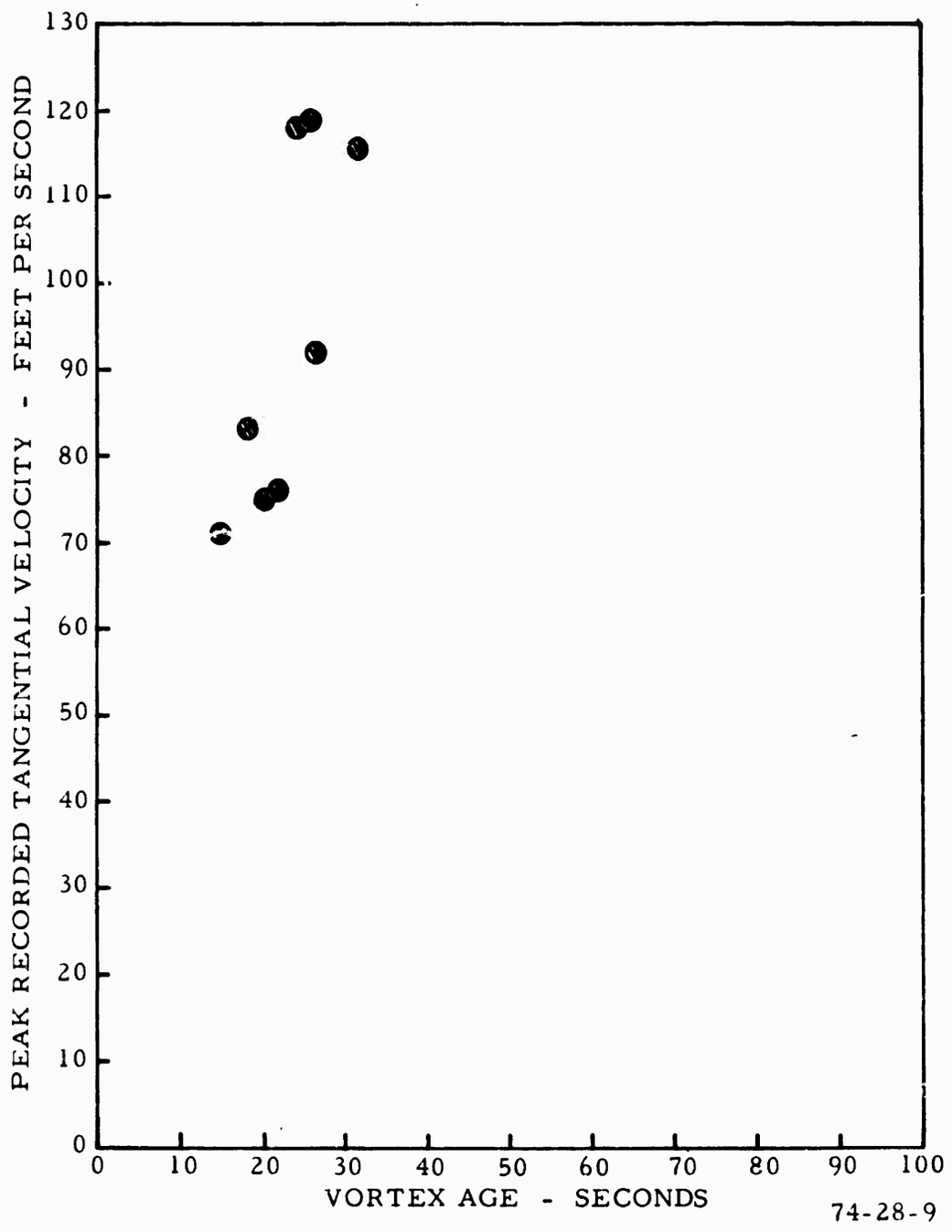

FIGURE 9. MCDONNELL-DOUGLAS DC9, SERIES 10, PEAK RECORDED TANGENTIAL VELOCITY VS. VORTEX AGE. TAKEOFF CONFIGURATION - UPWIND VORTICES (UNCORRECTED FOR WIND)

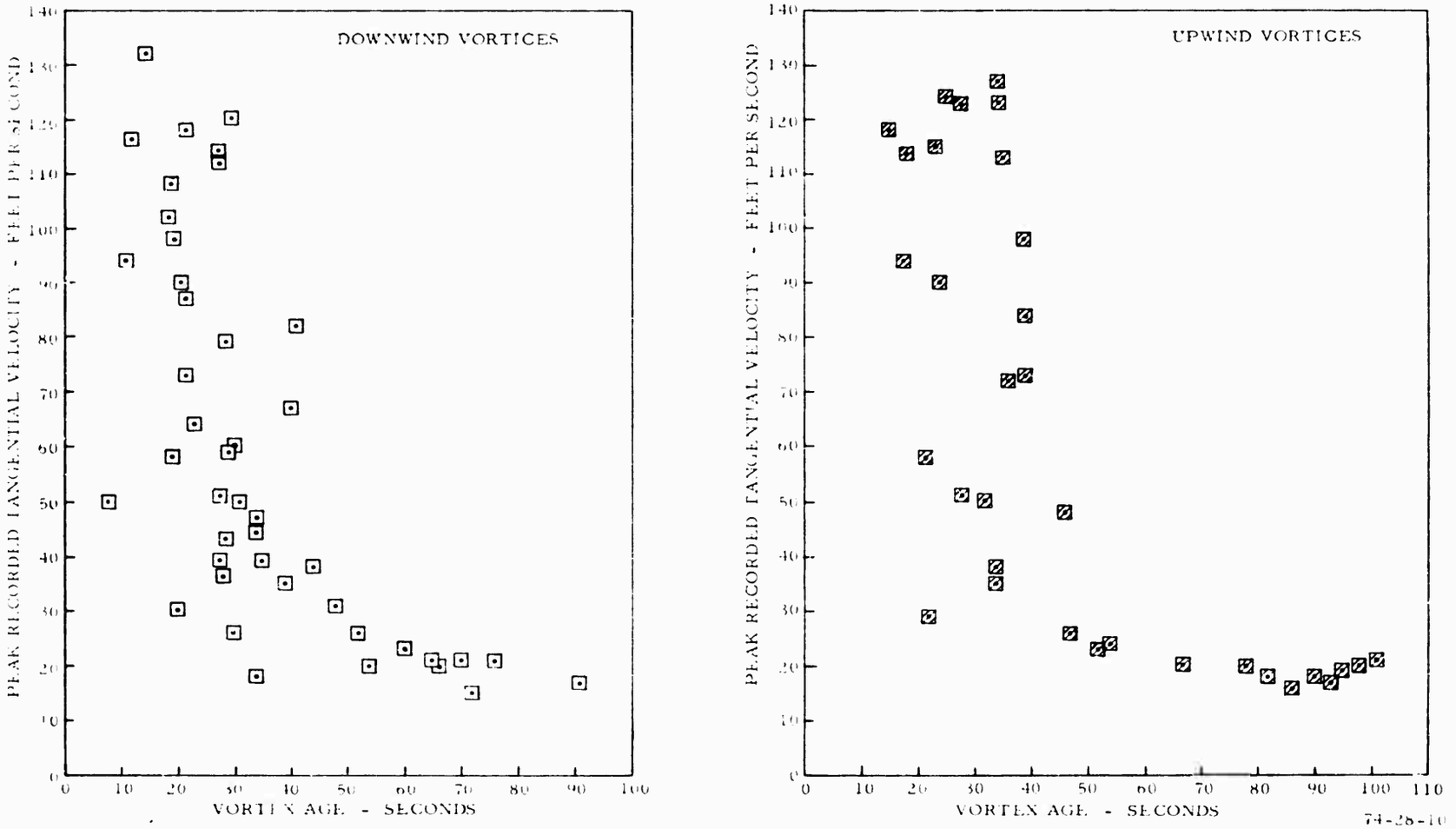

FIGURE 10. MCDONNELL-DOUGLAS DC9, SERIES 10, PEAK RECORDED TANGENTIAL VELOCITY VS. VORTEX AGE. LANDING CONFIGURATION (UNCORRECTED FOR WIND)

is a rapid falloff in the maximum velocity to be expected. An empirical curve fit to the data was made and the exponential equation $V_{\theta_{max}}=396\exp(-.0347t)$, with a half life of 20 seconds, is a fair description of the boundary of peak values over the time period 30 to 100 seconds after vortex generation. The inverse square root of elapsed time, which yielded a good fit to the data on the Boeing 747 and 727 (references 5 and 6) does not fit the present data at all. In the landing configuration data (figure 10), a comparison may be made between peak velocities in upwind and downwind vortices - and it is evident that over comparable times, there is little difference between them. This is in contrast to the findings in the Boeing 727 vortex flight tests, in which it was found, in landing configuration, that the boundary values of the peak tangential velocities were approximately 25 percent higher for upwind vortices as compared with downwind vortices.

Figures 11 and 12 show the variation of vortex lateral transport velocity with the crosswind velocity component. There is insufficient data on the takeoff configuration for comment, but in the landing configuration good correlation has been obtained over a wide range of crosswind values. For both upwind and downwind vortices, the lateral transport velocity is approximately equal to the crosswind velocity, which in this report was determined from the meteorological data at the 140-foot level. On balance, the downwind vortex lateral transport velocities exceed those of the upwind vortices by a small margin, which is the expected result (individual velocities are contained in appendix C).

In the absence of wind and viscous effects, the theoretical analysis of appendix D shows that the vortex lateral transport velocity tends to a limiting value given by

$$\dot{y} = \pm\frac{\Gamma}{4\pi s} \tag{1}$$

where s = semi-distance between vortices at time of generation

This value exists when the vortices have descended to the limiting height which is

$$z_\infty = s$$

Before reaching this height, the lateral transport velocity is

$$\dot{y} = \frac{\Gamma s^2}{4\pi z^3} \tag{2}$$

Taking a typical value of Γ=1660 feet squared per second and taking $s=.125\pi b$ (that is, 35 feet).

$$\frac{\Gamma}{4\pi s} = 3.8 \text{ ft/s}$$

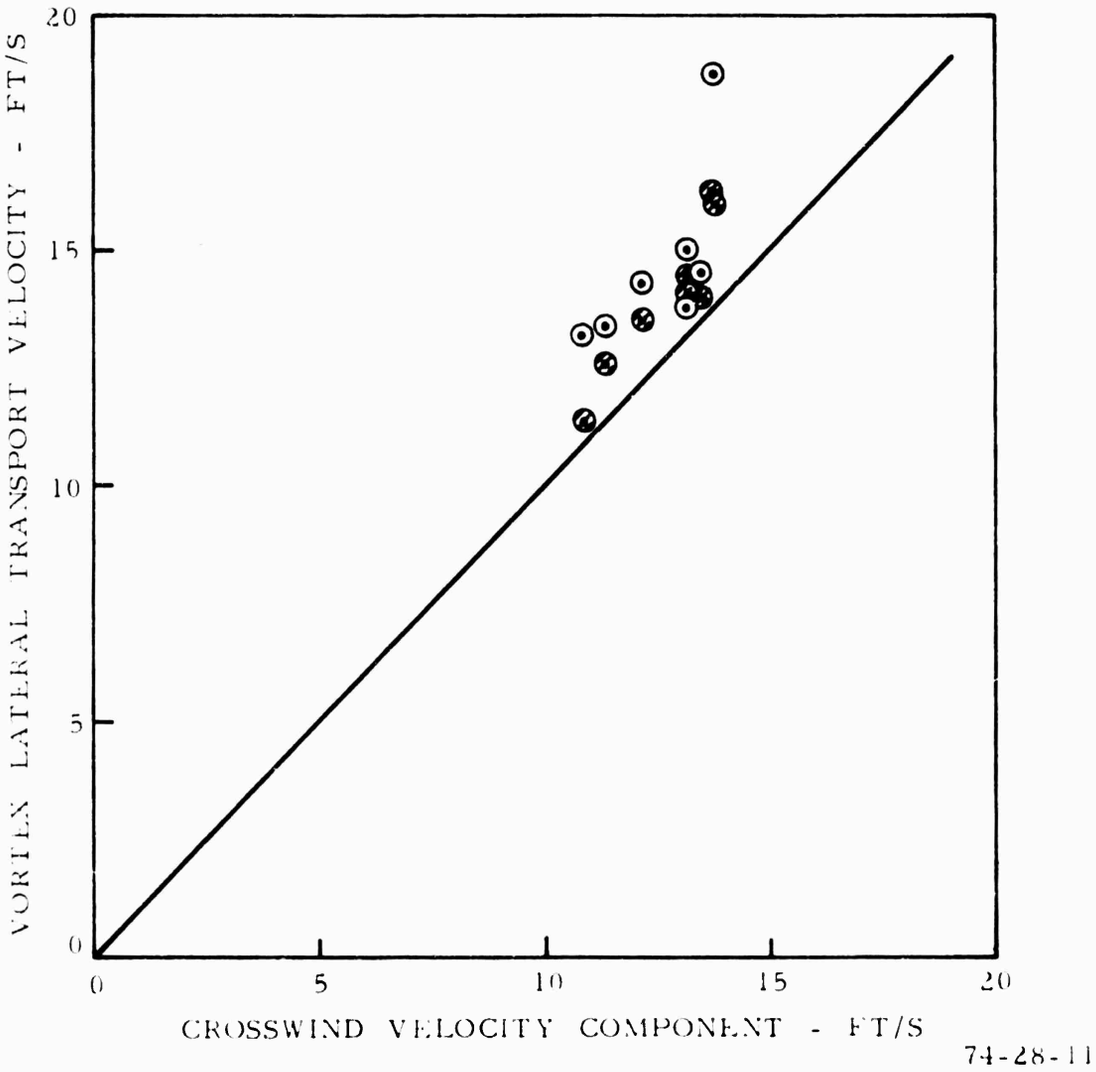

FIGURE 11. MCDONNELL-DOUGLAS DC9, SERIES 10, VORTEX LATERAL TRANSPORT VELOCITY VS. CROSSWIND VELOCITY COMPONENT - UPWIND AND DOWNWIND VORTICES. TAKEOFF CONFIGURATION

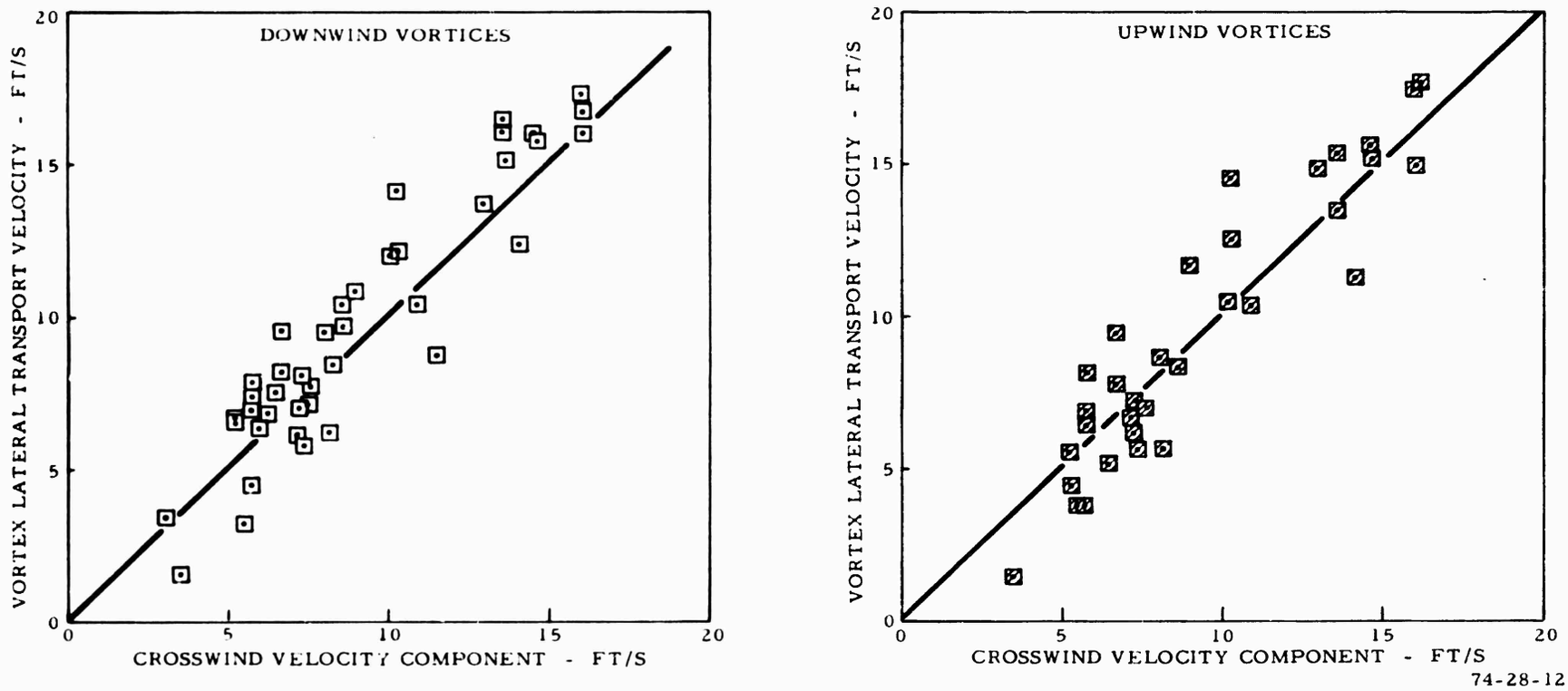

FIGURE 12. MCDONNELL-DOUGLAS DC9, SERIES 10, VORTEX LATERAL TRANSPORT VELOCITY VS. CROSSWIND VELOCITY COMPONENT. LANDING CONFIGURATION

and for z=2s, $z = 2s, \frac{\Gamma s^2}{4\pi z^3} = .47\ ft/s$

Thus, when the vortices strike the tower at heights greater than 2s (that is, 70 feet), the rate of induced drift (away from each other) is less than 1 foot per second (ft/s). Reference to appendix C shows that most vortices struck the tower at a greater height than this, which thus indicates that the vortex drift (that is, lateral transport) shown in figures 11 and 12 is almost entirely due to the wind. This is in agreement with the results presented in these figures, which show little difference between the drift rates of upwind and downwind vortices, and a slope of one-to-one, passing through the origin.

Figure 13 presents the measured vortex mean descent rates plotted against the theoretical values. The latter were determined using an expression developed from material published in reference 9. The development of the analysis appears in appendix D of this report. It yields the result that the time taken by a vortex pair to descend from height z_1 down to height z_2 is given by

$$T = \frac{8\pi s^2}{\Gamma}(\cot 2\phi_2 - \cot 2\phi_1) \tag{3}$$

where $\phi_{1,2} = \text{Arcsec } z_{1,2}/s$

It is also shown that the descent rate at height z is given by

$$\dot{z} = \frac{-\Gamma}{4\pi s} \frac{(z^2 - s^2)^{3/2}}{z^3} \tag{4}$$

When z is very large compared with s, this reduces to

$$\dot{z} = \frac{-\Gamma}{4\pi s} \tag{5}$$

With z equal to 2 seconds,

$$\dot{z} = \frac{-\Gamma}{4\pi s} \frac{\sqrt{27}}{8} \tag{6}$$

and with z equal to 1.5 seconds,

$$\dot{z} = \frac{-\Gamma}{4\pi s} \frac{1.25^{3/2}}{1.5^3} \tag{7}$$

The last two values are, respectively, 65 and 41 percent of the descent rate of out of ground effect. It is clear then that as the ground plane is approached, the rate of vortex descent diminishes very rapidly.

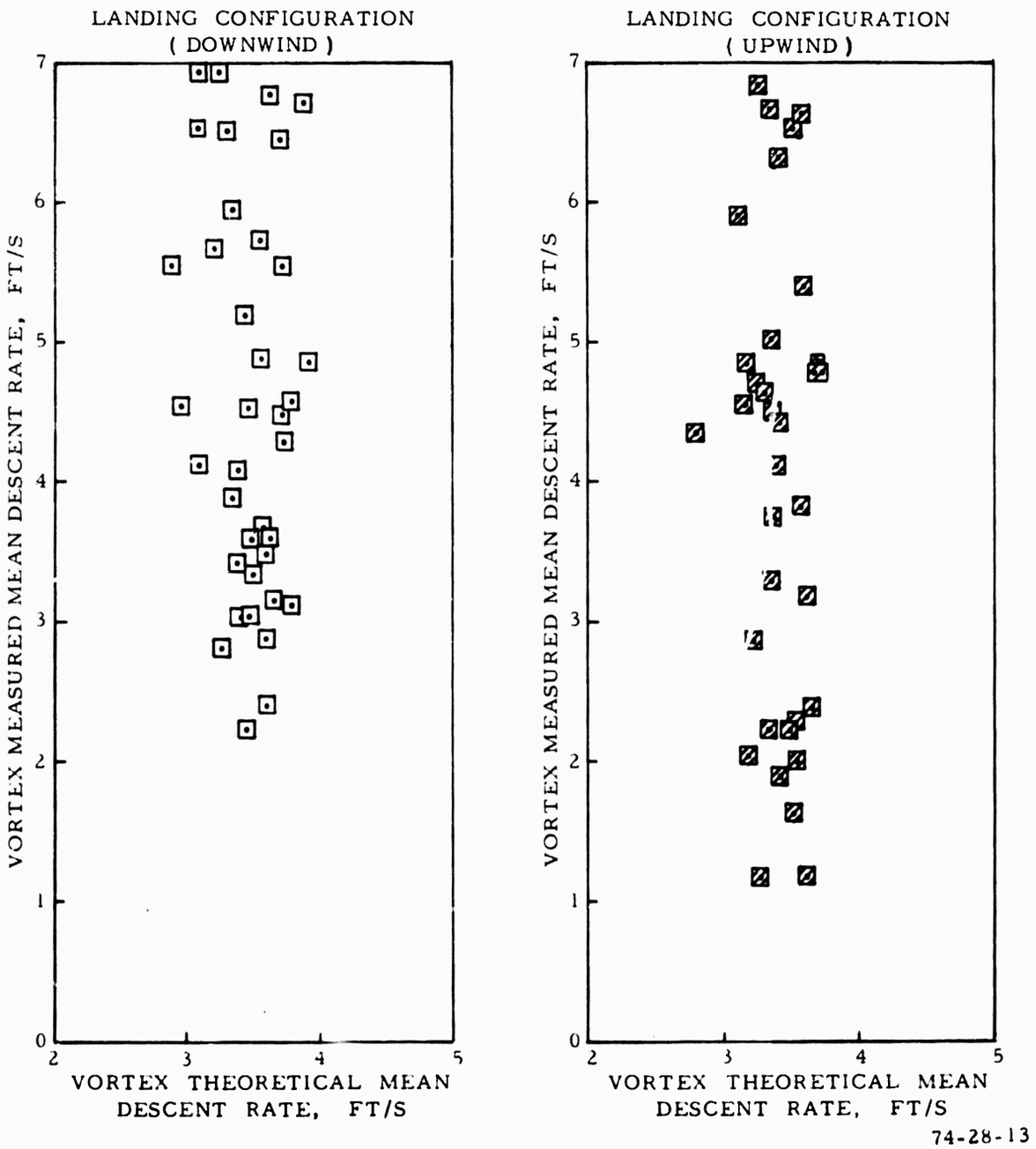

FIGURE 13. COMPARISON OF THEORETICAL AND MEASURED VORTEX MEAN DESCENT RATES

In the subject series of vortex-wake turbulence flight tests, no provision has been made for precise tracking of the vortices, if indeed this is yet possible and consequently transport velocities can only be determined as mean values over the time period between vortex generation and their striking the tower. Good results were obtained with the lateral transport velocities, which correlated quite well with the crosswind, largely because ground effect was very small in the height range over which the vortices were moving. Ground effect on descent velocity, however, is seen to be significant and the instantaneous value can be strongly influenced by small variations in the atmospheric density gradient, convection currents, and self-induced undulating movements developing within the vortex itself. The mean descent rate, even over an altitude range that is quite tightly controlled is, as a result, still subject to wide variations. The theoretical descent rate is a function only of the strength of the trailing vortices, the separation between them and the initial and final heights. Figure 13 serves to show that the calculation of the vertical situation of a vortex pair is not possible by any of the simple considerations that appear to work in determining the lateral situation.

In order to assess the effect of temperature inversion on vortex descent, the data points presented in figure 13 (measured descent rates are also tabulated in appendix C) were arbitrarily divided into those less than 4 ft/s descent rate and those greater. The low-altitude meteorological data of appendix A shows that a temperature inversion was present on many of the runs. Sixteen downwind vortices descended at less than 4 ft/s (run numbers 12-14, 19, 29-37, 39, 40, and 44), and of these, eleven (run numbers 12, 13, 29-34, 37, 39, and 40) were associated with a temperature inversion. Similarly, sixteen upwind vortices (run numbers 12, 13, 25, 29, 31-37, 39, 40, 43, 46, and 51) descended at less than 4 ft/s, and of these, eleven also (run numbers 12, 13, 29, 31-34, 37, 39, 40, and 43) were associated with an inversion.

Figures 14 and 15 present peak tangential velocity versus ambient windspeed, with the data grouped by vortex age (10-20 seconds, 20-30 seconds 30-40 seconds, and greater than 40 seconds). In the first three groups, the data points are randomly scattered and show no evidence of any correlation with windspeed. The final group merely reflect what is already shown in figure 8 - namely that beyond 40 seconds vortex age, peak velocities diminish very rapidly and are not likely to exceed 50 ft/s.

The possibility of a correlation between peak velocity and windspeed had been considered to exist because of wind shear, shown by the data of appendix A to be present at least to the altitude limit of the instrumentation.

In this series of tests, the range of altitude abreast of the tower was quite restricted, and when the data has been grouped according to age, it was found that in any one "age group," the range of altitude is further restricted - consequently, it is not possible to determine if any relationship exists between peak velocity in a vortex and the height above ground level at which it was generated. One result that was noted in previous work (reference 6), was that ground plane interference accelerated the flow - a result that is also predicted by potential flow theory.

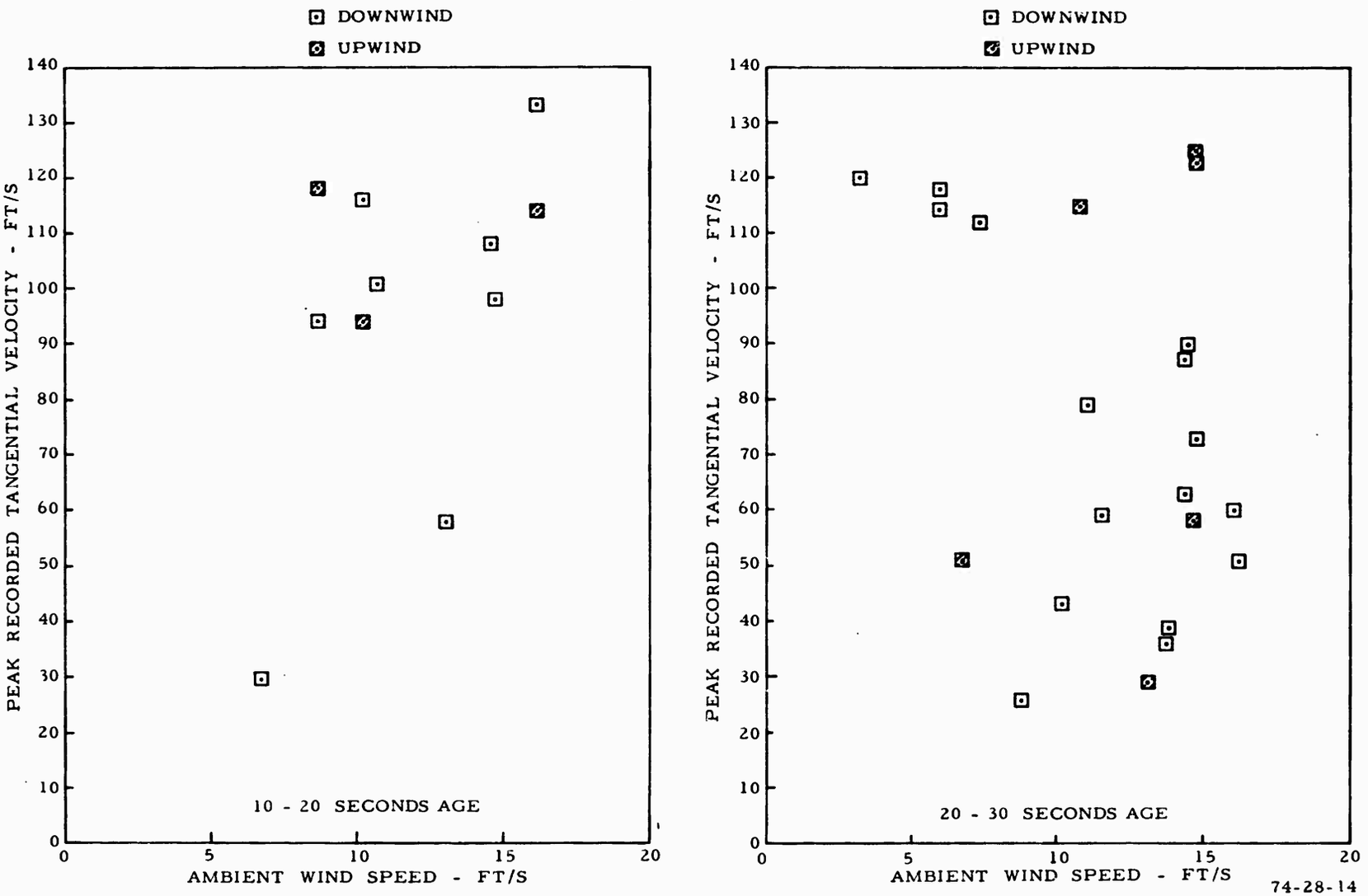

FIGURE 14. MCDONNELL-DOUGLAS DC9, SERIES 10, PEAK RECORDED TANGENTIAL VELOCITY VS. AMBIENT WINDSPEED. LANDING CONFIGURATION, UPWIND AND DOWNWIND VORTICES

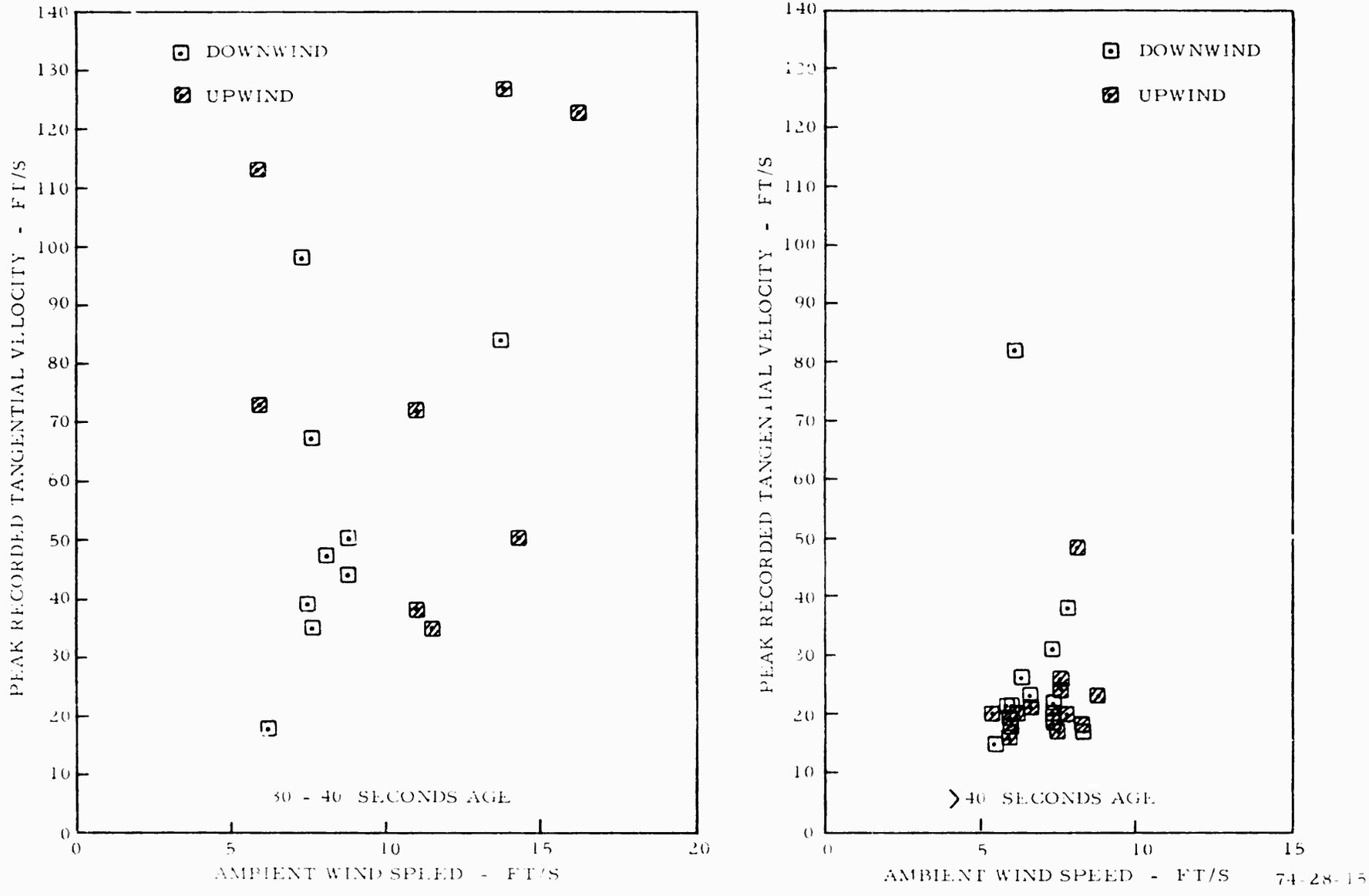

FIGURE 15. MCDONNELL-DOUGLAS DC9, SERIES 10, PEAK RECORDED TANGENTIAL VELOCITY VS. AMBIENT WINDSPEED. LANDING CONFIGURATION, UPWIND AND DOWNWIND VORTICES

The main body of the data is presented in appendices B and E, the distribution of tangential velocity for individual vortices. In appendix B, the tangential velocity plots are arranged by airplane flight configuration and by vortex age. Two configurations were tested - takeoff (flaps 20°, landing gear down), and landing (flaps 50°, landing gear down). Of the 61 runs made, the first 9 were in takeoff configuration, the remainder were in landing. Twenty-six of the runs yielded at least one good vortex 'hit' on the tower, the sensor data from which could be analyzed to produce a tangential velocity distribution.

It is evident from these distribution plots, which cover vortex ages between 20 and 40 seconds, that there is no detectable difference between the velocity distributions for vortices generated in the takeoff configuration, and those for landing configuration. All exhibit a consistently small core, the diameter of which is of the same order of magnitude as the sensor spacing (1 foot). At vortex ages greater than 40 seconds, figure 8 shows that there is a marked reduction in the maximum tangential velocity to be expected (the exponential decay curve that has been drawn is a very approximate fit to the data, and as figure 10 indicates, a different type of function, with small initial and final slope, and steep intermediate slope would be better), and it has not been possible with that data (that is, at 40 seconds and more) to deduce the velocity distributions and associated core diameters. All that could be done was to extract the peak tangential velocities and to note that past 50 seconds, at any rate, there is little structured flow and no region of high velocity remaining. There is no evidence of significant expansion of the vortex core with the passage of time, and this is supported by the findings of reference 6, from which tests it was possible to develop tangential velocity distributions of vortices up to 80 seconds in age, showing little or no core expansion.

In appendix E, composite plots are presented which illustrate the slowness with which the tangential velocity distributions change with time. This is best shown by comparison of figures E-2 and E-6, which cover a time span of 12 seconds vortex age to 41 seconds vortex age. All figures in the group E-2 through E-6 are for landing configuration, downwind vortices, and the airplane altitude abreast of the tower was between 200 and 230 feet. Thus, the variation among the vortices in this group is attributable to age, which in turn is determined by aircraft lateral clearance from the tower and the profile of crosswind velocity component. The solid lines in this group of figures represent an empirical envelope only, and were not mathematically determined.

The general form of the velocity distribution is close to that of the Hoffman-Joubert logarithmic distribution, which was shown to fit much of the data in references 5 and 6. As was found with the Boeing 727 airplane vortex cores are uniformly small in diameter - too small to measure accurately with the sensor spacing used in these tests. This spacing, namely 1 foot between sensors, probably represents a practical limit on resolution that can be obtained using the present type of anemometry, which necessarily involves heavy mounting hardware, and it is doubtful if any useful purpose would be

served by attempting to obtain more detailed information on the vortex core. The Hoffman-Joubert type of velocity distribution is presented in figure E-8 for three values of core radius - 1, 2, and 3 feet, with a maximum tangential velocity of 140 ft/s.

Figure 16 (A through F) presents six representative tangential velocity distributions, and illustrates clearly the absence of any clear difference between vortices generated in takeoff configuration and those generated in landing configuration (the respective flap angles are 20 and 50 degrees). The curves are calculated according to the Hoffman-Joubert logarithmic type of velocity distribution:

$$V_\theta = V_\theta(r_c)\,\frac{r_c}{r}\left(\ell_n \frac{r}{r_c} + 1\right)$$

The values of core radius r_c, and core radius tangential velocity $V_\theta(r_c)$ are noted separately for each plot.

It was indicated at the beginning of this report that there was some interest in comparing the subject airplane, the DC9, with the Boeing 727, since the two airplanes have certain design features in common - namely, swept-back wings, aft-mounted engines, and T-tail. The B727 vortex-wake flight tests are described in reference 6 and the principal findings of that report were as follows:

The highest peak recorded tangential velocities were found to exist in vortices generated in landing configuration, and of these, the upwind produced the higher peaks - up to a maximum value of 260 ft/s as compared with 210 ft/s for downwind. The only other flight configuration on which sufficient data was gathered for comment i.e., takeoff, also yielded absolute peak velocities on the order of 200 ft/s. In all three flight configurations in which the B727 was tested, the core diameters were uniformly small - too small in fact to be determined with sensor spacing of 1 foot. It was also found that the envelope defining the absolute peak velocities as a function of time could be approximated by the exponential equation

$$V_{\theta_{max}} = 341.5\exp(-.0126t)$$

with a half-life of 55 seconds. This was a surprising result, since the corresponding equation for the much larger and heavier B747 is

$$V_{\theta_{max}} = 336.4\exp(-.0173t),$$

with a half-life of 40 seconds. Another surprising result of the comparison between the B747 and B727 vortex flight tests was the fact that while with the former airplane, the vortex tangential velocity distribution as a function of radius was strongly influenced by the amount of flap detection (small deflections generated small-core vortices with high peak velocities, while large deflections generated large-core vortices with much lower peak velocities), the vortices generated by the B727, as has been seen, were insensitive to flap deflection, with regard to both the peak tangential velocity and the vortex-core diameter.

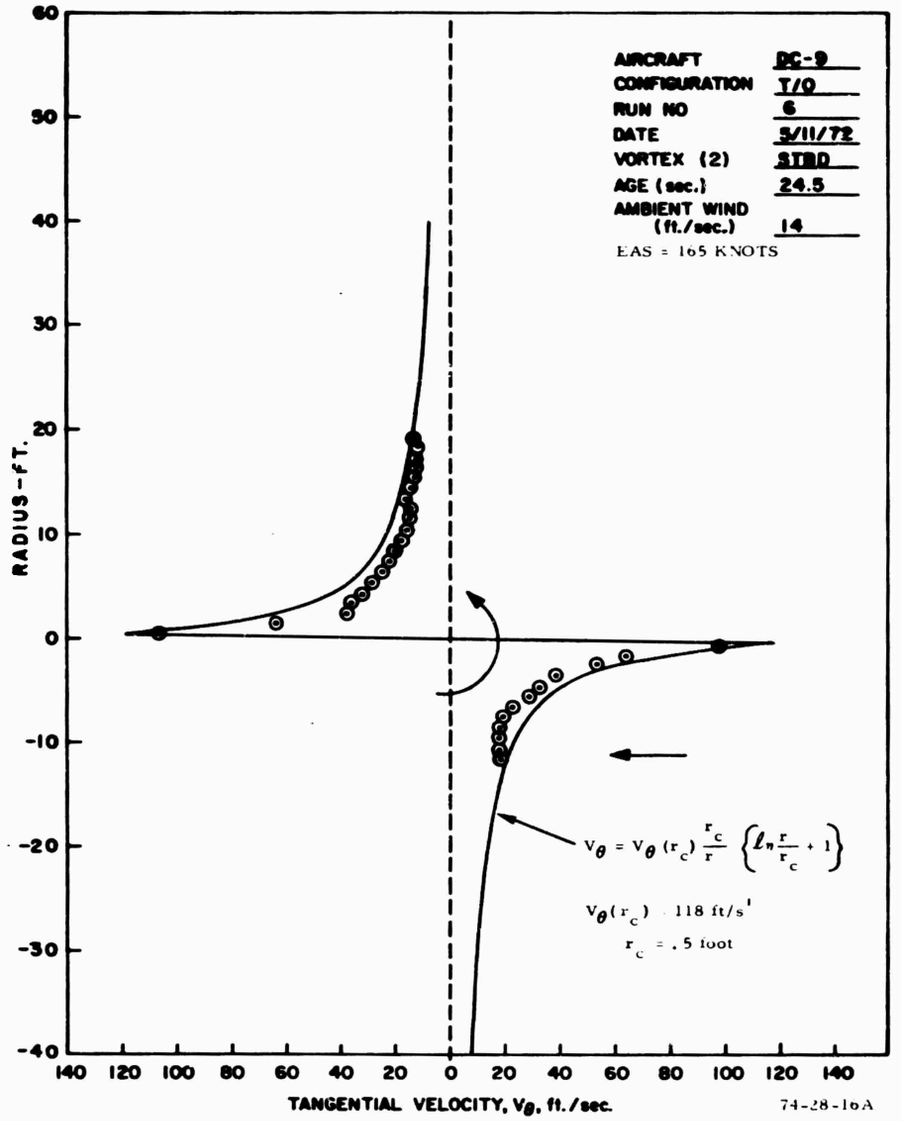

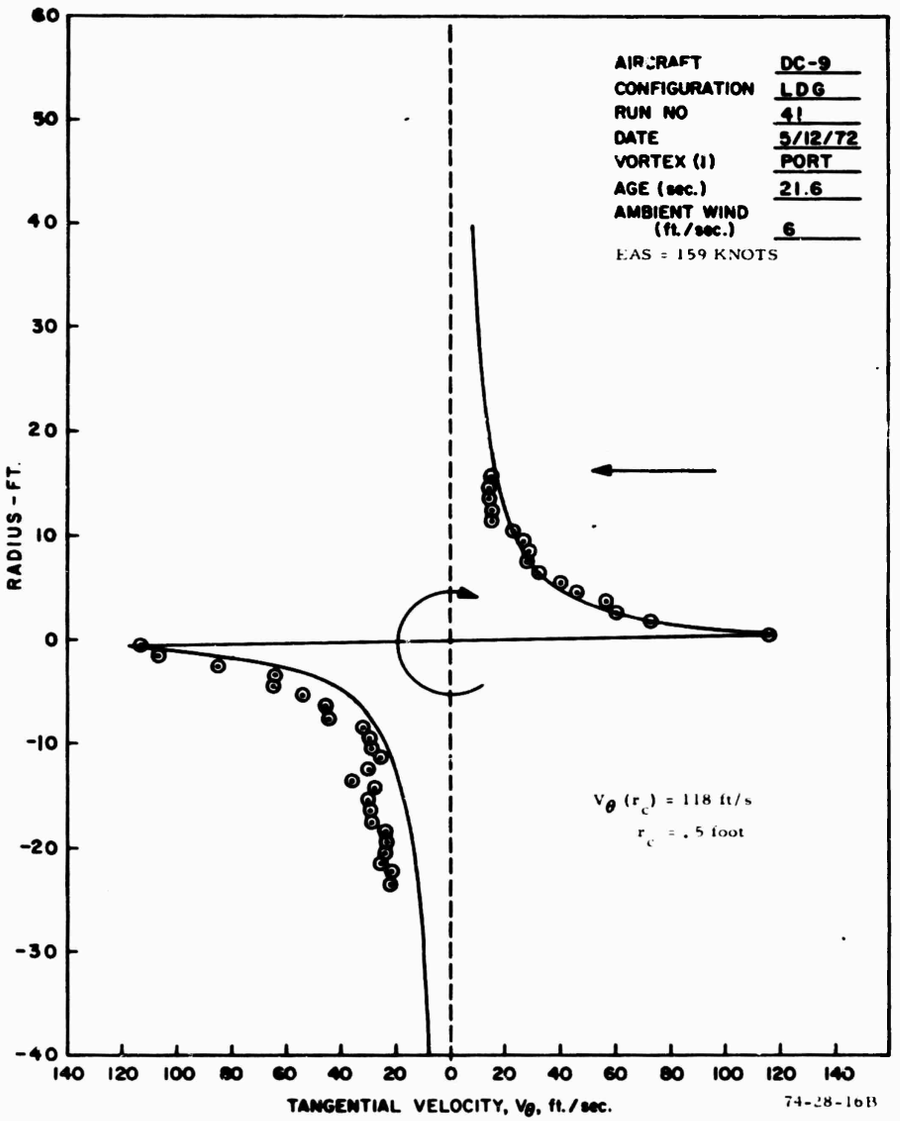

FIGURE 16A/B. EXAMPLES SHOWING FIT OF HOFFMAN-JOUBERT LOGARITHMIC VELOCITY DISTRIBUTION TO EXPERIMENTAL DATA (Page 1 of 3)

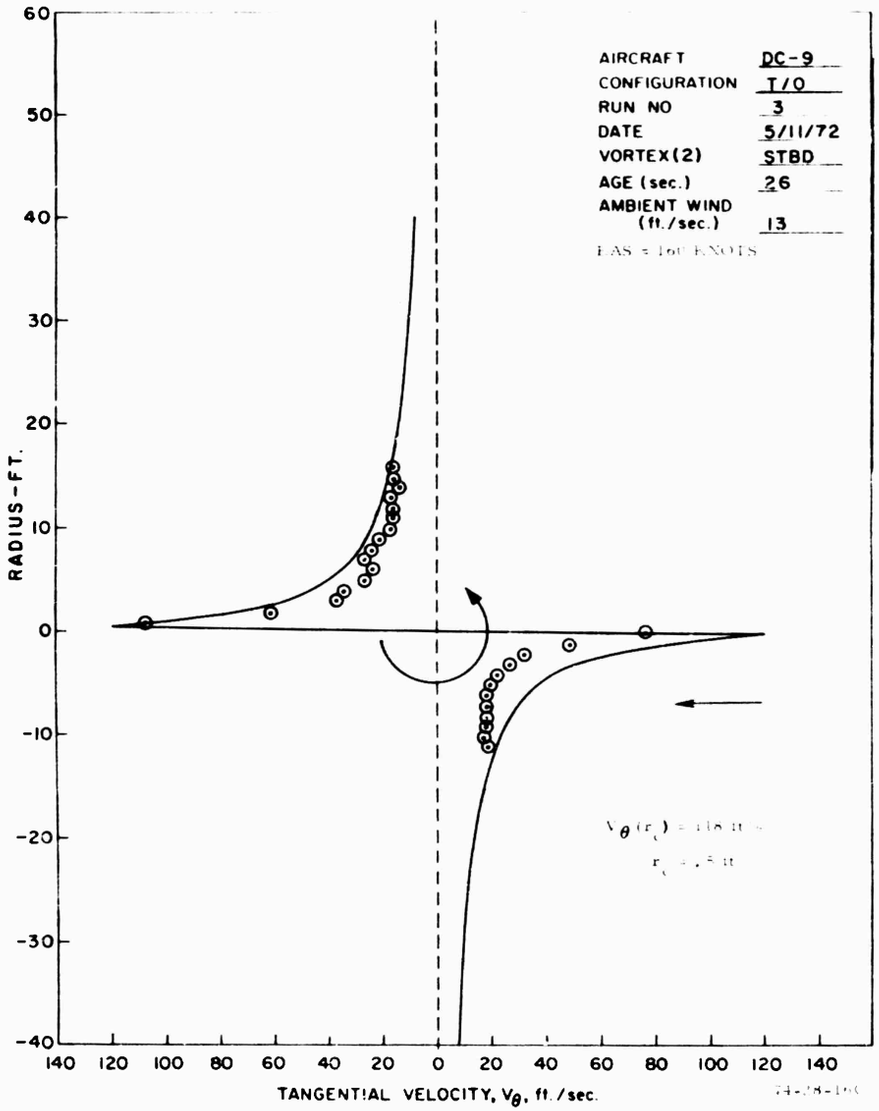

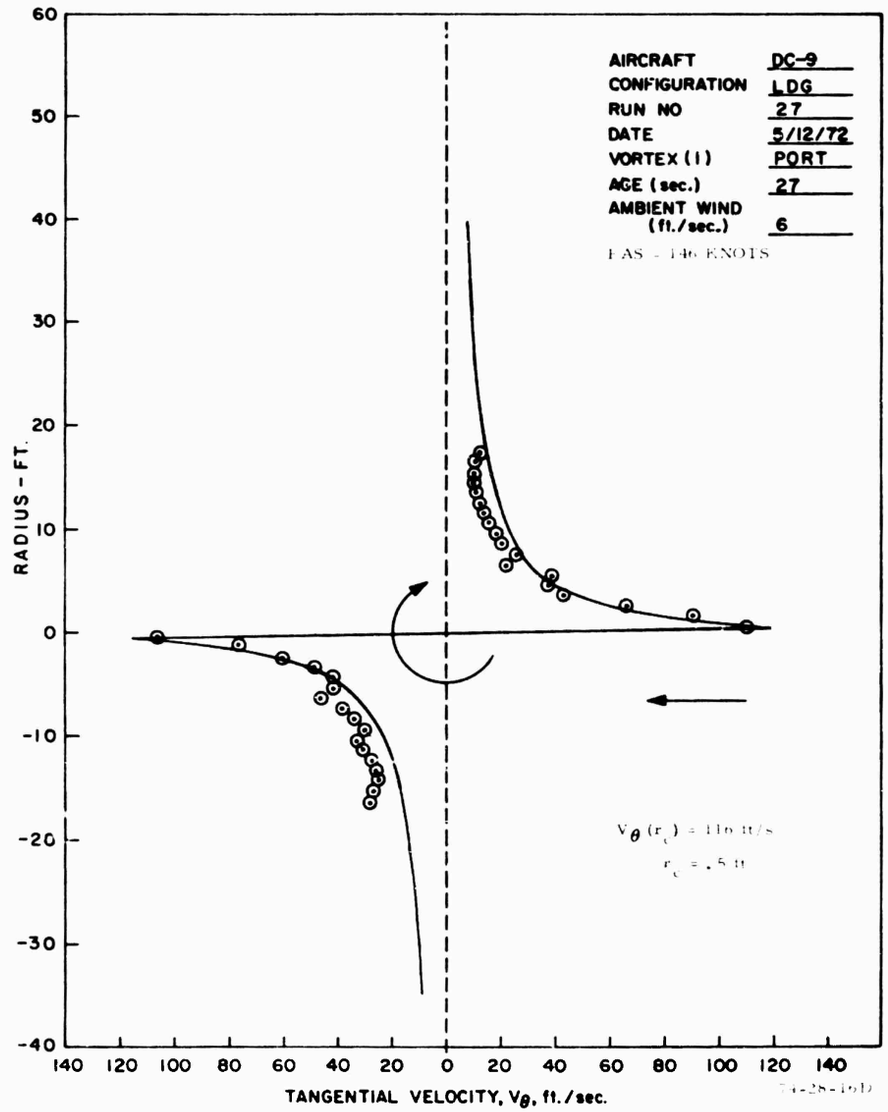

FIGURE 16C/D. EXAMPLES SHOWING FIT OF HOFFMAN-JOUBERT LOGARITHMIC VELOCITY DISTRIBUTION TO EXPERIMENTAL DATA (Page 2 of 3)

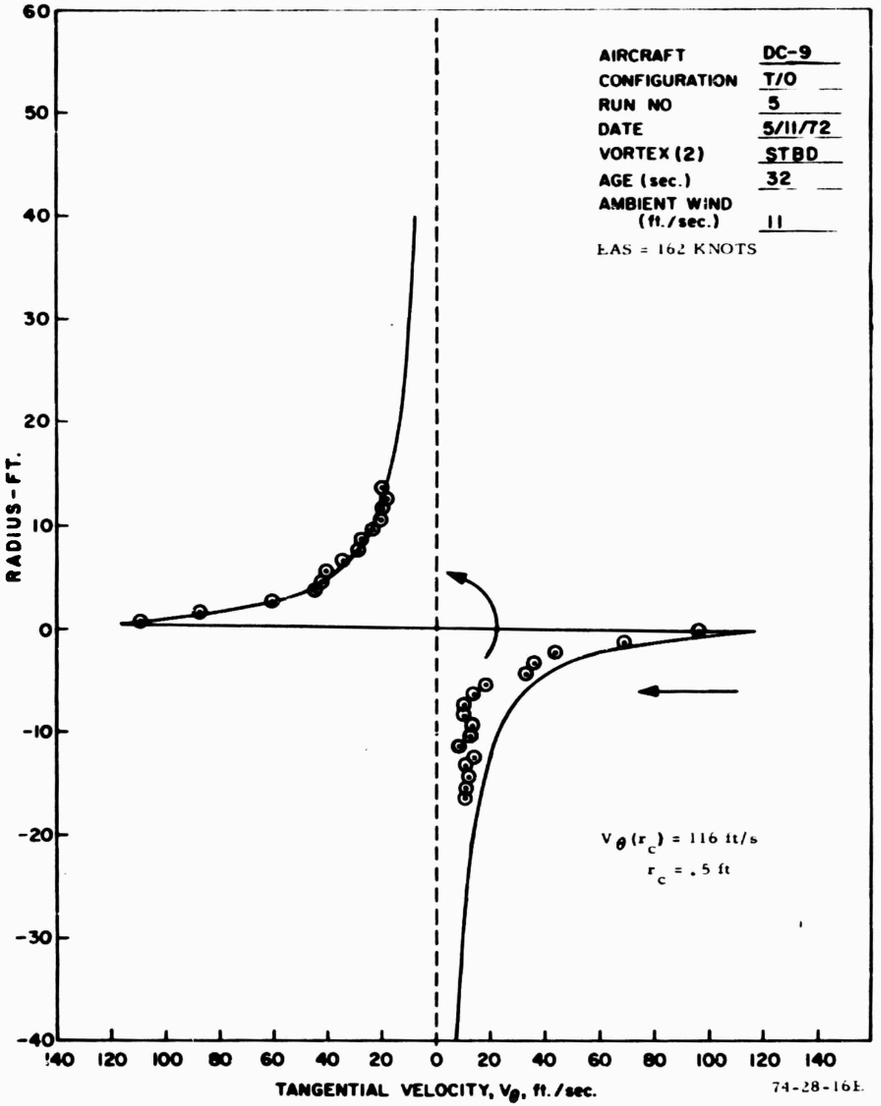

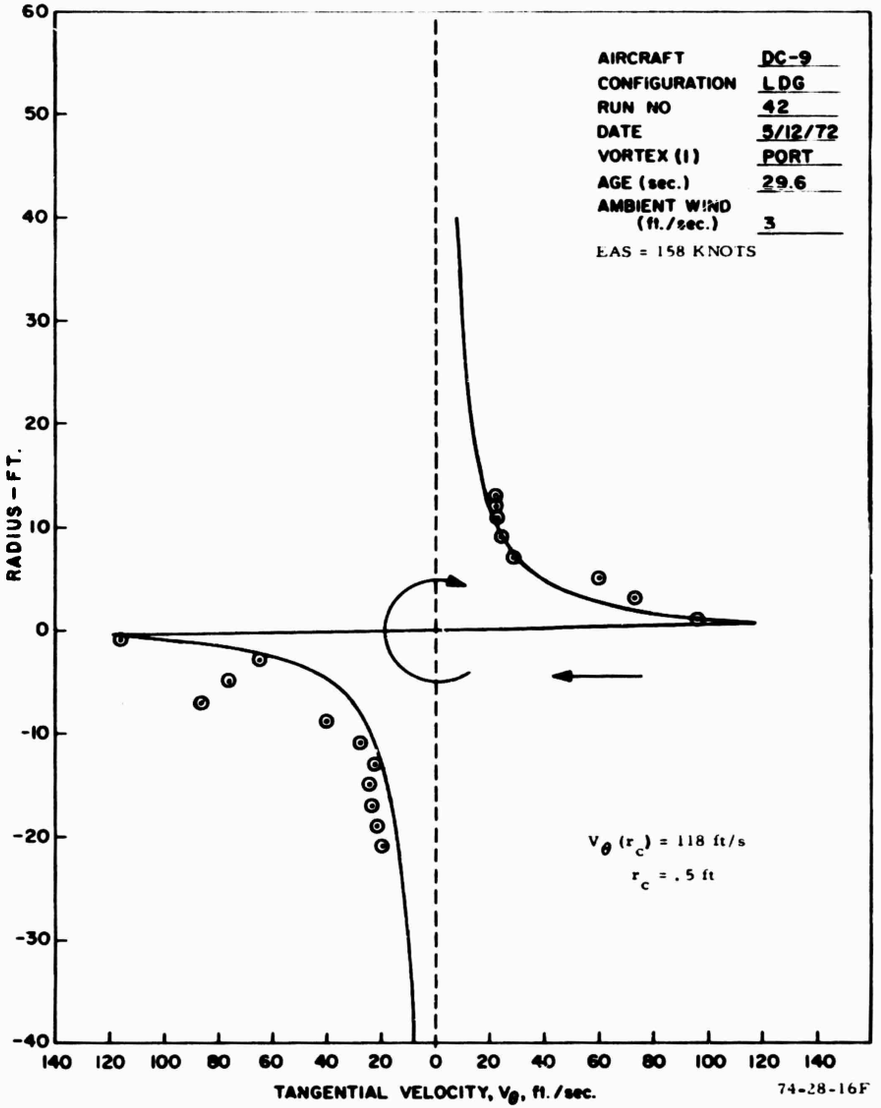

FIGURE 16E/F. EXAMPLES SHOWING FIT OF HOFFMAN-JOUBERT LOGARITHMIC VELOCITY DISTRIBUTION TO EXPERIMENTAL DATA (Page 3 of 3)

In one respect, the DC9 results are similar to the B727 results - namely, the vortex-core diameters have been found to be uniformly small (on the order of 1 foot) and the peak velocities and shape of the tangential velocity distribution are apparently independent of flap deflection. This result is possibly subject to revision, however, as the entire series of test runs were made in landing configuration, with the exception of the first nine, made in takeoff configuration. The magnitude of the peak velocities however, is much smaller (130 ft/s versus 260 ft/s), and the half-life is little more than a third of the value found for the B727 (20 seconds versus 55 seconds).

Appendixes A, D, and F contain summaries of low-altitude meteorological data, flight test data, and windspeed/direction at 140 ft, airplane track and date/time of each run.

CONCLUSIONS

1. The peak-velocity envelope uncorrected for wind, for vortex ages between 30 and 100 seconds, decays according to the equation

$$V_{\theta_{max}} = 396 \exp(-.0347t),$$

which has a half-life of 20 seconds.

2. Little or no difference due to configuration could be detected between vortices of comparable age.

3. Vortex lateral transport velocities correlate well with crosswind velocity component measured at 140 feet, indicating the vortices were out of ground effect.

4. Vortex descent velocities varied widely, even though test altitudes were held within close limits. It was found that the lower descent velocities usually occurred in the presence of a temperature inversion.

5. Tangential velocity distributions conform quite well to the Hoffman-Joubert logarithmic velocity distribution. No peak velocities greater than 140 ft/s were found, and all vortex cores were small in diameter, on the order of 1 foot, regardless of age or airplane flight configuration, a characteristic found also in the Boeing 727 airplane.

REFERENCES

1. Garodz, Leo J., Measurements of the Vortex Wake Characteristics of the Boeing 747, Lockheed C5A and Other Aircraft, Data Report, Project 177-621-03X (Special Task No. 1), April 1970.

2. Condit, Philip M., Results of the Boeing Wake-Turbulence Test Program, Boeing Document No. D6-30851, April 1970.

3. Andrews, William H., Robinson, Glenn H., Krier, Gary E., and Drinkwater, Fred J., III, Flight-Test Evaluation of the Wing Vortex Wake Generated by Large Jet Transport Aircraft, FWP-18, 1970.

4. Garodz, Leo J., FAA Full-Scale Aircraft Vortex Wake Turbulence Flight Test Investigations: Past, Present, Future, AIAA 9th Aerospace Sciences Meeting, New York, AIAA Paper Number 71-97, January 25 through 27, 1971.

5. Garodz, Leo J., Miller, Nelson J., and Lawrence, David, The Measurement of the Boeing 747 Trailing Vortex System Using the Tower Fly-By Technique, FAA Report No. RD-73-156.

6. Garodz, Leo J., Miller, Nelson J., and Lawrence, David, The Measurement of the Boeing 727 Trailing Vortex System Using the Tower Fly-By Technique, FAA Report No. RD-73-90.

7. Garodz, Leo J., Miller, Nelson J., and Lawrence, David, The Measurement of the Douglas DC7 Trailing Vortex System Using the Tower Fly-By Technique, FAA Report No. RD-73-141.

8. Schaufele, Roger D., and Ebeling, Ann W., Aerodynamic Design of the DC9 Wing and High-Lift System, Society of Automotive Engineers, Paper No. No. 670846.

9. Lamb, Horace, Hydrodynamics. Sixth Edition, Dover Publications, (Article Number 155), New York, 1945.

DC9 VORTEX FLIGHT TESTS

LOW-ALTITUDE METEOROLOGICAL DATA
May 11 through 12, 1972

	Run Numbers 1-5			Run Numbers 6-10			Run Numbers 11-15		
Level ft.	Temp. °C	Vel. ft/s	Direc. °Mag.	Temp. °C	Vel. ft/s	Direc. °Mag.	Temp. °C	Vel. ft/s	Direc. °Mag.
23	5.1	0.4	323	4.5	0.4	318	-	-	312
45	5.7	5.3	333	7.7	5.6	332	-	-	324
70	8.4	7.1	326	8.6	7.3	332	-	-	308
100	10.2	9.8	-	9.5	9.2	340	-	-	296
140	10.9	12.3	(360)	10.7	13.6	(350)	-	(14.7)	(340)
23	4.5	0.4	323	4.8	0.4	326	7.3	0.5	314
45	7.7	3.5	340	6.0	6.1	338	9.3	4.5	241
70	8.0	6.3	339	8.5	7.7	330	8.9	6.5	337
100	9.5	9.6	-	9.4	9.5	335	9.5	9.1	296
140	10.2	13.5	(350)	10.3	14.2	(340)	9.3	13.7	(350)
23	4.7	0.4	315	-	-	-	7.7	0.5	321
45	6.0	4.9	345	-	-	-	10.2	5.5	265
70	8.5	7.3	340	-	-	-	9.0	7.3	335
100	10.2	10.0	-	-	-	-	9.7	9.1	267
140	11.2	13.4	(350)	-	(14.7)	(340)	10.0	13.8	(350)
23	4.9	0.4	300	6.1	0.5	-	-	-	315
45	6.2	3.8	334	11.2	3.5	336	-	-	265
70	8.6	5.9	330	8.4	6.1	331	-	-	299
100	9.8	8.3	-	9.4	9.0	329	-	-	-
140	10.7	11.5	(350)	10.3	13.8	(340)	-	(16.2)	341
23	4.9	0.4	332	-	-	-	11.4	8.0	308
45	5.6	3.0	328	-	-	-	13.7	8.7	30
70	8.7	5.1	322	-	-	-	11.5	9.4	56
100	9.8	7.7	322	-	-	-	11.5	9.9	15
140	10.7	11.4	(350)	-	(14.7)	(350)	11.3	11.0	345

NOTES:
1. Data points are mean values obtained over a 2-minute period prior to passage of airplane past test tower. Period excludes final 10 seconds prior to passage.
2. Temperature sensor at 45-foot level suspect on some runs.
3. Numbers in parenthesis are spot readings recorded manually, from backup instrumentation at 140-foot level. Readings were taken approximately 5 seconds prior to passage of aircraft past test tower.

DC9 VORTEX FLIGHT TESTS

LOW-ALTITUDE METEOROLOGICAL DATA
May 11 through 12, 1972

	Run Numbers 16-20			Run Numbers 21-25			Run Numbers 26-30		
Level ft.	Temp. °C	Vel. ft/s	Direc. °Mag.	Temp. °C	Vel. ft/s	Direc. °Mag.	Temp. °C	Vel. ft/s	Direc. °Mag.
23	11.5	7.7	306	-	-	-	12.8	10.5	282
45	13.9	8.6	15	-	-	-	13.8	11.1	298
70	11.6	9.0	64	-	-	-	12.8	11.0	296
100	11.6	9.4	15	-	-	-	13.2	12.1	304
140	11.4	10.7	308	-	(13.2)	(360)	10.3	14.9	315
23	11.8	10.5	252	-	-	260	8.8	0.7	28
45	13.7	11.6	5	-	-	302	12.3	5.2	17
70	11.9	12.2	11	-	-	290	11.9	6.2	33
100	12.0	12.5	18	-	-	252	12.5	10.1	56
140	11.7	14.4	288	-	(13.2)	349	12.7	13.5	50
23	11.9	8.5	256	12.7	11.3	303	-	-	-
45	13.9	9.7	68	13.6	12.3	322	-	-	-
70	12.0	10.2	146	12.6	13.1	313	-	-	-
100	12.0	10.3	28	11.8	13.4	322	-	-	-
140	11.8	11.5	273	12.5	16.0	342	-	(7.3)	17.5
23	12.2	7.9	317	12.7	11.8	301	9.3	0.4	-
45	14.7	8.4	238	16 5	12.5	320	10.8	4.0	17
70	12.1	8.6	242	12.7	13.4	314	11.8	3.4	23
100	12.3	8.7	159	11.0	13.6	327	12.5	4.6	38
140	12.0	10.1	338	12.6	16.1	347	12.7	(7.3)	36
23	-	-	-	12.9	12.1	291	10.0	0.5	-
45	-	-	-	16.1	12.5	307	12.7	3.9	21
70	-	-	-	12.9	12.6	304	12.1	4.0	24
100	-	-	-	12.2	12.5	312	12.5	4.2	41
140	-	(13.2)	(350)	11.2	14.3	335	12.6	6.2	39

DC9 VORTEX FLIGHT TESTS

LOW-ALTITUDE METEOROLOGICAL DATA
May 11 through 12, 1972

	Run Numbers 31-35			Run Numbers 36-40			Run Numbers 41-45		
Level ft.	Temp. °C	Vel. ft/s	Direc. °Mag.	Temp. °C	Vel. ft/s	Direc. °Mag.	Temp. °C	Vel. ft/s	Direc. °Mag.
23	6.7	0.5	316	-	-	-	8.9	0.5	328
45	10.8	4.5	294	-	-	-	8.6	5.3	318
70	11.3	4.9	-	-	-	-	11.7	6.0	335
100	12.2	5.6	31	-	-	-	12.2	7.3	7
140	12.6	5.4	27	-	(5.9)	(30)	12.4	(5.9)	(20)
23	6.9	0.5	312	9.3	2.2	307	10.0	0.4	278
45	13.3	5.1	4	12.9	5.2	286	12.1	3.7	308
70	11.8	5.0	8	12.9	6.5	299	11.8	3.3	320
100	12.3	6.0	32	13.4	7.4	48	12.3	3.9	319
140	12,5	6.6	33	13.7	8.3	31	13.4	3.2	(20)
23	8.0	0.6	348	-	-	-	9.8	1.0	280
45	12.5	5.7	5	-	-	-	12.0	5.8	321
70	12.0	6.2	15	-	-	-	12.1	5.9	322
100	12.4	6.8	36	-	-	-	12.7	7.0	270
140	12.6	6.0	26	-	(7.3)	(30)	12.9	7.5	338
23	9.2	4.3	345	6.2	0.5	207	12.6	0.8	299
45	13.1	6.6	5	3.7	3.4	274	14.6	5.4	318
70	11.9	6.6	15	11.4	4.4	288	12.7	4.5	320
100	12.3	7.6	34	12.2	5.5	21	11.8	4.5	326
140	12.5	7.8	24	12.5	5.9	25	12.9	6.1	338
23	-	-	-	8.4	0.5	337	12.8	0.9	290
45	-	-	-	18.4	4.7	329	15.0	4.9	304
70	-	-	-	11.9	5.6	-	13.1	5.0	299
100	-	-	-	12.4	6.0	17	13.1	5.6	303
140	-	(7.3)	(30)	12.6	6.2	10	13.3	6.7	325

DC9 VORTEX FLIGHT TESTS

LOW-ALTITUDE METEOROLOGICAL DATA
May 11 through 12, 1972

	Run Numbers 46-50			Run Numbers 51-55			Run Numbers 56-60		
Level ft.	Temp. °C	Vel. ft/s	Direc. °Mag.	Temp. °C	Vel. ft/s	Direc. °Mag.	Temp. °C	Vel. ft/s	Direc. °Mag.
23	13.3	2.1	295	14.0	6.4	300	14.6	7.1	302
45	15.7	6.0	314	16.3	7.2	320	15.7	8.5	64
70	13.4	6.1	315	14.1	7.1	313	14.7	8.5	112
100	13.5	6.5	320	14.1	7.3	319	14.6	8.9	44
140	13.6	7.6	339	14.2	8.8	340	14.4	10.2	298
23	13.5	0.8	301	-	-	-	14.6	5.4	88
45	15.9	6.2	319	-	-	-	16.8	6.5	76
70	13.6	5.9	316	-	-	-	14.7	6.7	148
100	13.6	6.3	321	-	-	-	14.8	7.2	151
140	13.8	7.6	343	-	(8.8)	(310)	14.7	8.7	270
23	13.1	3.9	271	14.5	3.3	294	14.9	5.4	313
45	15.3	6.5	293	16.5	6.4	310	17.8	6.8	263
70	13.3	6.1	292	-	6.4	306	15.0	6.8	267
100	13.2	6.4	298	14.5	6.8	312	15.0	7.1	201
140	13.4	7.8	311	14.7	7.8	334	14.8	8.7	311
23	-	-	-	14.7	5.9	305	14.9	8.8	-
45	-	-	-	16.3	7.4	322	17.5	10.2	-
70	-	-	-	14.7	8.3	313	15.0	10.8	-
100	-	-	-	14.7	8.6	325	14.9	11.5	-
140	-	(8.8)	(310)	14.7	9.8	348	14.7	13.1	(350)
23	13.8	5.5	281	14.5	9.0	330	14.9	10.4	-
45	16.0	6.6	296	15.6	10.2	35	17.3	11.8	-
70	13.9	6.4	294	14.6	10.4	-	15.0	12.3	-
100	13.8	6.7	301	14.6	10.2	34	15.0	12.5	-
140	14.0	8.1	325	14.5	11.5	326	14.7	14.3	(350)

Run Number 61

Level ft.	Temp °C	Vel. ft/s	Direc. °Mag.
23	14.1	11.3	253
45	-	11.8	255
70	11.6	11.2	273
100	18.1	12.6	-
140	13.5	14.6	263

APPENDIX B

VORTEX TANGENTIAL VELOCITY DISTRIBUTIONS

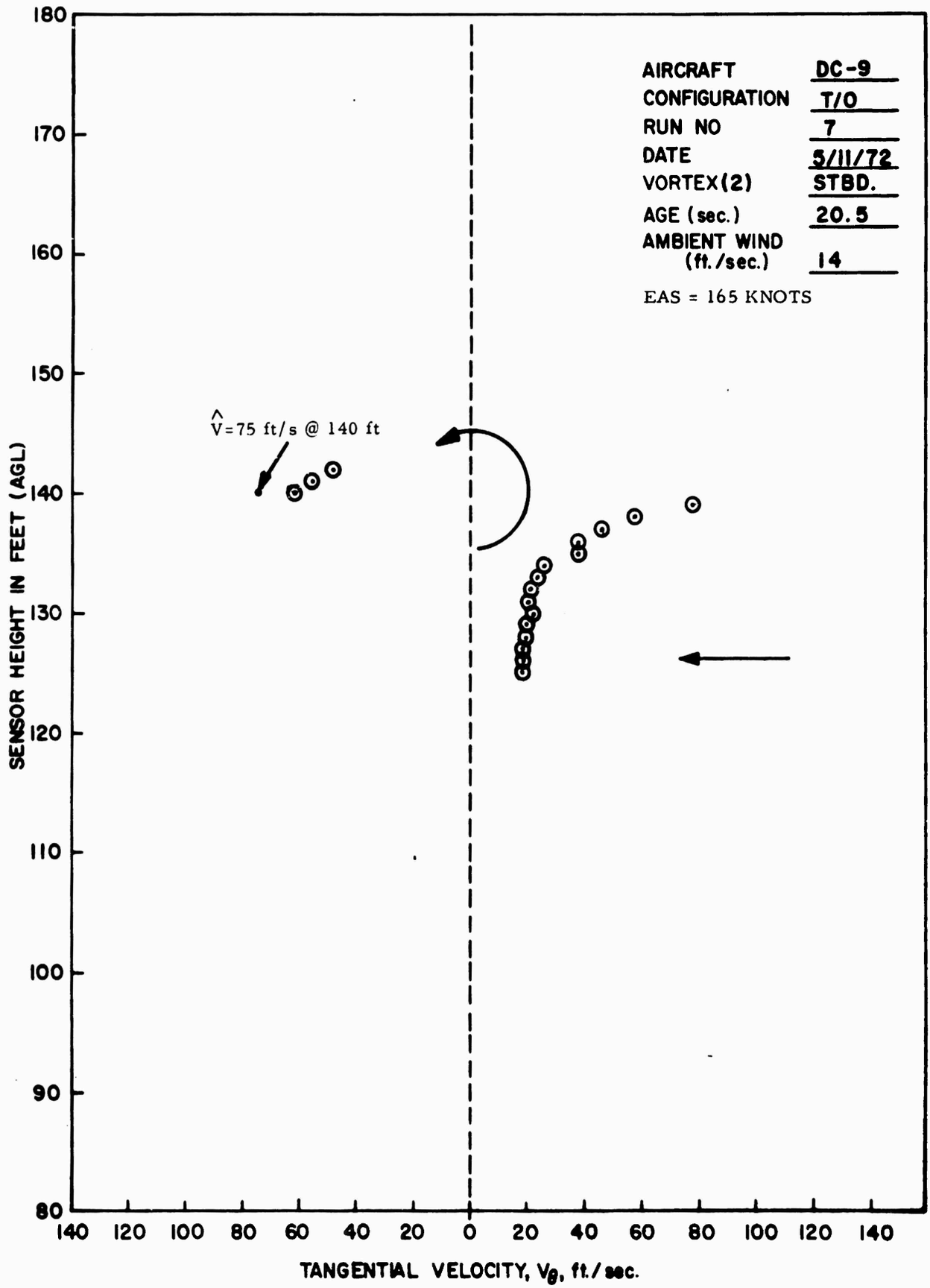
AIRCRAFT DC-9
CONFIGURATION T/O
RUN NO 7
DATE 5/11/72
VORTEX(2) STBD.
AGE (sec.) 20.5
AMBIENT WIND (ft./sec.) 14
EAS = 165 KNOTS
V̂=75 ft/s @ 140 ft
SENSOR HEIGHT IN FEET (AGL)
180
170
160
150
140
130
120
110
100
90
80
140 120 100 80 60 40 20 0 20 40 60 80 100 120 140
TANGENTIAL VELOCITY, Vθ, ft./sec.

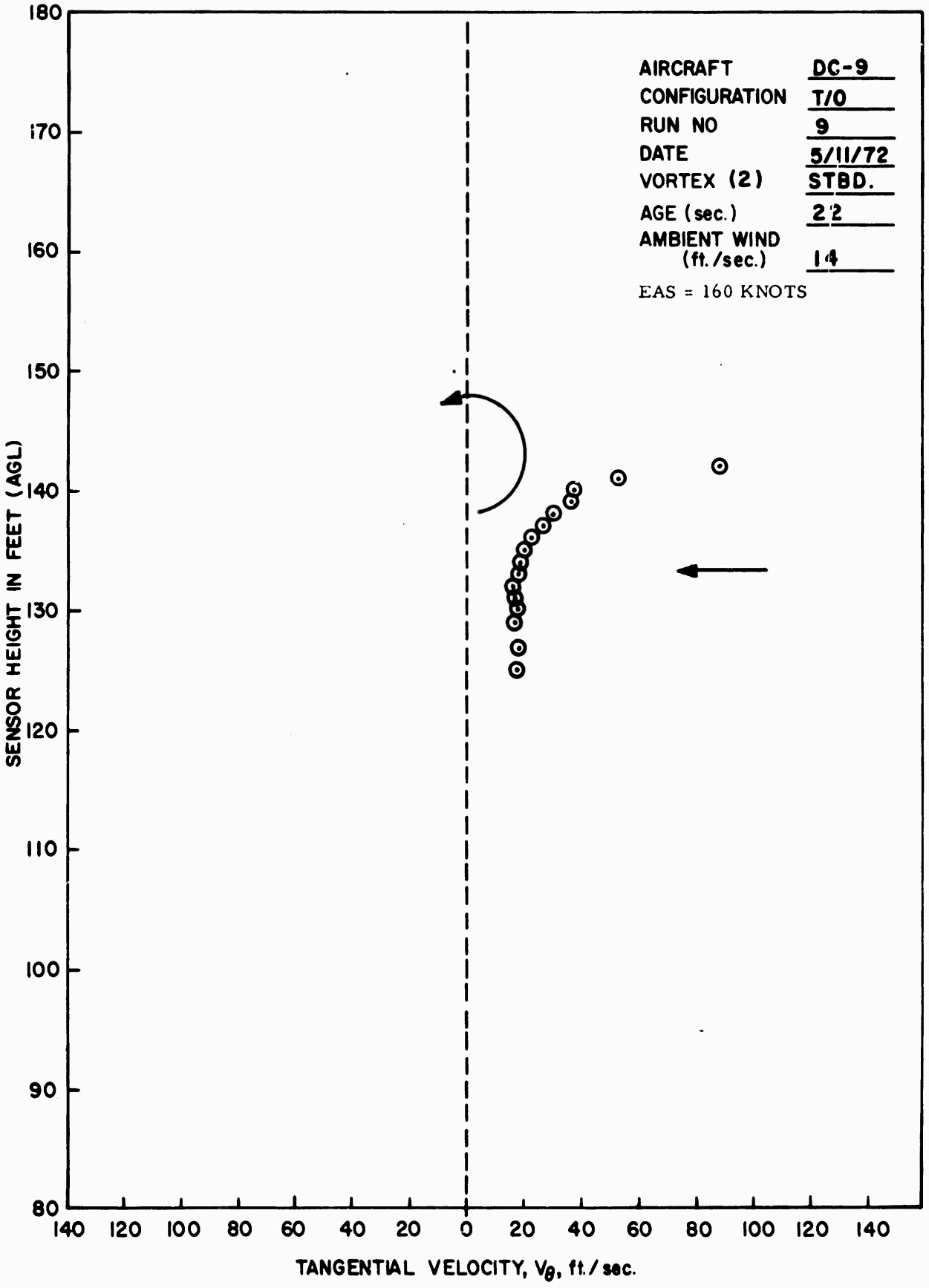
AIRCRAFT DC-9
CONFIGURATION T/O
RUN NO 9
DATE 5/11/72
VORTEX (2) STBD.
AGE (sec.) 22
AMBIENT WIND (ft./sec.) 14
EAS = 160 KNOTS
SENSOR HEIGHT IN FEET (AGL)
180
170
160
150
140
130
120
110
100
90
80
140 120 100 80 60 40 20 0 20 40 60 80 100 120 140
TANGENTIAL VELOCITY, V_θ, ft./sec.

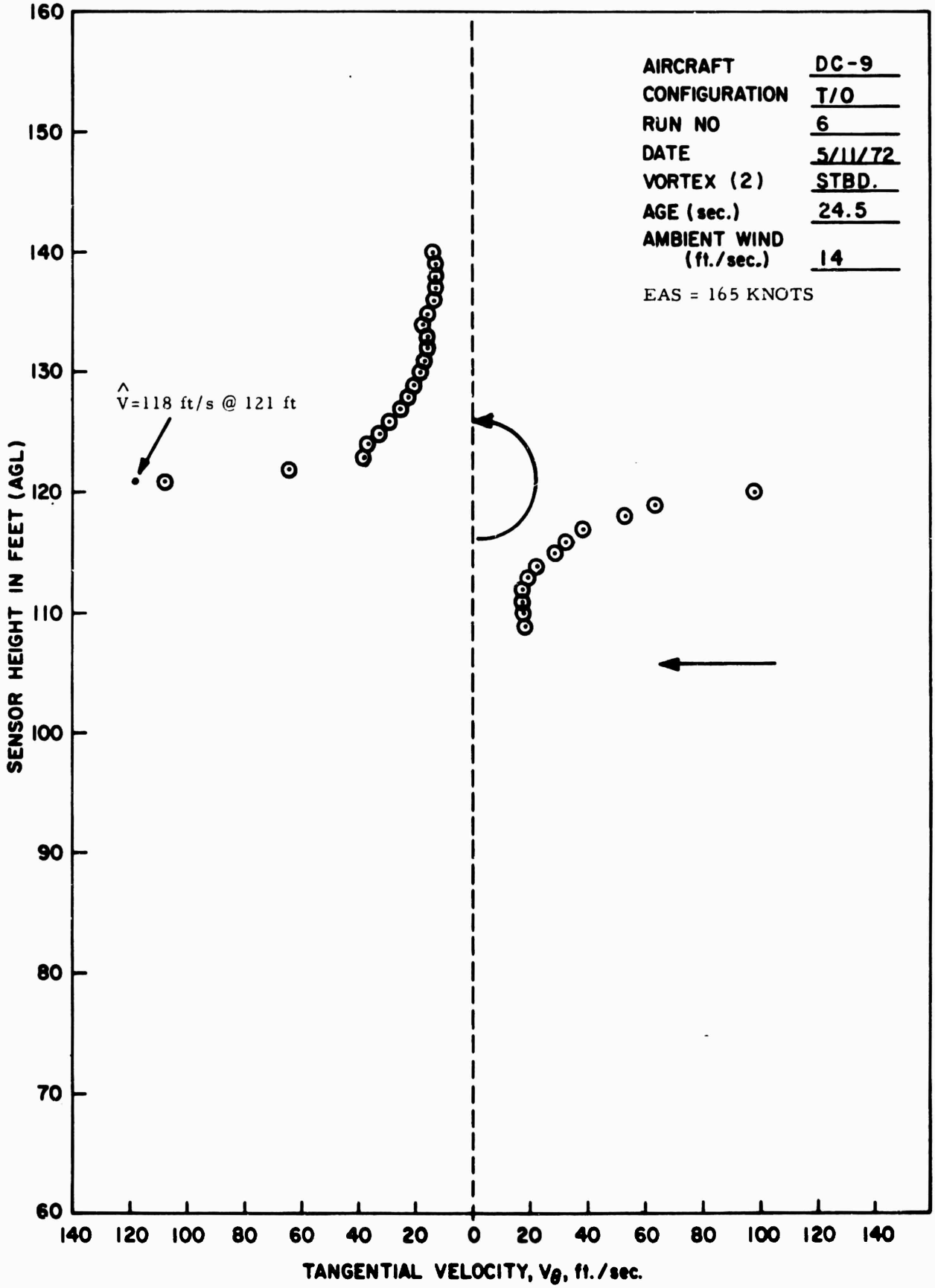
AIRCRAFT DC-9
CONFIGURATION T/O
RUN NO 6
DATE 5/11/72
VORTEX (2) STBD.
AGE (sec.) 24.5
AMBIENT WIND (ft./sec.) 14
EAS = 165 KNOTS
$\hat{V}$=118 ft/s @ 121 ft
SENSOR HEIGHT IN FEET (AGL)
160
150
140
130
120
110
100
90
80
70
60
140 120 100 80 60 40 20 0 20 40 60 80 100 120 140
TANGENTIAL VELOCITY, V_θ, ft./sec.

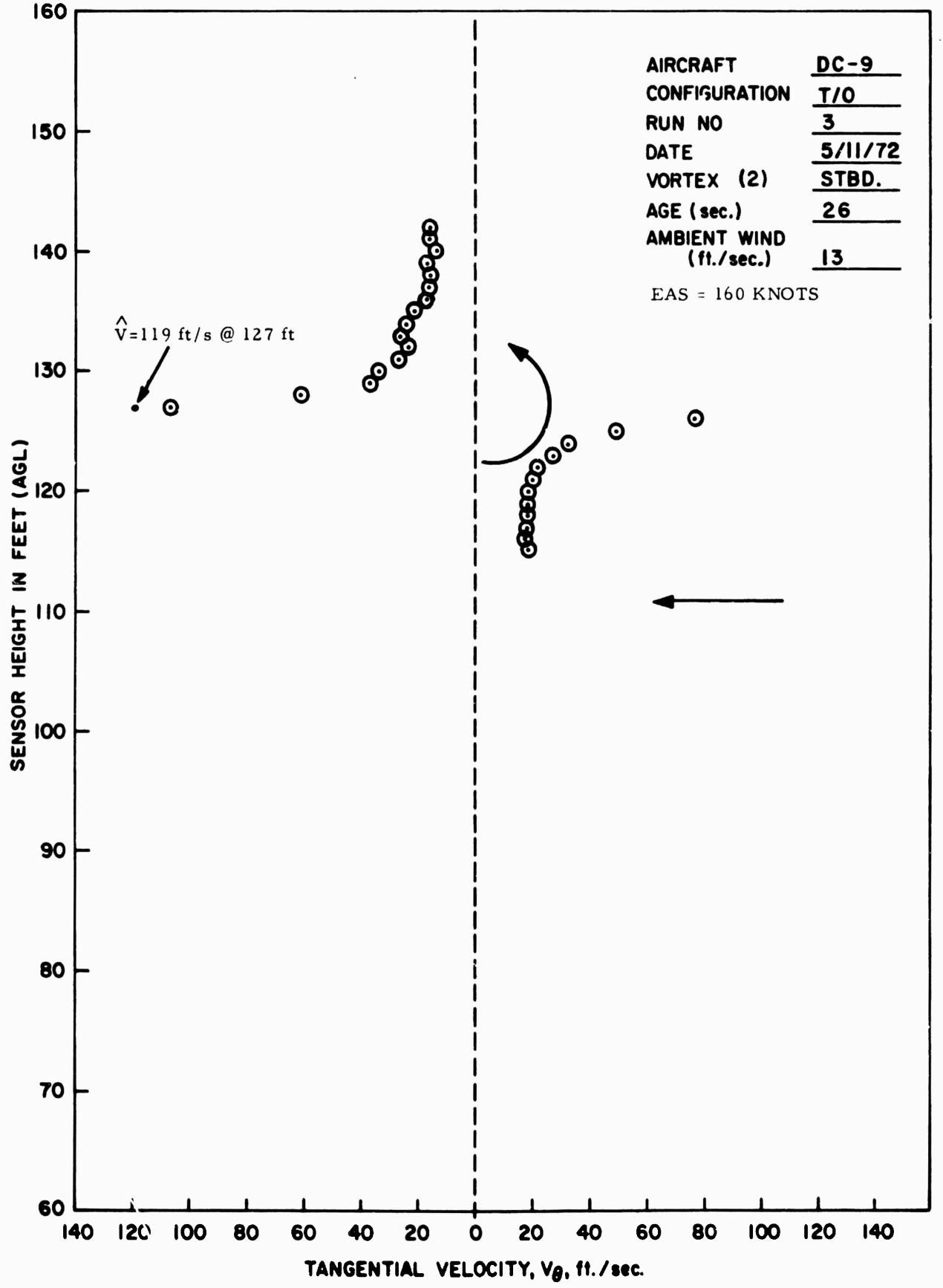
AIRCRAFT DC-9
CONFIGURATION T/O
RUN NO 3
DATE 5/11/72
VORTEX (2) STBD.
AGE (sec.) 26
AMBIENT WIND (ft./sec.) 13
EAS = 160 KNOTS
$\hat{V}$=119 ft/s @ 127 ft
SENSOR HEIGHT IN FEET (AGL)
160
150
140
130
120
110
100
90
80
70
60
140 120 100 80 60 40 20 0 20 40 60 80 100 120 140
TANGENTIAL VELOCITY, V_θ, ft./sec.

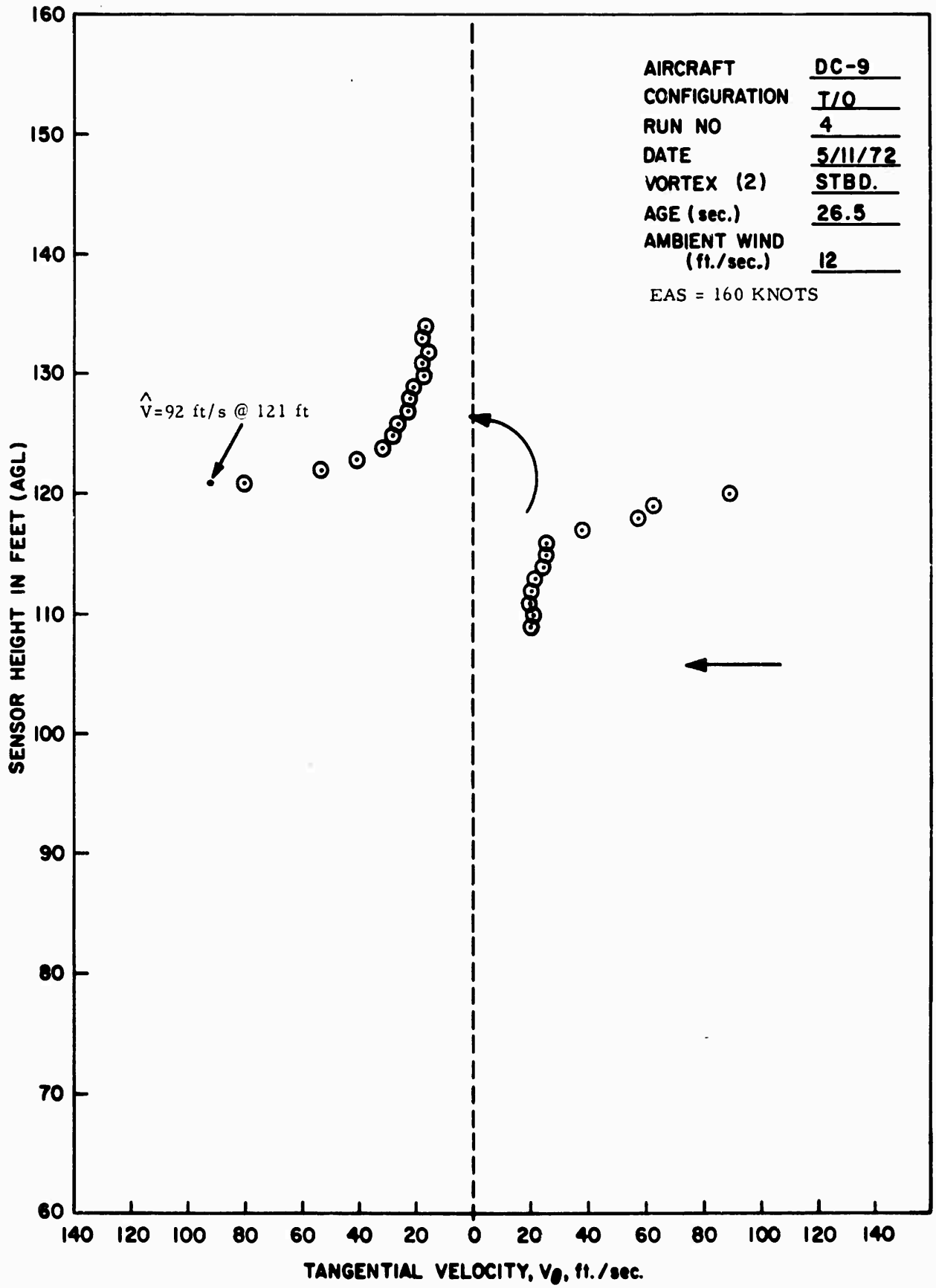
AIRCRAFT DC-9
CONFIGURATION T/O
RUN NO 4
DATE 5/11/72
VORTEX (2) STBD.
AGE (sec.) 26.5
AMBIENT WIND (ft./sec.) 12
EAS = 160 KNOTS
$\hat{V}$=92 ft/s @ 121 ft
SENSOR HEIGHT IN FEET (AGL)
160
150
140
130
120
110
100
90
80
70
60
140 120 100 80 60 40 20 0 20 40 60 80 100 120 140
TANGENTIAL VELOCITY, V_θ, ft./sec.

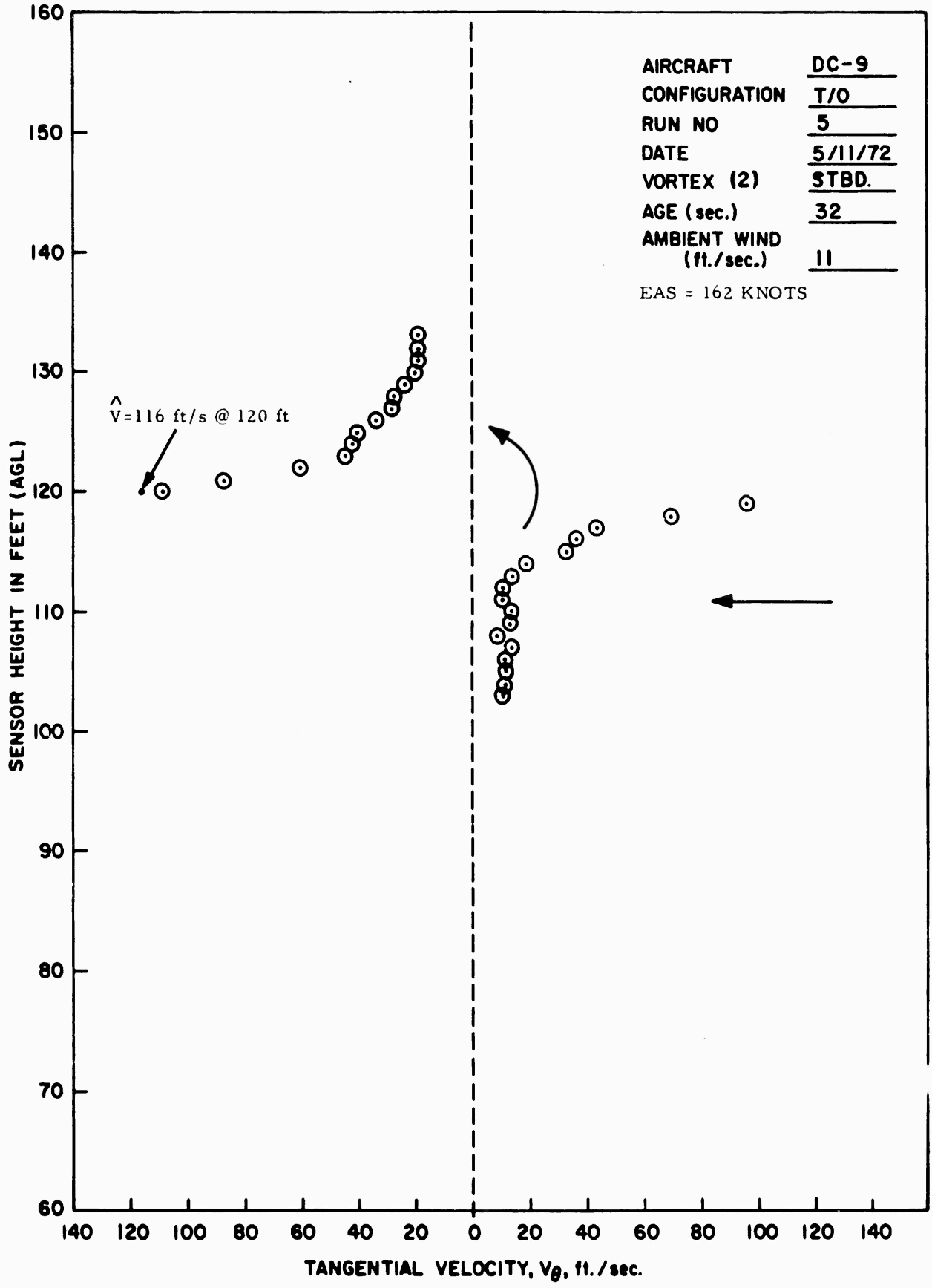
AIRCRAFT DC-9
CONFIGURATION T/O
RUN NO 5
DATE 5/11/72
VORTEX (2) STBD.
AGE (sec.) 32
AMBIENT WIND (ft./sec.) 11
EAS = 162 KNOTS
$\hat{V}$=116 ft/s @ 120 ft
SENSOR HEIGHT IN FEET (AGL)
160
150
140
130
120
110
100
90
80
70
60
140 120 100 80 60 40 20 0 20 40 60 80 100 120 140
TANGENTIAL VELOCITY, V_θ, ft./sec.

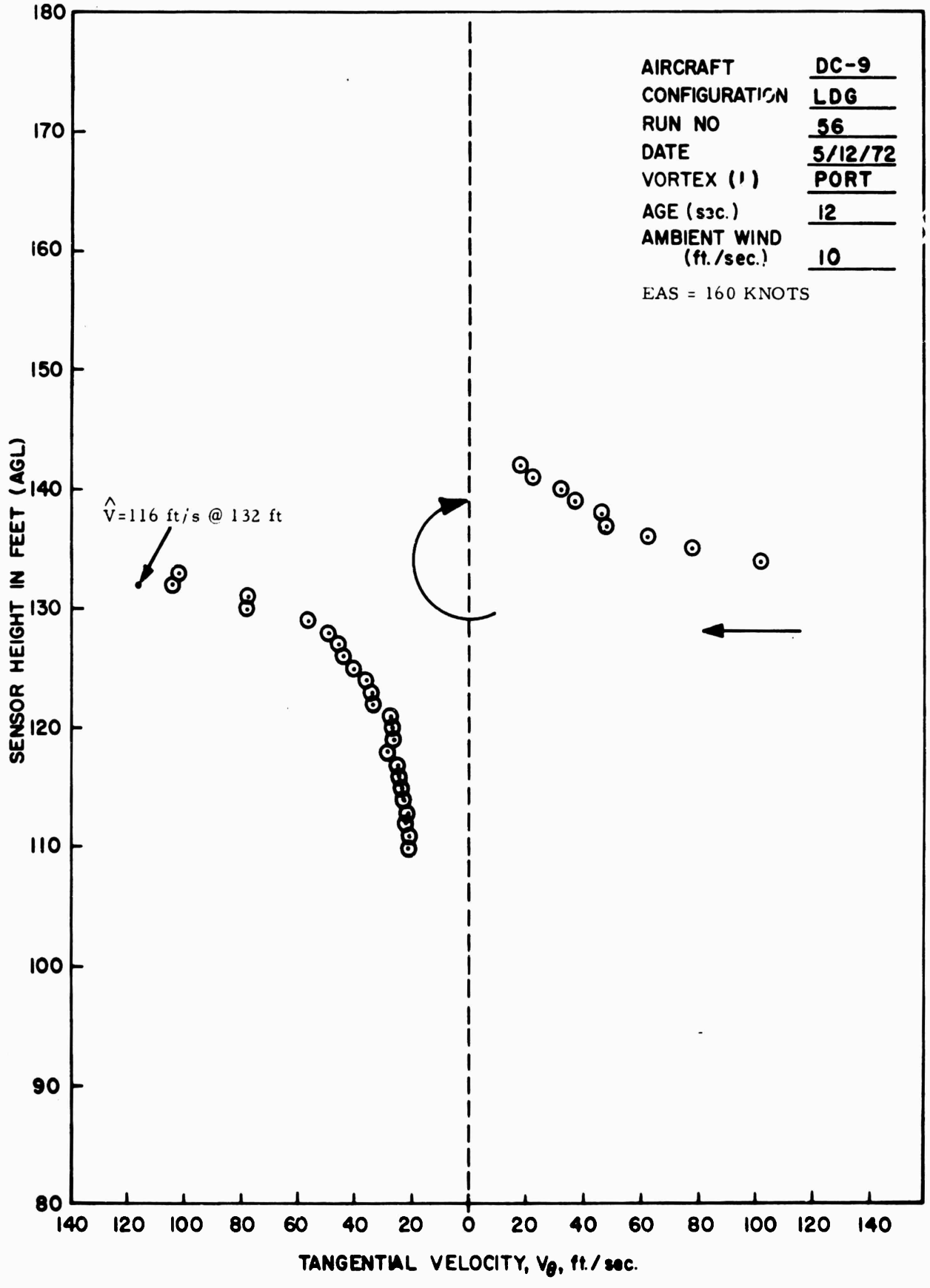
AIRCRAFT DC-9
CONFIGURATION LDG
RUN NO 56
DATE 5/12/72
VORTEX (1) PORT
AGE (sec.) 12
AMBIENT WIND (ft./sec.) 10
EAS = 160 KNOTS
$\hat{V}$=116 ft/s @ 132 ft
SENSOR HEIGHT IN FEET (AGL)
180
170
160
150
140
130
120
110
100
90
80
140 120 100 80 60 40 20 0 20 40 60 80 100 120 140
TANGENTIAL VELOCITY, V_θ, ft./sec.

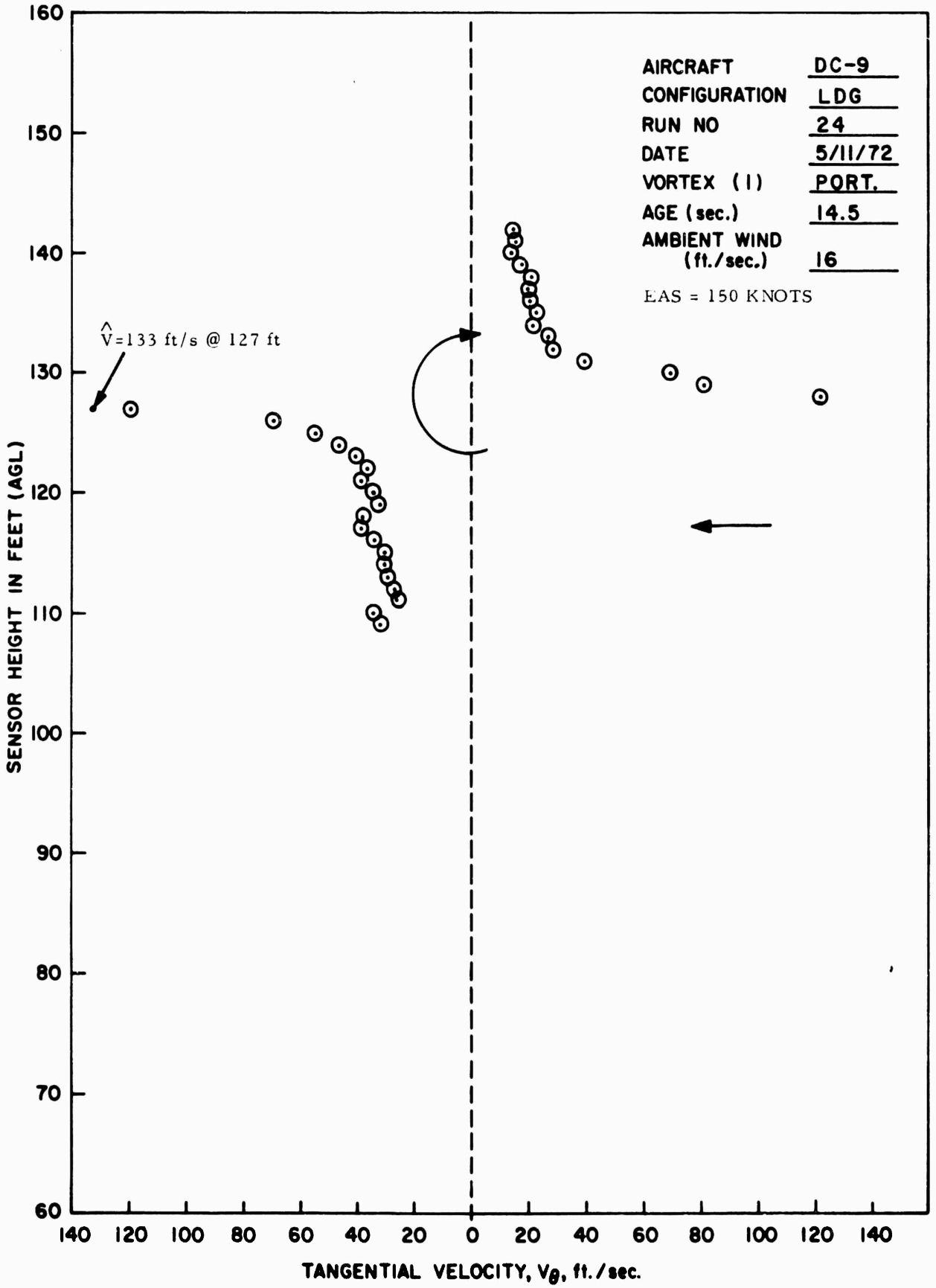
AIRCRAFT DC-9
CONFIGURATION LDG
RUN NO 24
DATE 5/11/72
VORTEX (1) PORT.
AGE (sec.) 14.5
AMBIENT WIND (ft./sec.) 16
EAS = 150 KNOTS
$\hat{V}$=133 ft/s @ 127 ft
SENSOR HEIGHT IN FEET (AGL)
160
150
140
130
120
110
100
90
80
70
60
140 120 100 80 60 40 20 0 20 40 60 80 100 120 140
TANGENTIAL VELOCITY, V_θ, ft./sec.

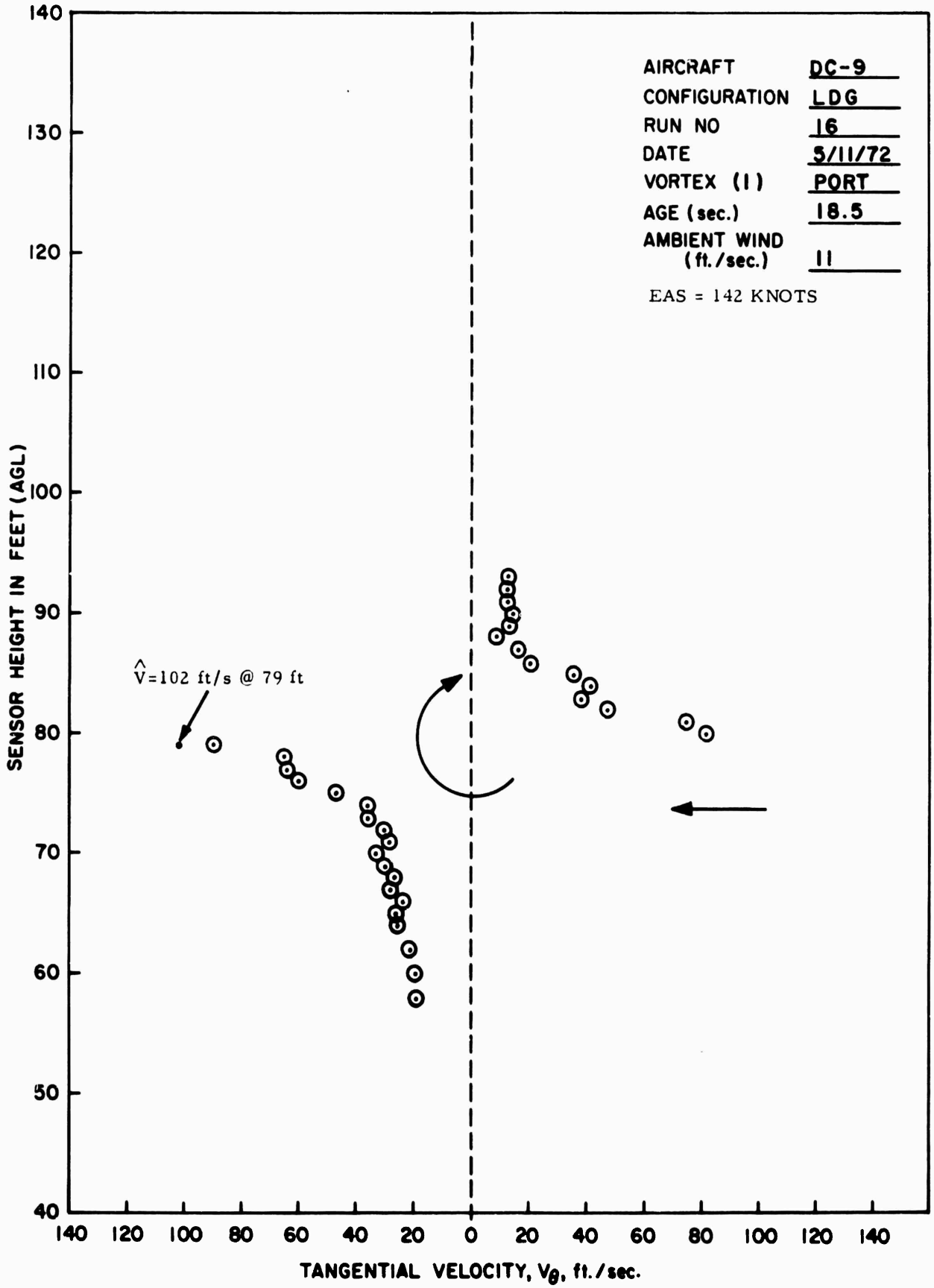
AIRCRAFT DC-9
CONFIGURATION LDG
RUN NO 16
DATE 5/11/72
VORTEX (1) PORT
AGE (sec.) 18.5
AMBIENT WIND (ft./sec.) 11
EAS = 142 KNOTS
$\hat{V}$=102 ft/s @ 79 ft
SENSOR HEIGHT IN FEET (AGL)
140
130
120
110
100
90
80
70
60
50
40
140 120 100 80 60 40 20 0 20 40 60 80 100 120 140
TANGENTIAL VELOCITY, V_θ, ft./sec.

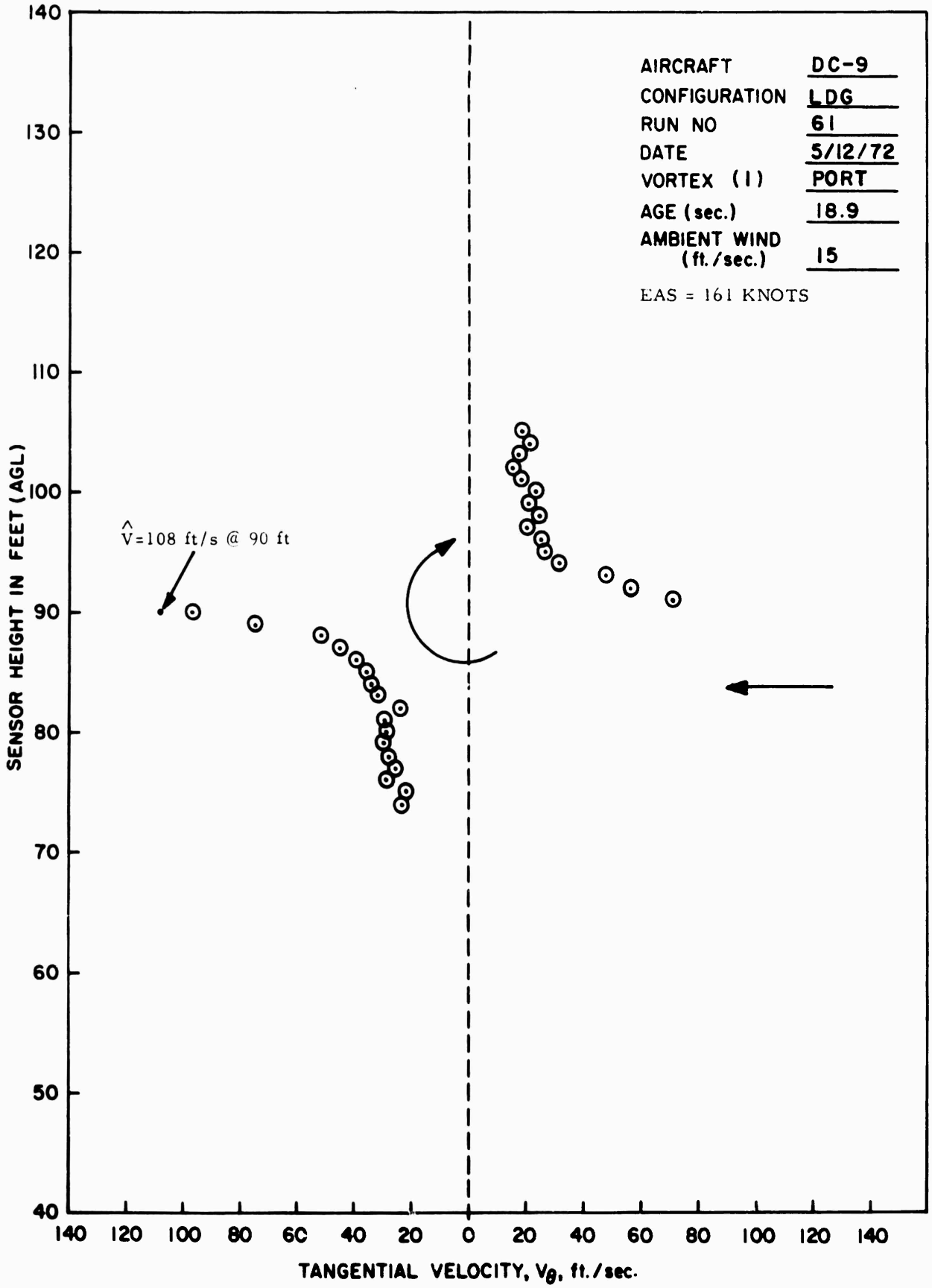
AIRCRAFT DC-9
CONFIGURATION LDG
RUN NO 61
DATE 5/12/72
VORTEX (1) PORT
AGE (sec.) 18.9
AMBIENT WIND (ft./sec.) 15
EAS = 161 KNOTS
$\hat{V}$=108 ft/s @ 90 ft
SENSOR HEIGHT IN FEET (AGL)
140
130
120
110
100
90
80
70
60
50
40
140 120 100 80 60 40 20 0 20 40 60 80 100 120 140
TANGENTIAL VELOCITY, V_θ, ft./sec.

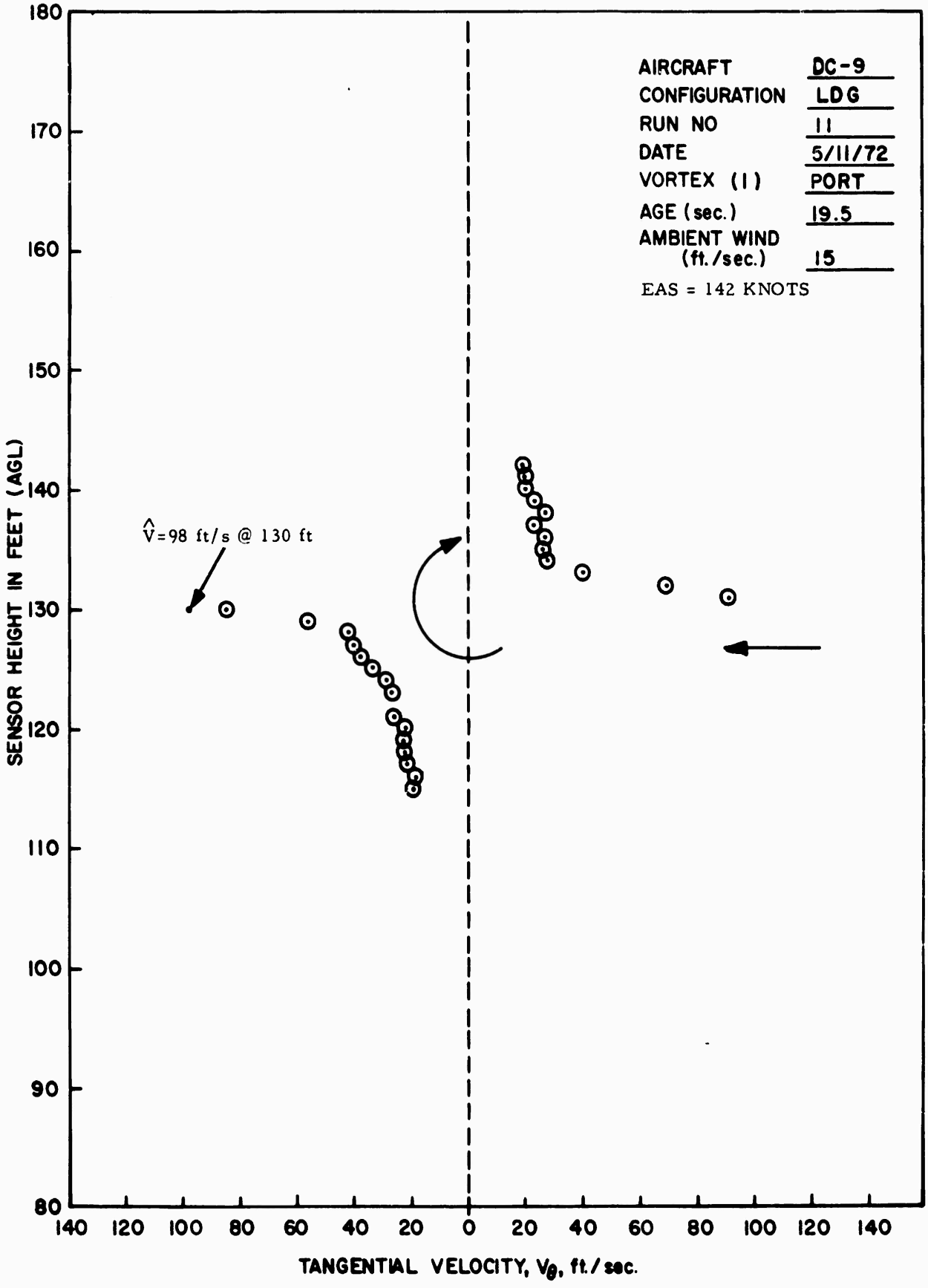
AIRCRAFT DC-9
CONFIGURATION LDG
RUN NO 11
DATE 5/11/72
VORTEX (1) PORT
AGE (sec.) 19.5
AMBIENT WIND (ft./sec.) 15
EAS = 142 KNOTS
$\hat{V}$=98 ft/s @ 130 ft
SENSOR HEIGHT IN FEET (AGL)
180
170
160
150
140
130
120
110
100
90
80
140 120 100 80 60 40 20 0 20 40 60 80 100 120 140
TANGENTIAL VELOCITY, V_θ, ft./sec.

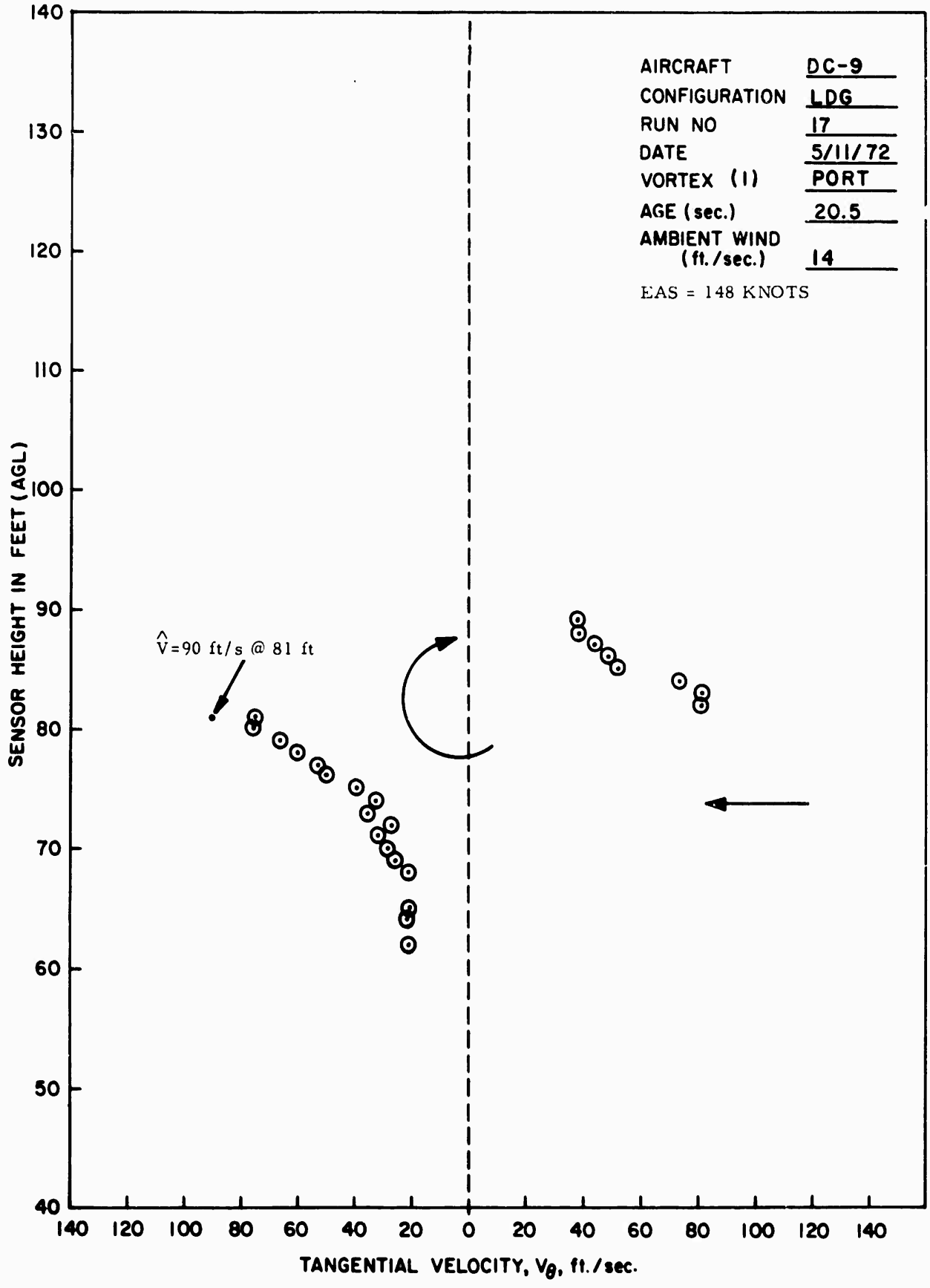
AIRCRAFT DC-9
CONFIGURATION LDG
RUN NO 17
DATE 5/11/72
VORTEX (1) PORT
AGE (sec.) 20.5
AMBIENT WIND (ft./sec.) 14
EAS = 148 KNOTS
$\hat{V}$=90 ft/s @ 81 ft
SENSOR HEIGHT IN FEET (AGL)
140
130
120
110
100
90
80
70
60
50
40
140 120 100 80 60 40 20 0 20 40 60 80 100 120 140
TANGENTIAL VELOCITY, V_θ, ft./sec.

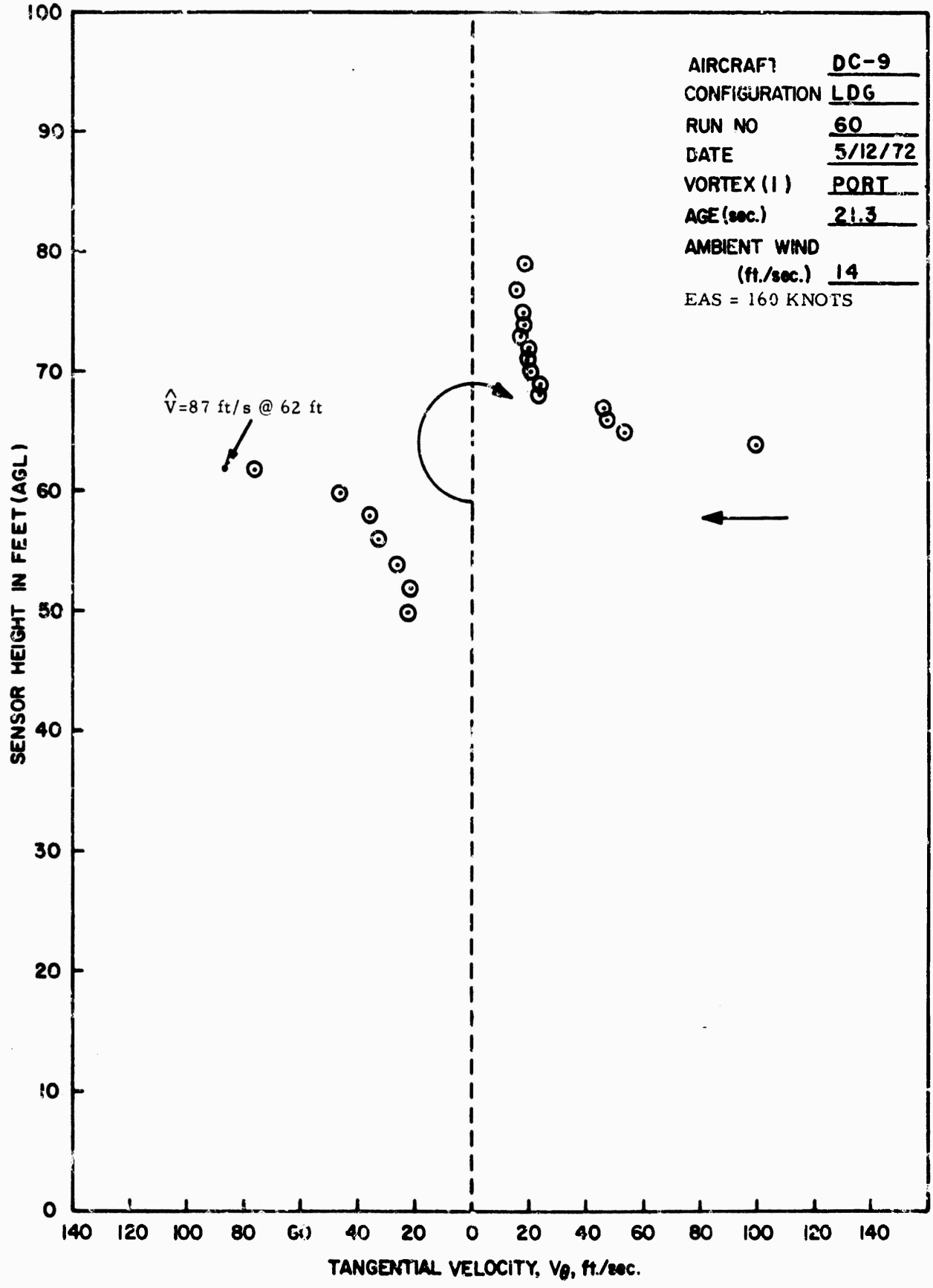
AIRCRAFT DC-9
CONFIGURATION LDG
RUN NO 60
DATE 5/12/72
VORTEX (1) PORT
AGE (sec.) 21.3
AMBIENT WIND (ft./sec.) 14
EAS = 160 KNOTS
$\hat{V}$=87 ft/s @ 62 ft
SENSOR HEIGHT IN FEET (AGL)
TANGENTIAL VELOCITY, V_θ, ft./sec.
100
90
80
70
60
50
40
30
20
10
0
140 120 100 80 60 40 20 0 20 40 60 80 100 120 140

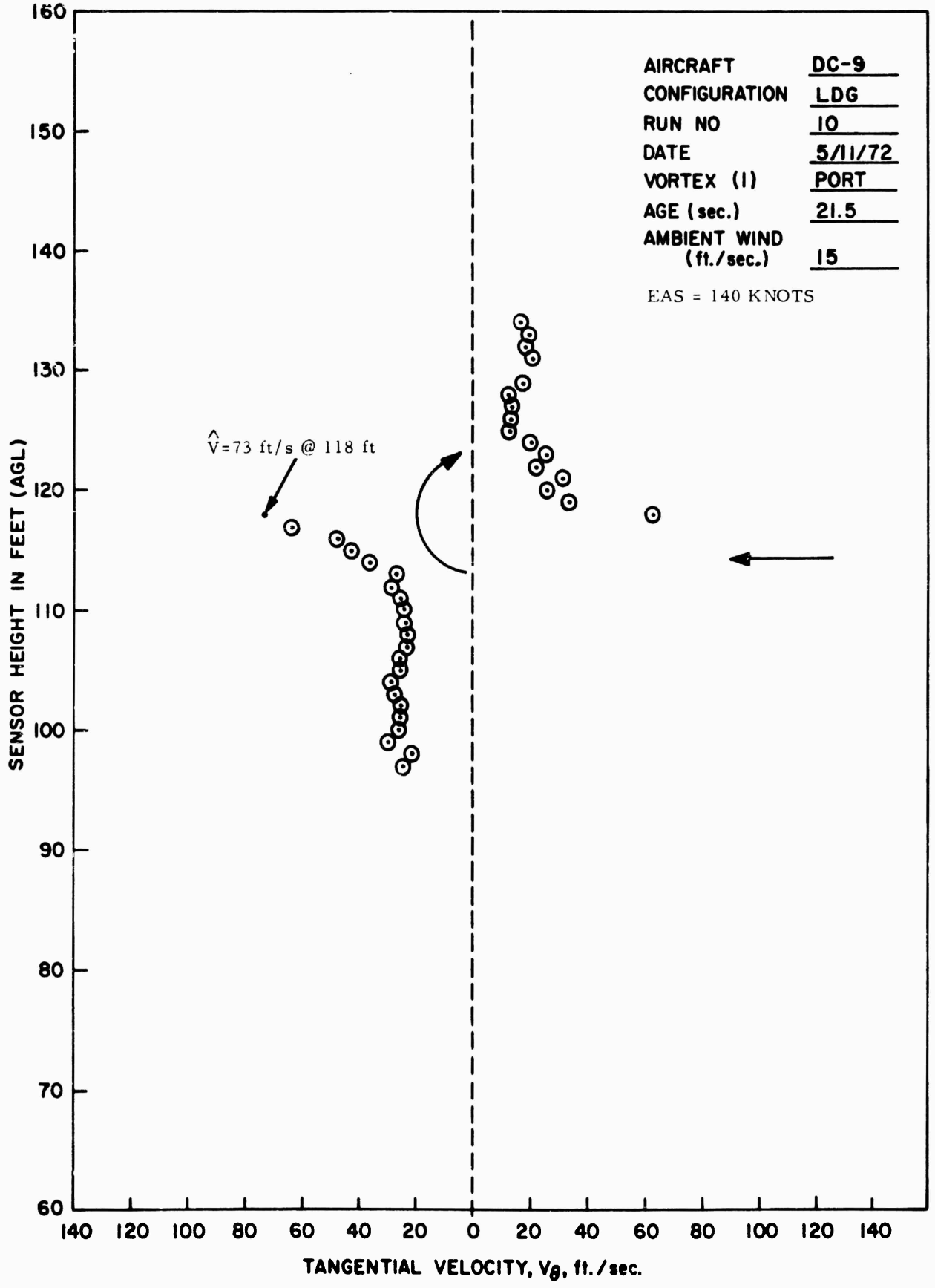
AIRCRAFT DC-9
CONFIGURATION LDG
RUN NO 10
DATE 5/11/72
VORTEX (1) PORT
AGE (sec.) 21.5
AMBIENT WIND (ft./sec.) 15
EAS = 140 KNOTS
$\hat{V}$=73 ft/s @ 118 ft
SENSOR HEIGHT IN FEET (AGL)
160
150
140
130
120
110
100
90
80
70
60
140 120 100 80 60 40 20 0 20 40 60 80 100 120 140
TANGENTIAL VELOCITY, V_θ, ft./sec.

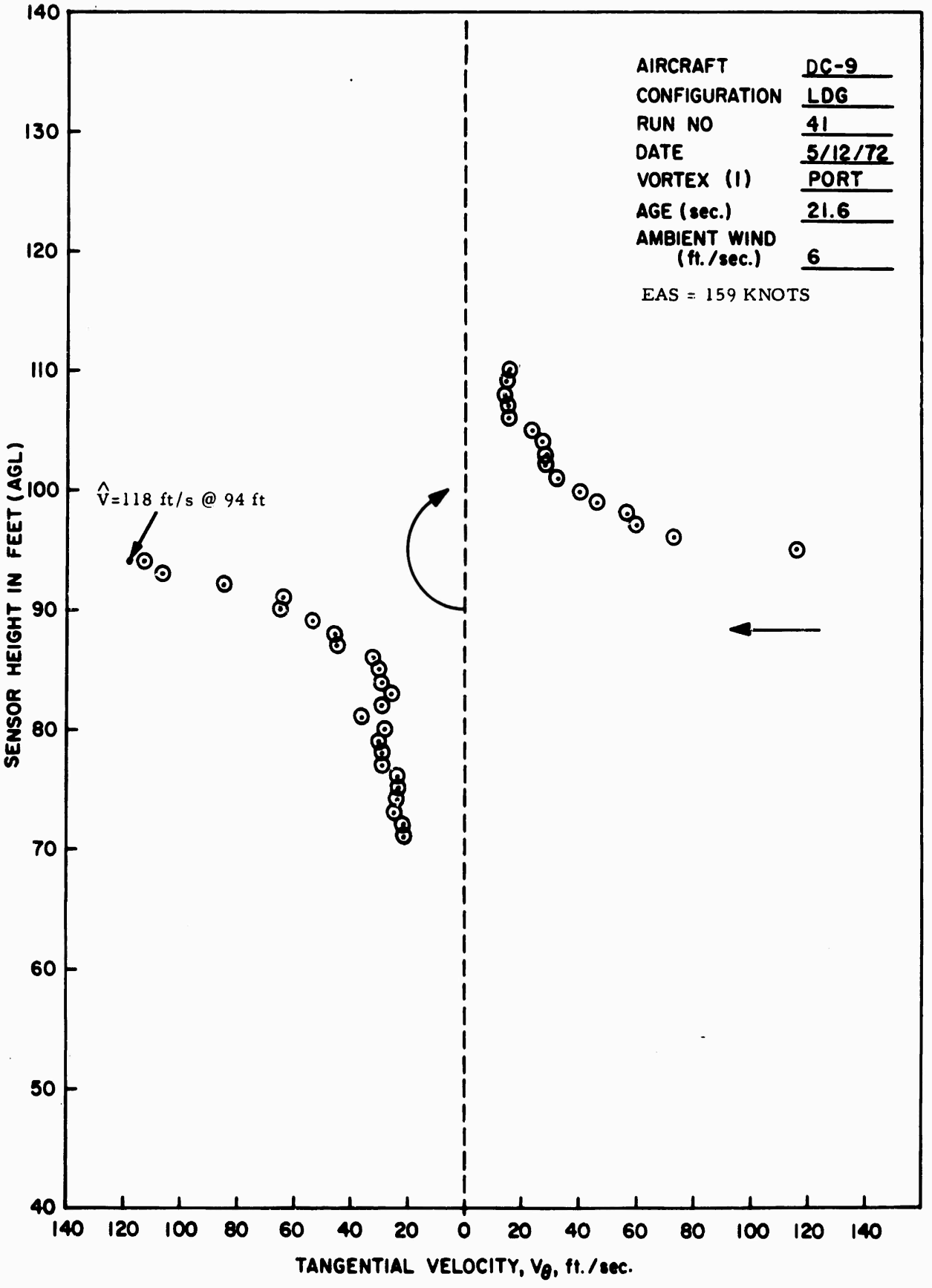
AIRCRAFT DC-9
CONFIGURATION LDG
RUN NO 41
DATE 5/12/72
VORTEX (1) PORT
AGE (sec.) 21.6
AMBIENT WIND (ft./sec.) 6
EAS = 159 KNOTS
$\hat{V}$=118 ft/s @ 94 ft
SENSOR HEIGHT IN FEET (AGL)
140
130
120
110
100
90
80
70
60
50
40
140 120 100 80 60 40 20 0 20 40 60 80 100 120 140
TANGENTIAL VELOCITY, V_θ, ft./sec.

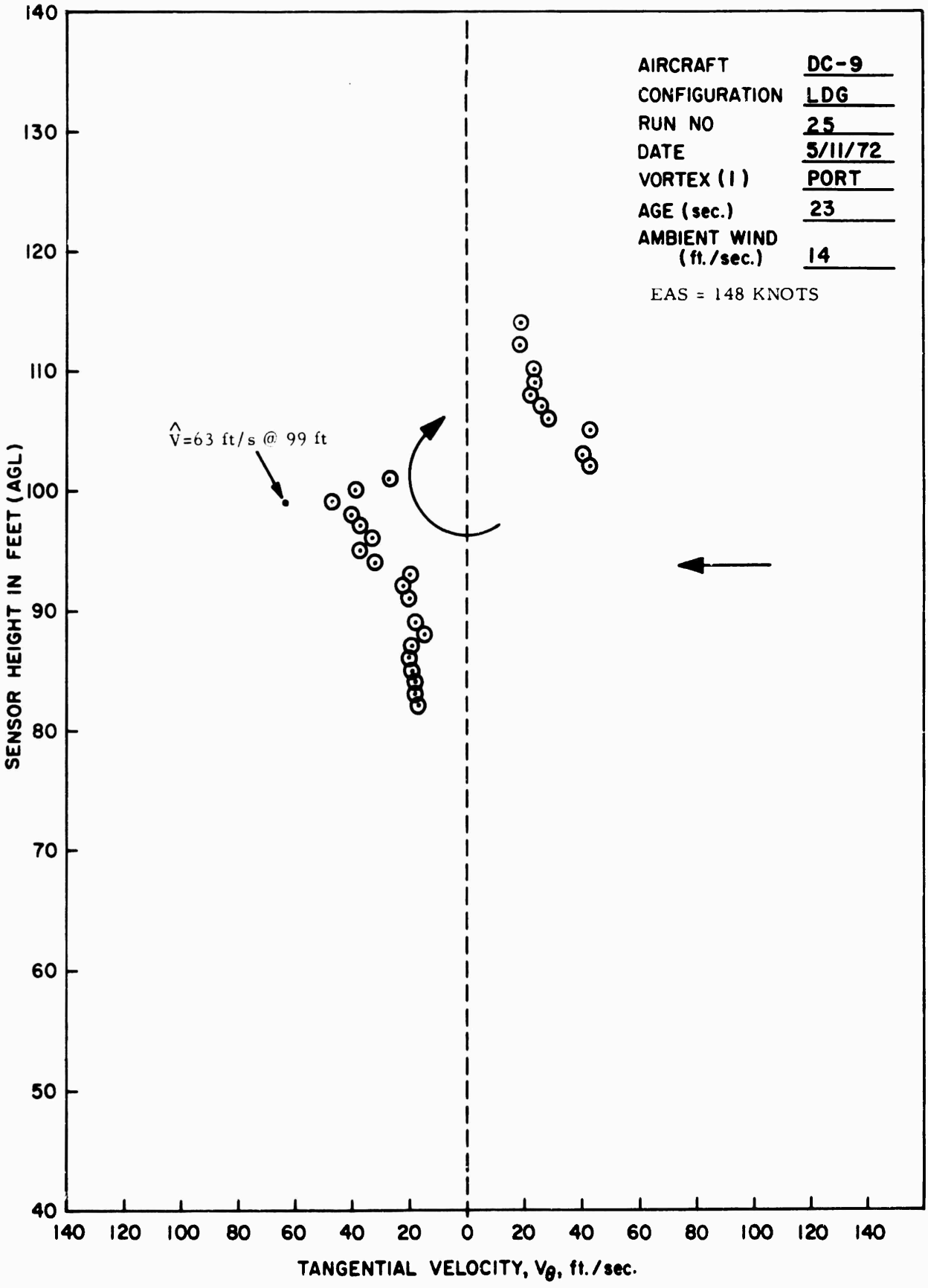
AIRCRAFT DC-9
CONFIGURATION LDG
RUN NO 25
DATE 5/11/72
VORTEX (1) PORT
AGE (sec.) 23
AMBIENT WIND (ft./sec.) 14
EAS = 148 KNOTS
$\hat{V}$=63 ft/s @ 99 ft
SENSOR HEIGHT IN FEET (AGL)
140
130
120
110
100
90
80
70
60
50
40
140 120 100 80 60 40 20 0 20 40 60 80 100 120 140
TANGENTIAL VELOCITY, V_θ, ft./sec.

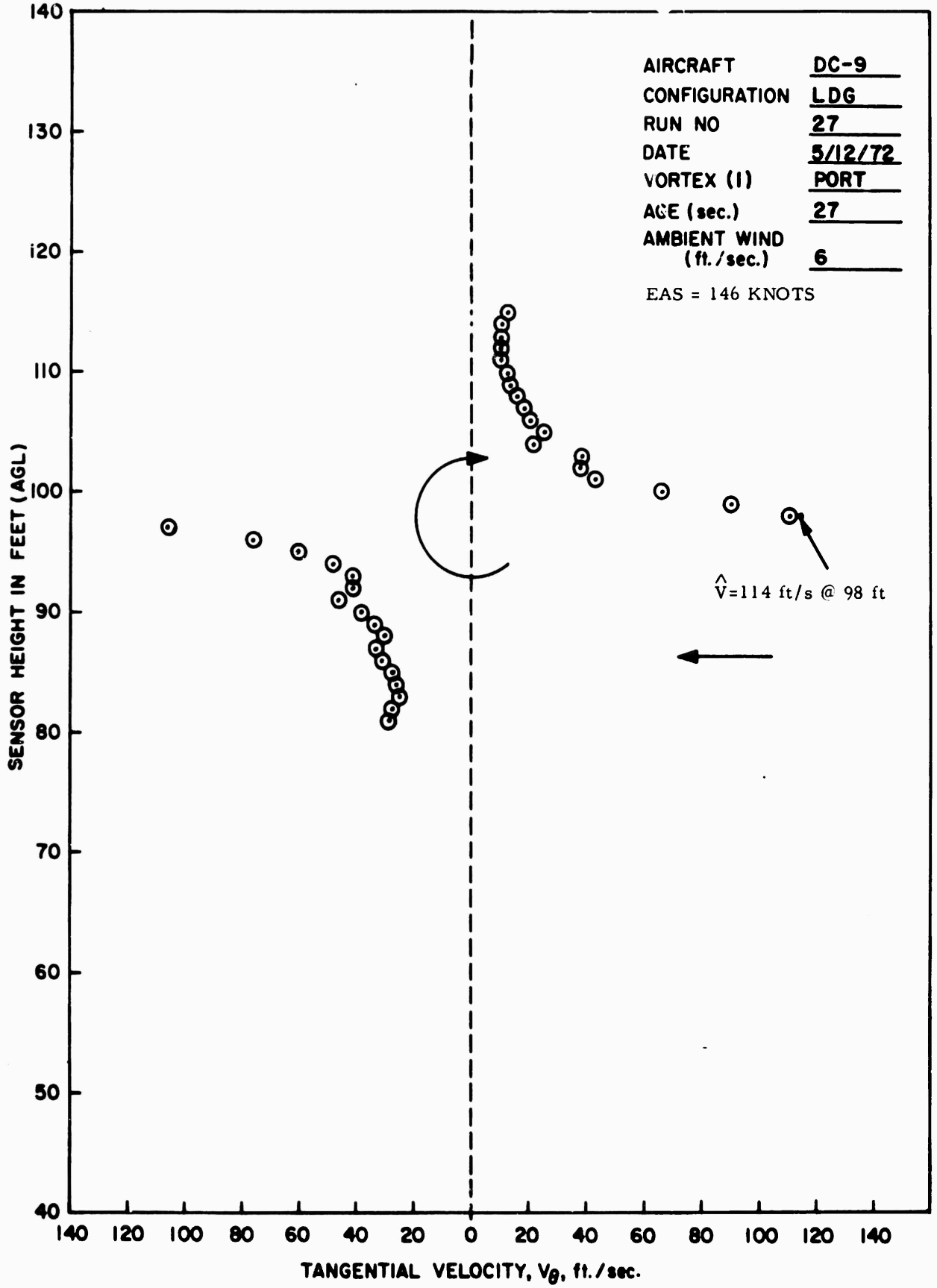
AIRCRAFT DC-9
CONFIGURATION LDG
RUN NO 27
DATE 5/12/72
VORTEX (1) PORT
AGE (sec.) 27
AMBIENT WIND (ft./sec.) 6
EAS = 146 KNOTS
$\hat{V}$=114 ft/s @ 98 ft
SENSOR HEIGHT IN FEET (AGL)
140
130
120
110
100
90
80
70
60
50
40
140 120 100 80 60 40 20 0 20 40 60 80 100 120 140
TANGENTIAL VELOCITY, V_θ, ft./sec.

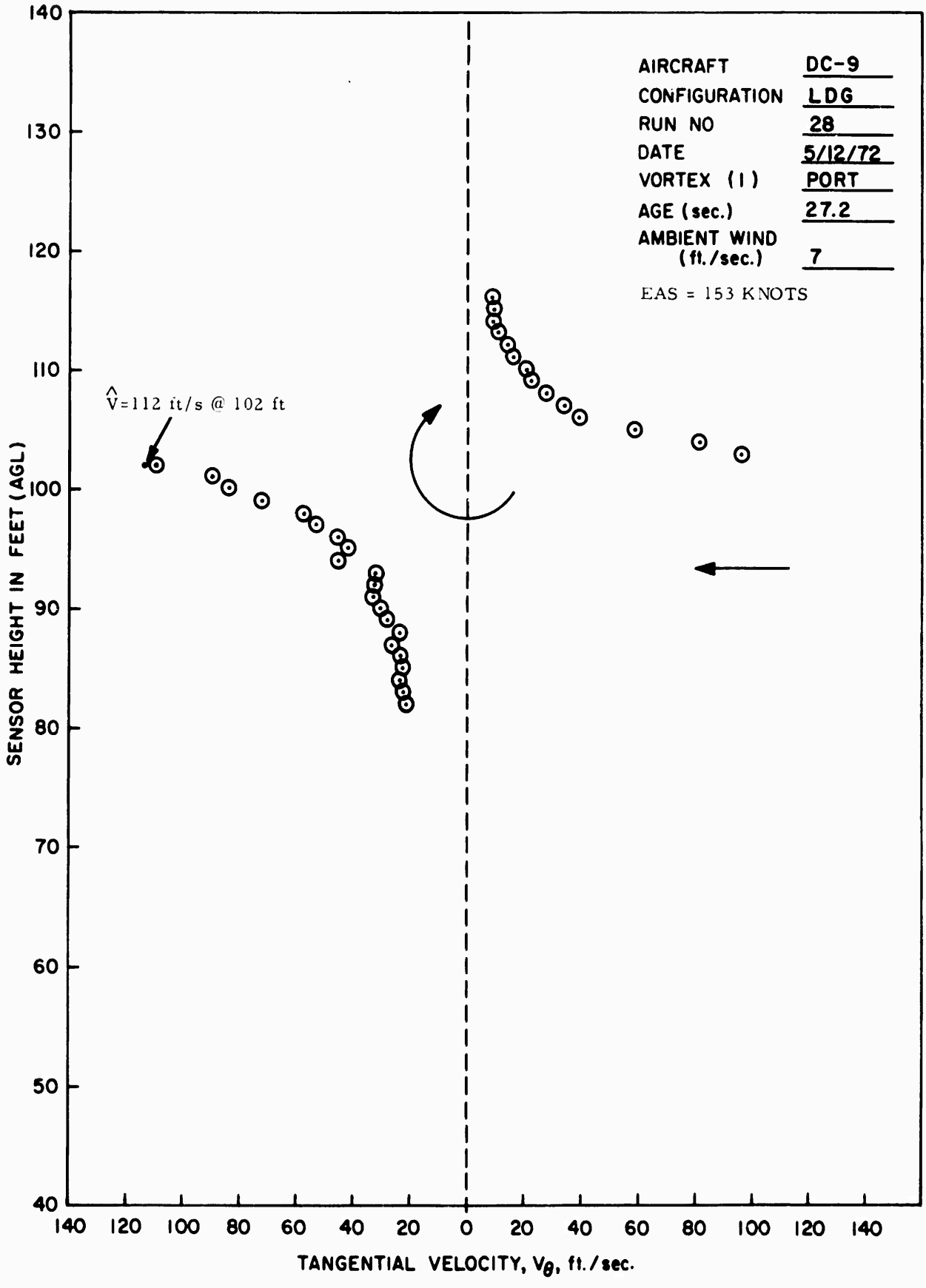
AIRCRAFT DC-9
CONFIGURATION LDG
RUN NO 28
DATE 5/12/72
VORTEX (1) PORT
AGE (sec.) 27.2
AMBIENT WIND (ft./sec.) 7
EAS = 153 KNOTS
$\hat{V}$=112 ft/s @ 102 ft
SENSOR HEIGHT IN FEET (AGL)
140
130
120
110
100
90
80
70
60
50
40
140 120 100 80 60 40 20 0 20 40 60 80 100 120 140
TANGENTIAL VELOCITY, V_θ, ft./sec.

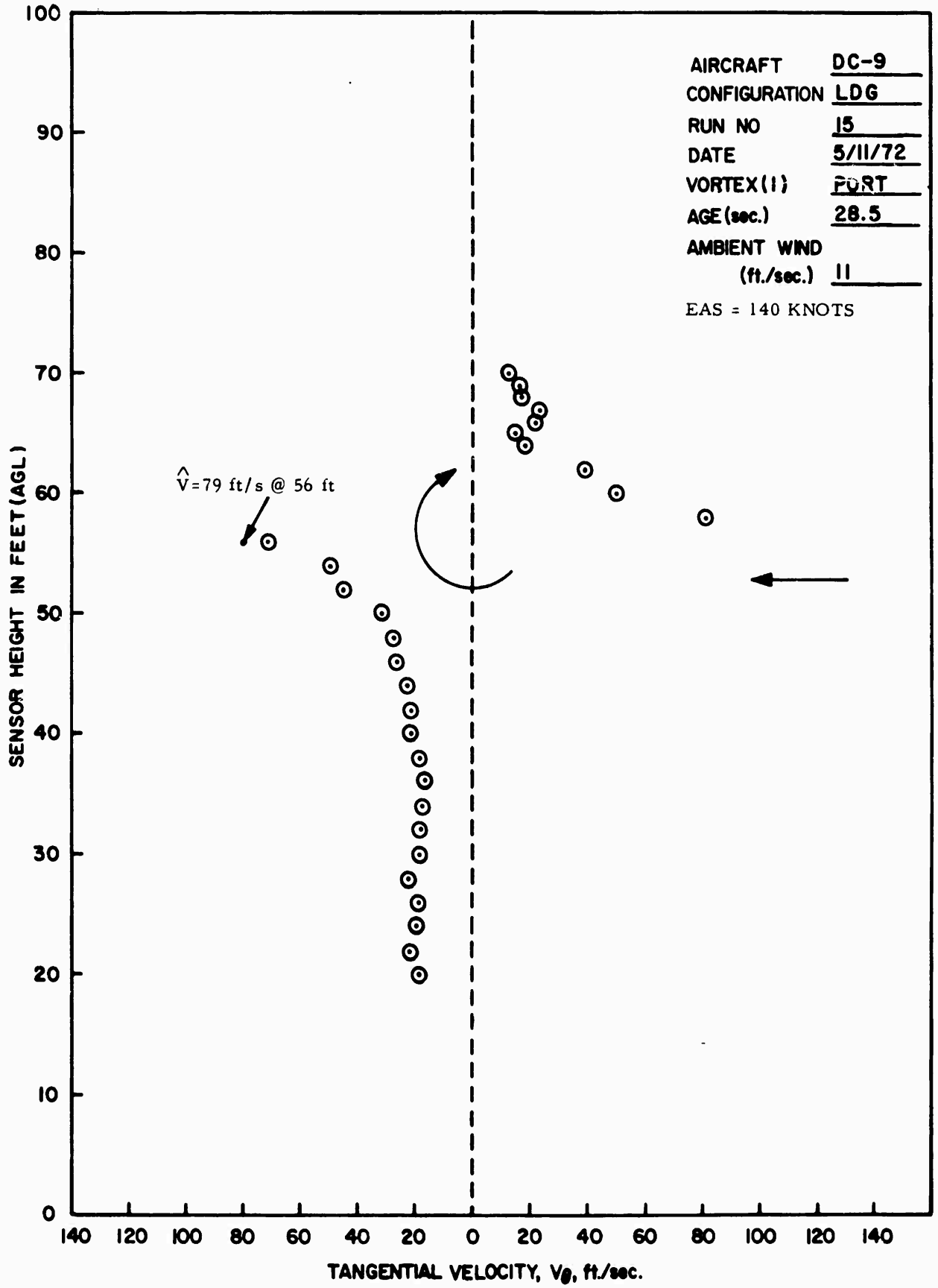
AIRCRAFT DC-9
CONFIGURATION LDG
RUN NO 15
DATE 5/11/72
VORTEX(1) PORT
AGE(sec.) 28.5
AMBIENT WIND (ft./sec.) 11
EAS = 140 KNOTS
$\hat{V}$=79 ft/s @ 56 ft
SENSOR HEIGHT IN FEET(AGL)
TANGENTIAL VELOCITY, V_θ, ft./sec.
100
90
80
70
60
50
40
30
20
10
0
140 120 100 80 60 40 20 0 20 40 60 80 100 120 140

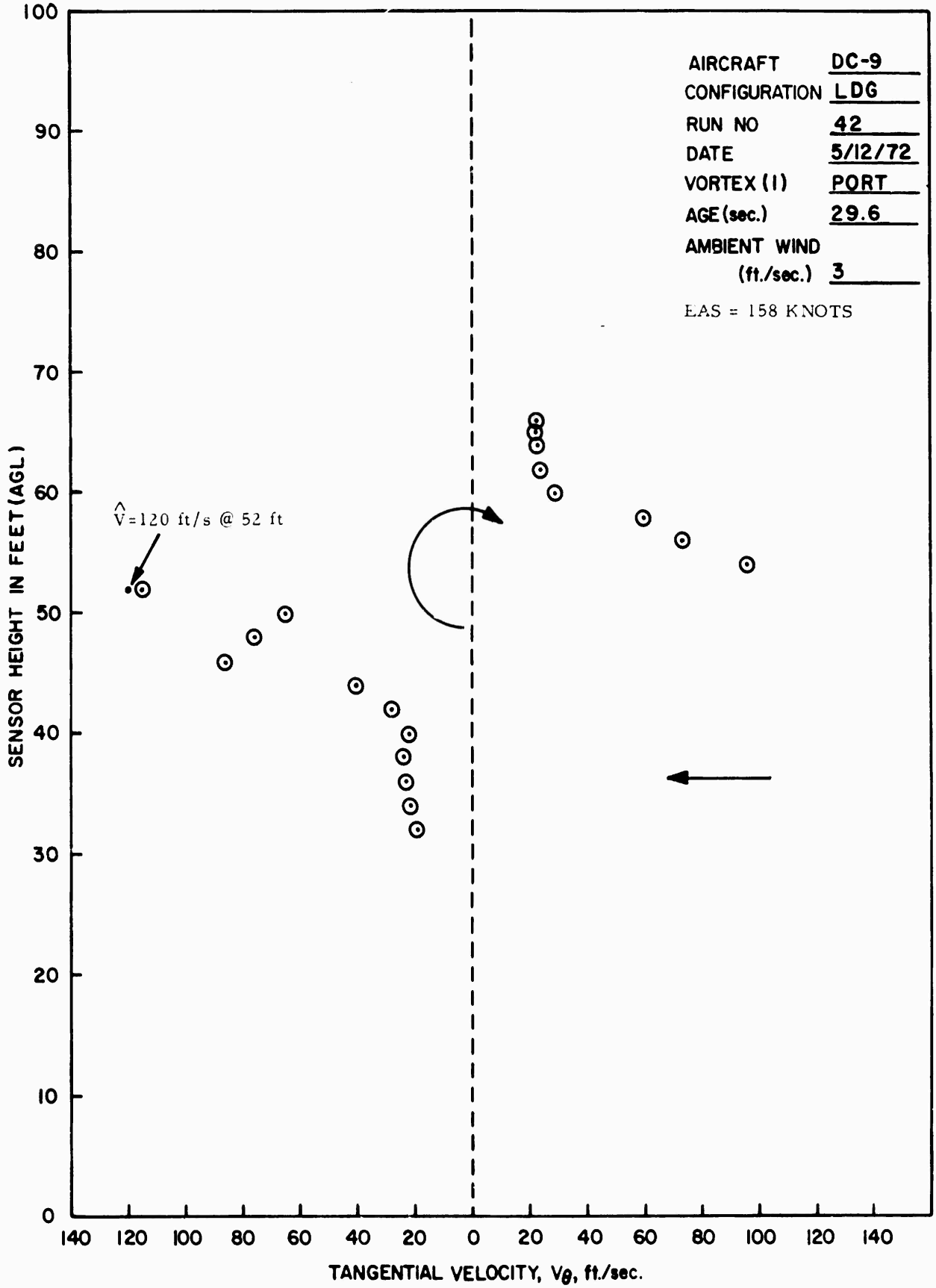
AIRCRAFT DC-9
CONFIGURATION LDG
RUN NO 42
DATE 5/12/72
VORTEX (1) PORT
AGE (sec.) 29.6
AMBIENT WIND (ft./sec.) 3
EAS = 158 KNOTS
$\hat{V}$=120 ft/s @ 52 ft
SENSOR HEIGHT IN FEET (AGL)
TANGENTIAL VELOCITY, V_θ, ft./sec.
100
90
80
70
60
50
40
30
20
10
0
140 120 100 80 60 40 20 0 20 40 60 80 100 120 140

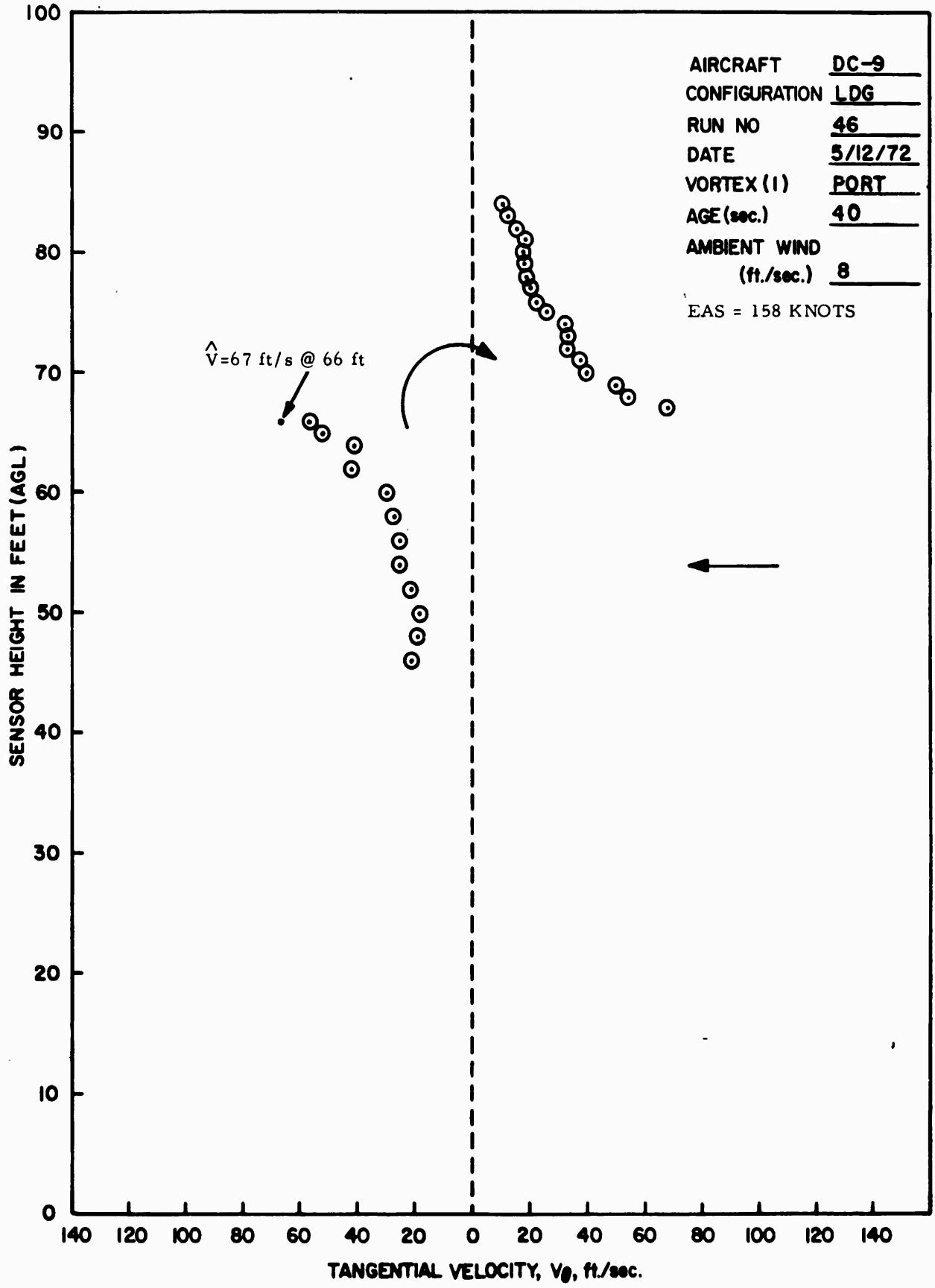
AIRCRAFT DC-9
CONFIGURATION LDG
RUN NO 46
DATE 5/12/72
VORTEX (1) PORT
AGE (sec.) 40
AMBIENT WIND (ft./sec.) 8
EAS = 158 KNOTS
$\hat{V}$=67 ft/s @ 66 ft
SENSOR HEIGHT IN FEET (AGL)
TANGENTIAL VELOCITY, Vθ, ft./sec.
100
90
80
70
60
50
40
30
20
10
0
140 120 100 80 60 40 20 0 20 40 60 80 100 120 140

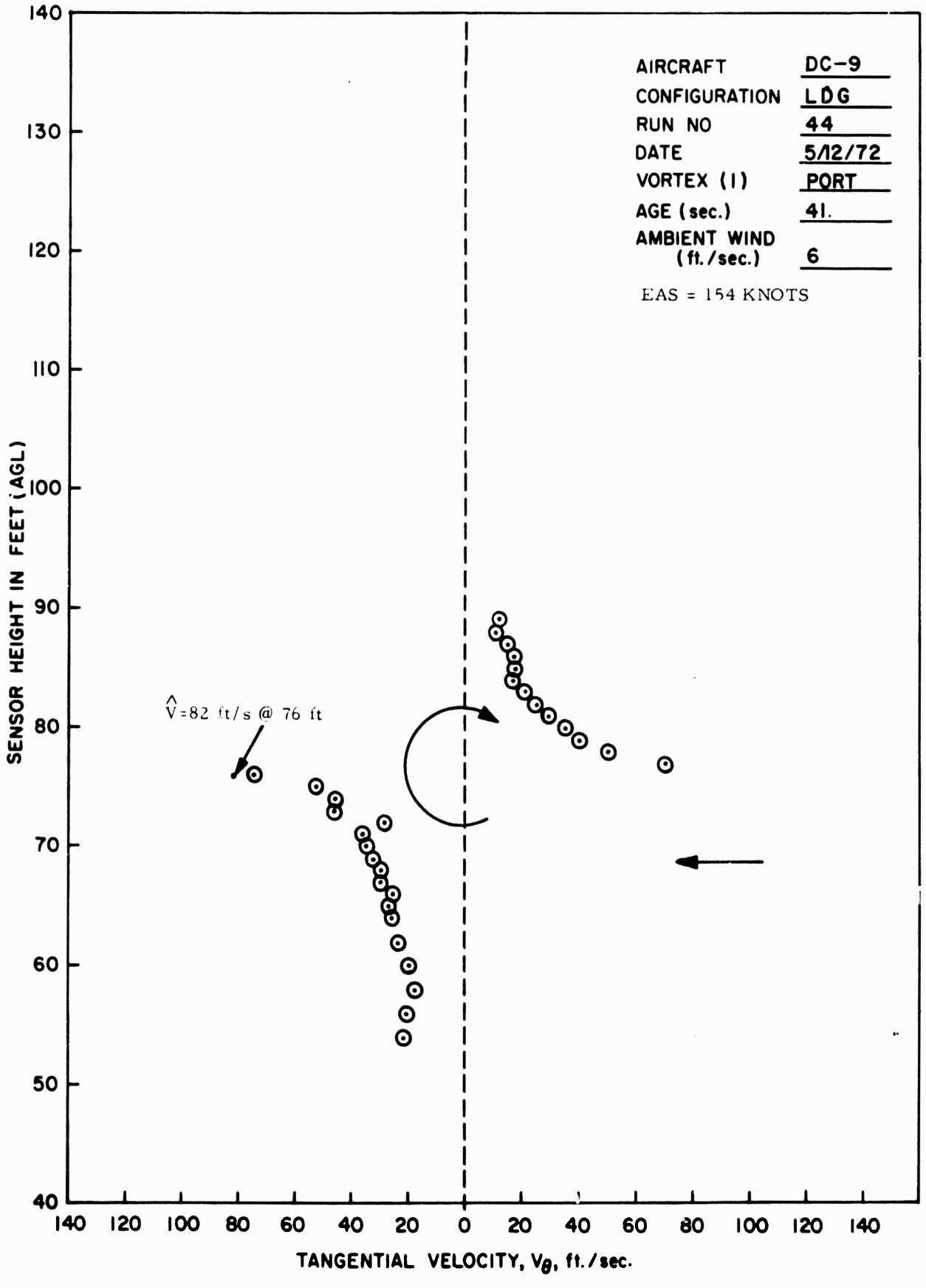
AIRCRAFT DC-9
CONFIGURATION LDG
RUN NO 44
DATE 5/12/72
VORTEX (1) PORT
AGE (sec.) 41.
AMBIENT WIND (ft./sec.) 6
EAS = 154 KNOTS
$\hat{V}$=82 ft/s @ 76 ft
SENSOR HEIGHT IN FEET (AGL)
140
130
120
110
100
90
80
70
60
50
40
140 120 100 80 60 40 20 0 20 40 60 80 100 120 140
TANGENTIAL VELOCITY, V_θ, ft./sec.

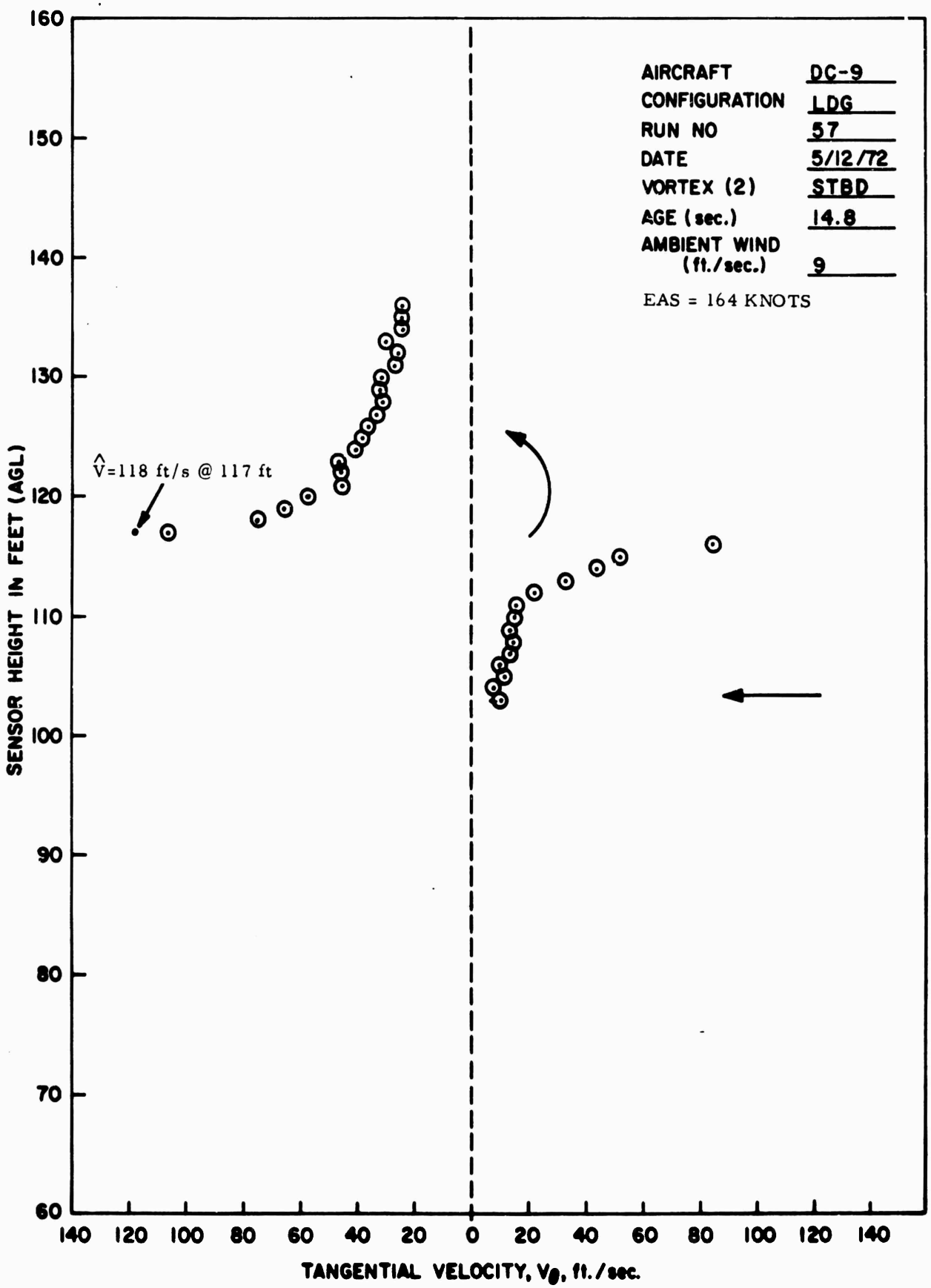
AIRCRAFT DC-9
CONFIGURATION LDG
RUN NO 57
DATE 5/12/72
VORTEX (2) STBD
AGE (sec.) 14.8
AMBIENT WIND (ft./sec.) 9
EAS = 164 KNOTS
$\hat{V}$=118 ft/s @ 117 ft
SENSOR HEIGHT IN FEET (AGL)
160
150
140
130
120
110
100
90
80
70
60
140 120 100 80 60 40 20 0 20 40 60 80 100 120 140
TANGENTIAL VELOCITY, V_θ, ft./sec.

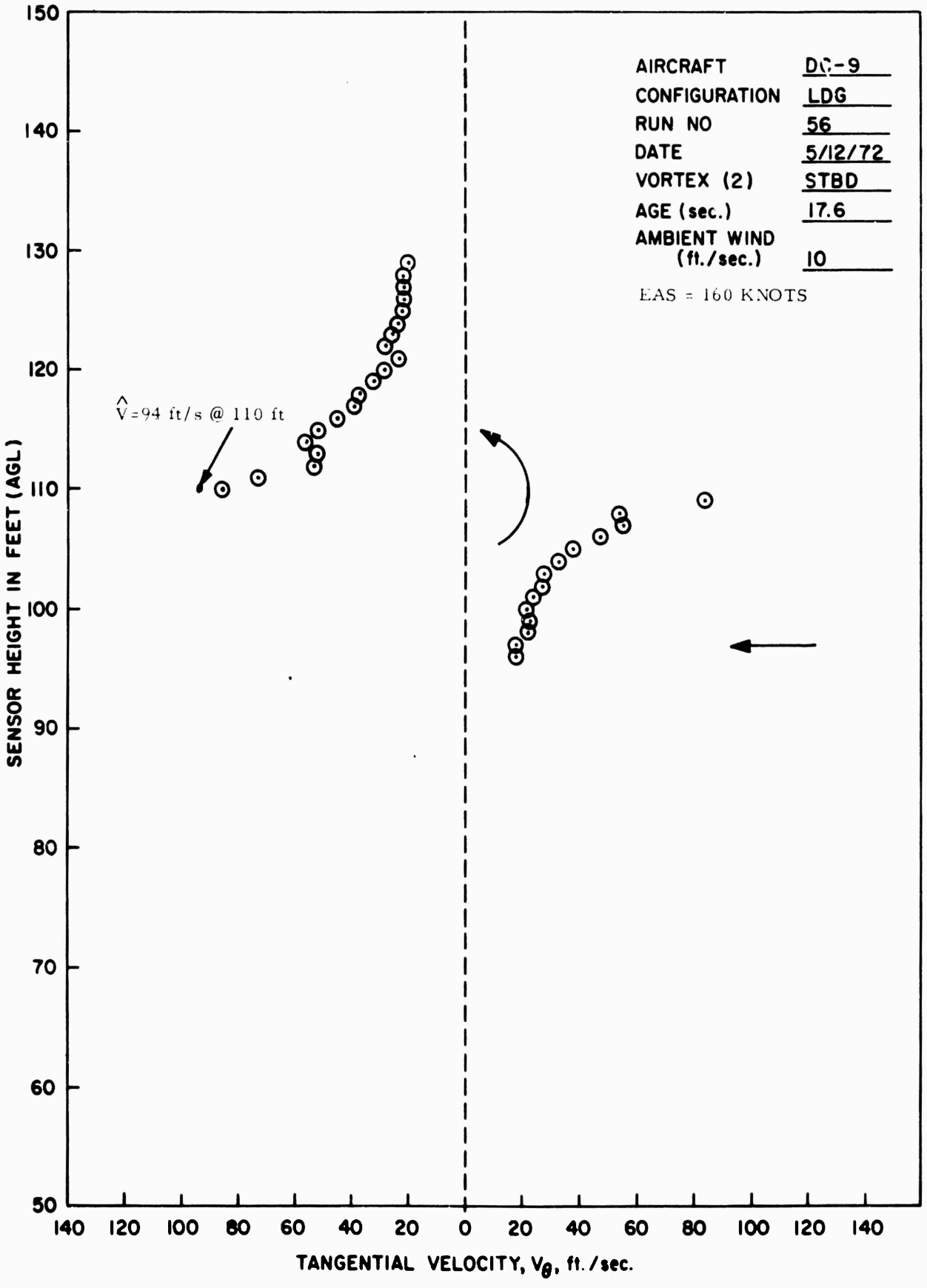
AIRCRAFT DC-9
CONFIGURATION LDG
RUN NO 56
DATE 5/12/72
VORTEX (2) STBD
AGE (sec.) 17.6
AMBIENT WIND (ft./sec.) 10
EAS = 160 KNOTS
$\hat{V}$=94 ft/s @ 110 ft
SENSOR HEIGHT IN FEET (AGL)
150
140
130
120
110
100
90
80
70
60
50
140 120 100 80 60 40 20 0 20 40 60 80 100 120 140
TANGENTIAL VELOCITY, V_θ, ft./sec.

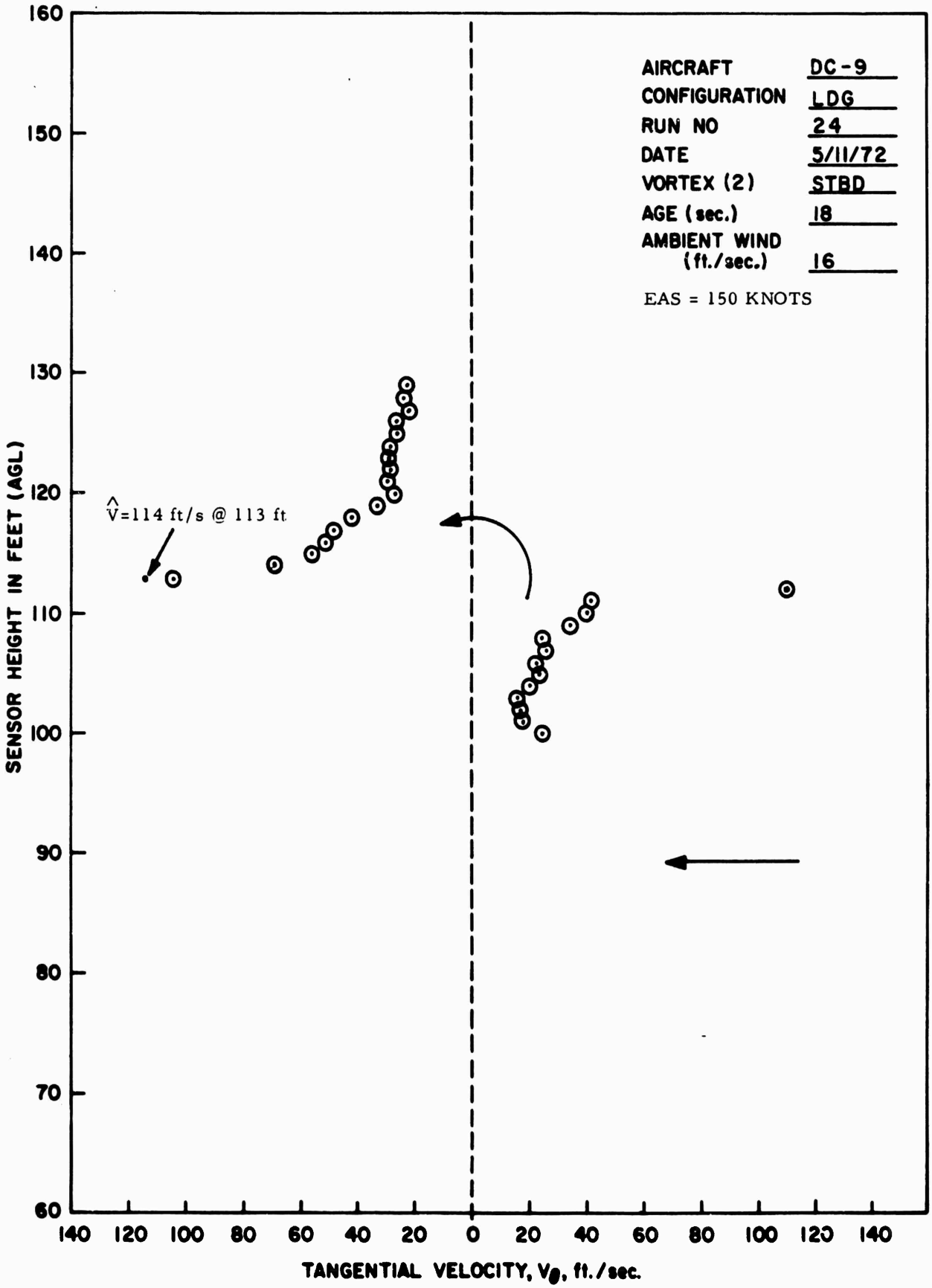
AIRCRAFT DC-9
CONFIGURATION LDG
RUN NO 24
DATE 5/11/72
VORTEX (2) STBD
AGE (sec.) 18
AMBIENT WIND (ft./sec.) 16
EAS = 150 KNOTS
$\hat{V}$=114 ft/s @ 113 ft
SENSOR HEIGHT IN FEET (AGL)
160
150
140
130
120
110
100
90
80
70
60
140 120 100 80 60 40 20 0 20 40 60 80 100 120 140
TANGENTIAL VELOCITY, V_θ, ft./sec.

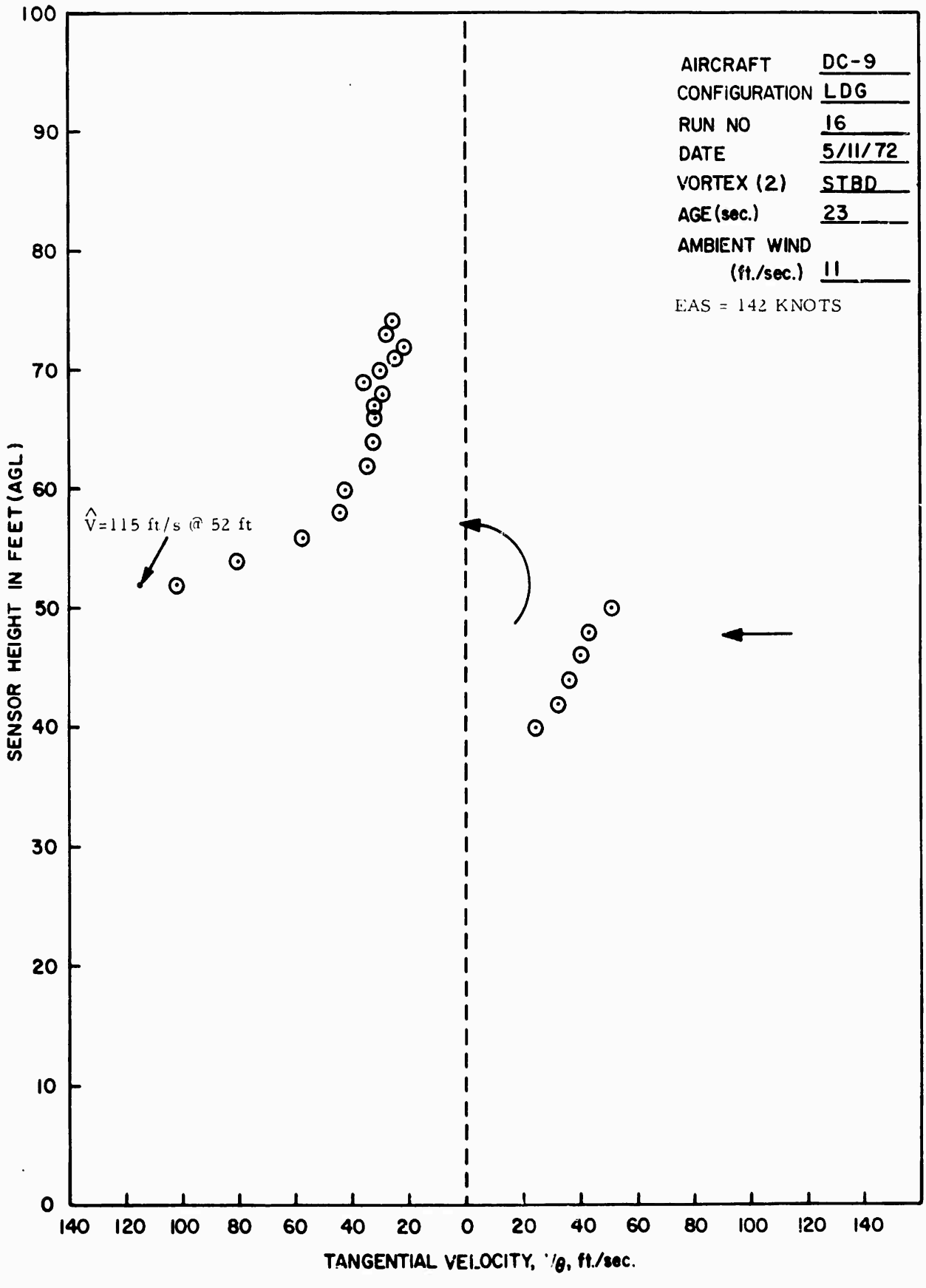
AIRCRAFT DC-9
CONFIGURATION LDG
RUN NO 16
DATE 5/11/72
VORTEX (2) STBD
AGE (sec.) 23
AMBIENT WIND (ft./sec.) 11
EAS = 142 KNOTS
$\hat{V}$=115 ft/s @ 52 ft
SENSOR HEIGHT IN FEET (AGL)
TANGENTIAL VELOCITY, v/g, ft./sec.
100
90
80
70
60
50
40
30
20
10
0
140 120 100 80 60 40 20 0 20 40 60 80 100 120 140

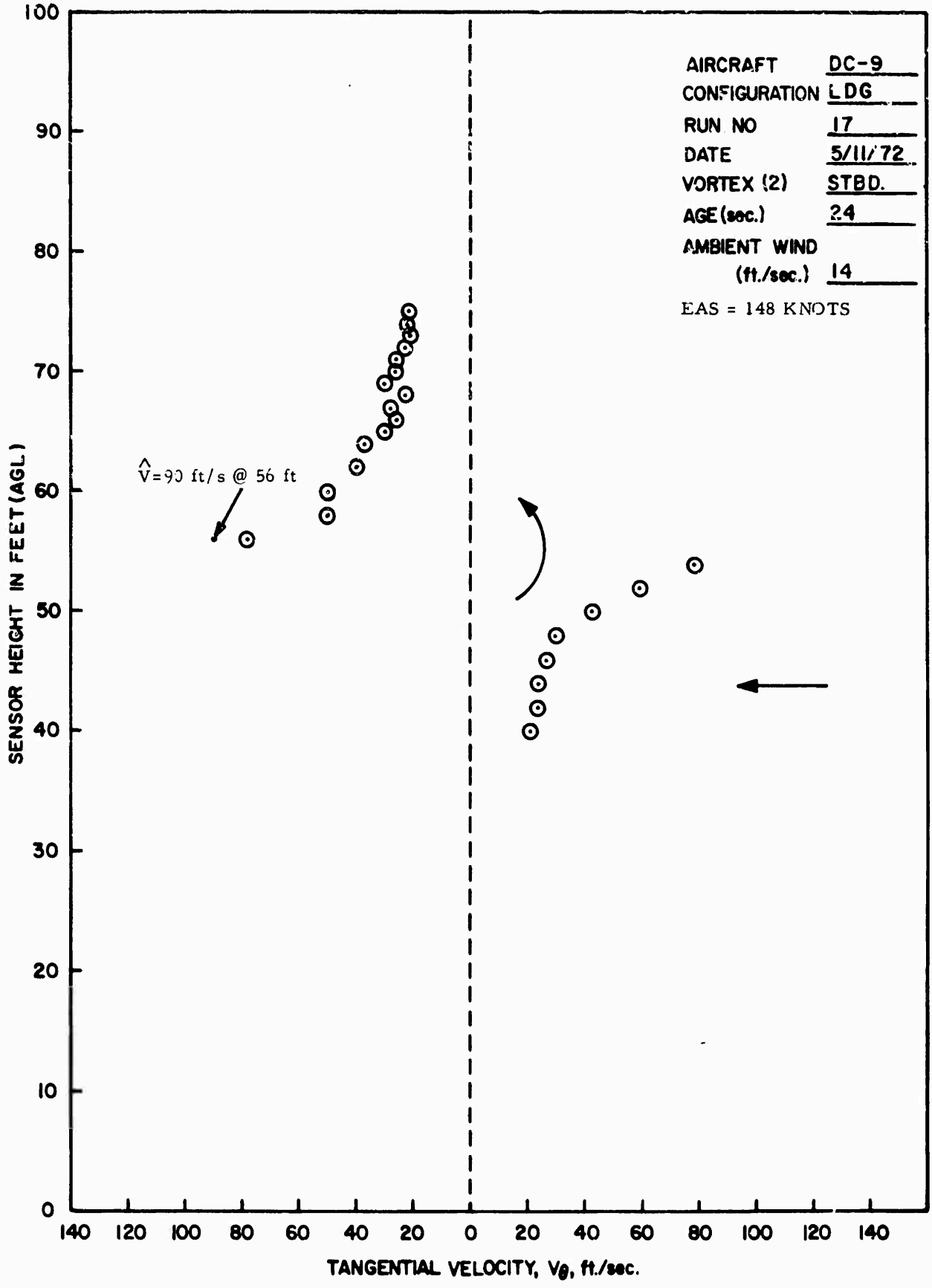
AIRCRAFT DC-9
CONFIGURATION LDG
RUN NO 17
DATE 5/11/72
VORTEX (2) STBD.
AGE (sec.) 24
AMBIENT WIND (ft./sec.) 14
EAS = 148 KNOTS
$\hat{V}$=90 ft/s @ 56 ft
SENSOR HEIGHT IN FEET (AGL)
TANGENTIAL VELOCITY, V_θ, ft./sec.
100
90
80
70
60
50
40
30
20
10
0
140 120 100 80 60 40 20 0 20 40 60 80 100 120 140

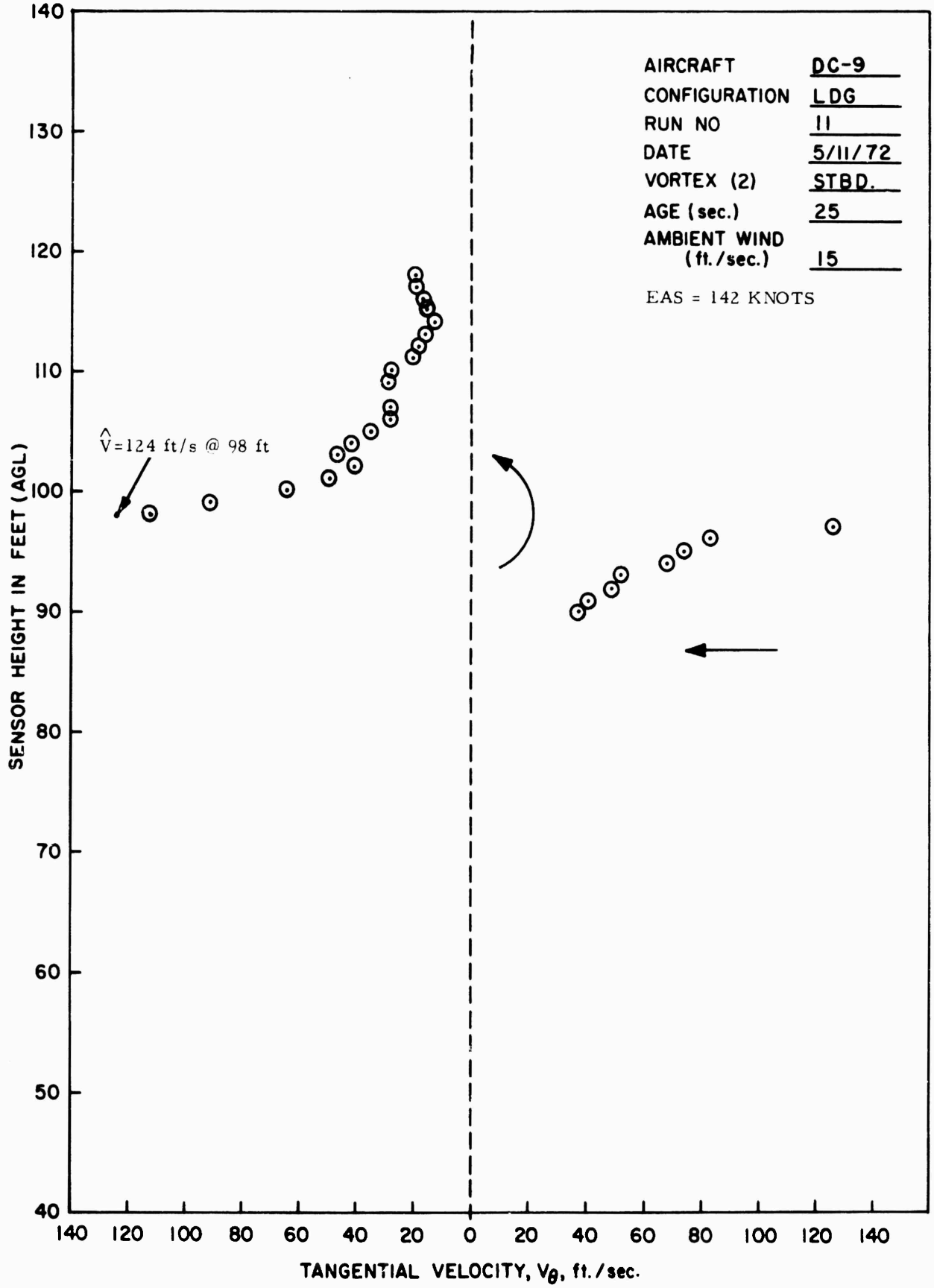
AIRCRAFT DC-9
CONFIGURATION LDG
RUN NO 11
DATE 5/11/72
VORTEX (2) STBD.
AGE (sec.) 25
AMBIENT WIND (ft./sec.) 15
EAS = 142 KNOTS
$\hat{V}$=124 ft/s @ 98 ft
SENSOR HEIGHT IN FEET (AGL)
140
130
120
110
100
90
80
70
60
50
40
140 120 100 80 60 40 20 0 20 40 60 80 100 120 140
TANGENTIAL VELOCITY, V_θ, ft./sec.

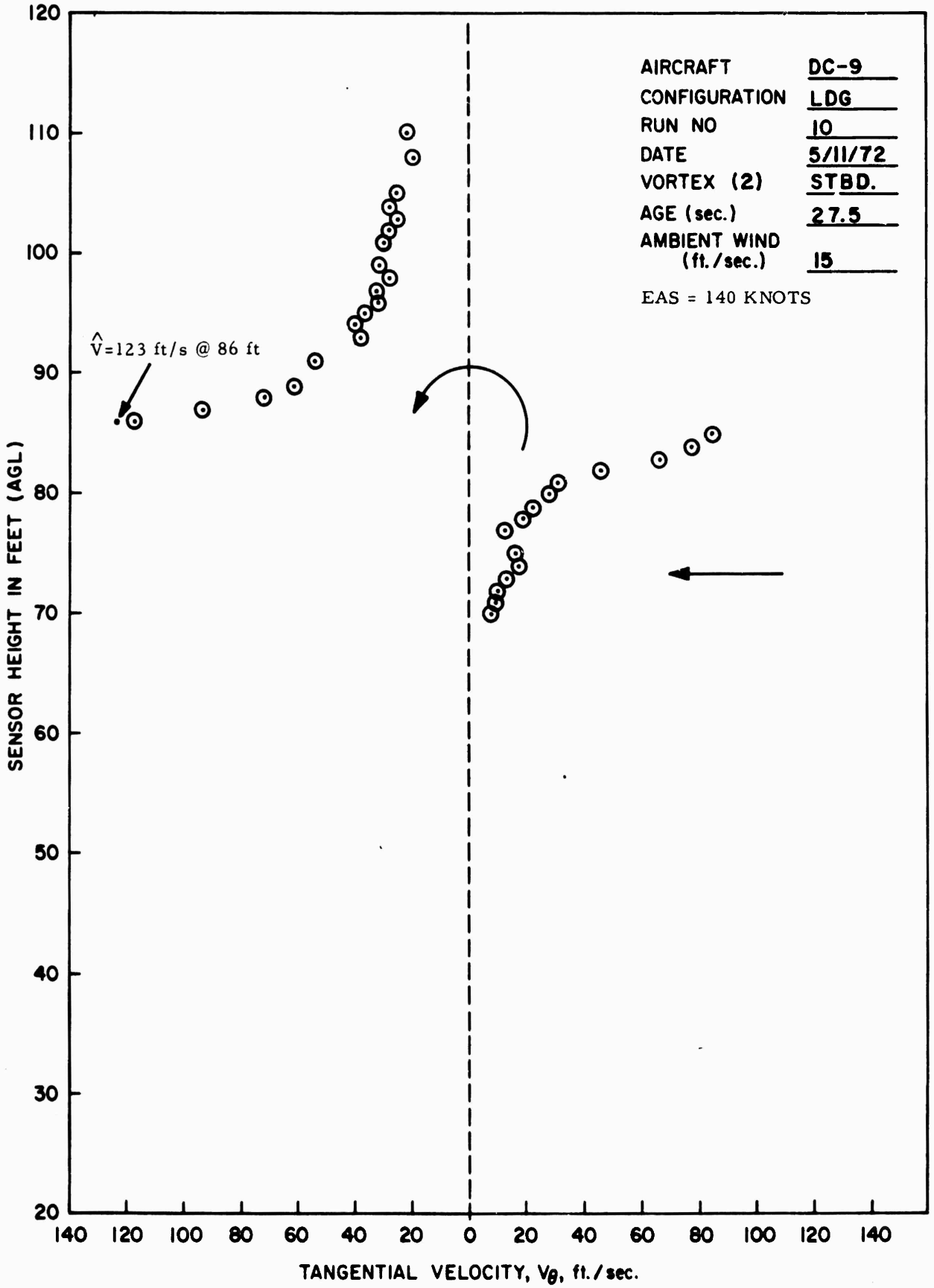
AIRCRAFT DC-9
CONFIGURATION LDG
RUN NO 10
DATE 5/11/72
VORTEX (2) STBD.
AGE (sec.) 27.5
AMBIENT WIND (ft./sec.) 15
EAS = 140 KNOTS
$\hat{V}$=123 ft/s @ 86 ft
SENSOR HEIGHT IN FEET (AGL)
120
110
100
90
80
70
60
50
40
30
20
140 120 100 80 60 40 20 0 20 40 60 80 100 120 140
TANGENTIAL VELOCITY, V_θ, ft./sec.

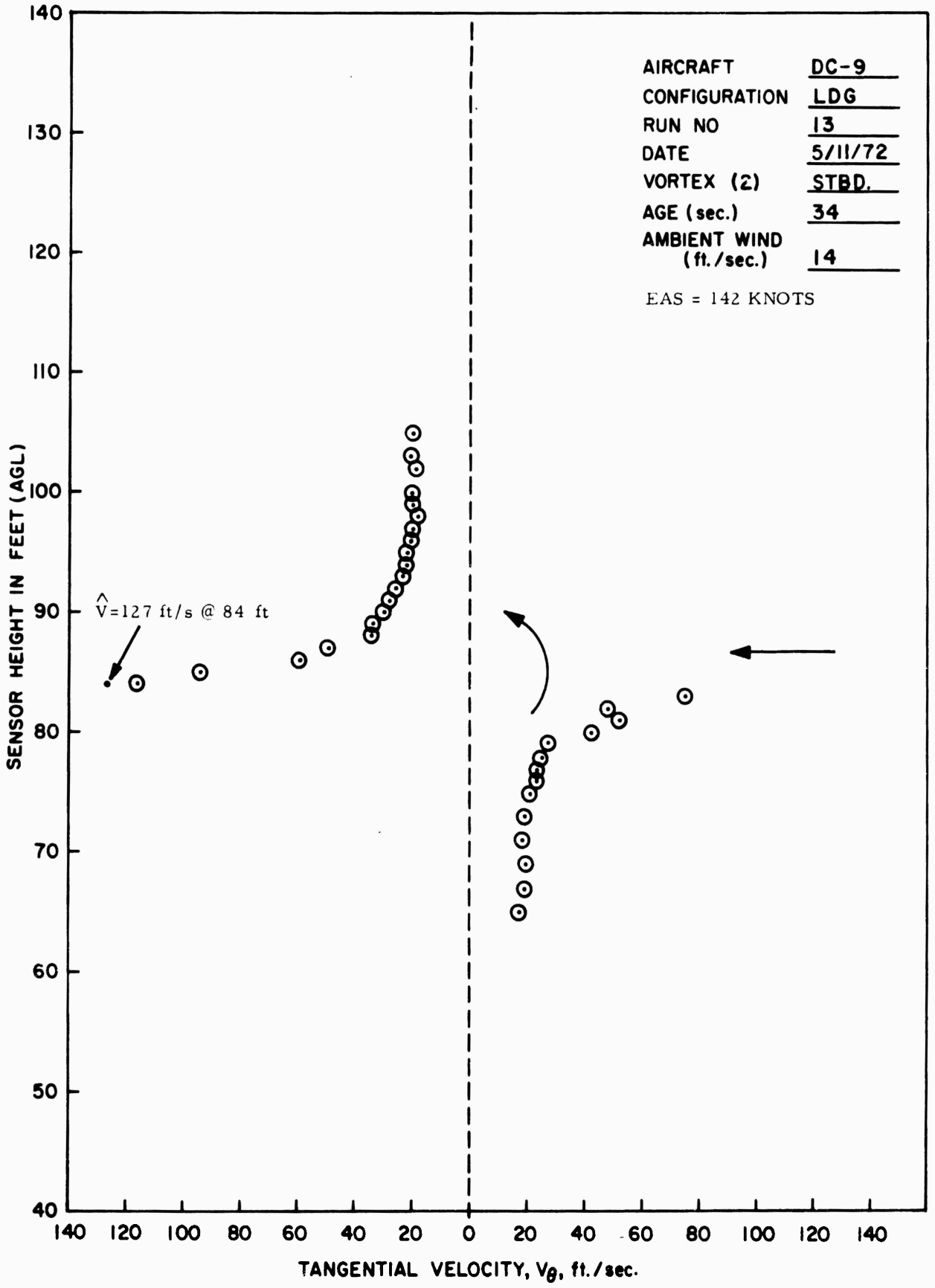
AIRCRAFT DC-9
CONFIGURATION LDG
RUN NO 13
DATE 5/11/72
VORTEX (2) STBD.
AGE (sec.) 34
AMBIENT WIND (ft./sec.) 14
EAS = 142 KNOTS
$\hat{V}$=127 ft/s @ 84 ft
SENSOR HEIGHT IN FEET (AGL)
140
130
120
110
100
90
80
70
60
50
40
140 120 100 80 60 40 20 0 20 40 60 80 100 120 140
TANGENTIAL VELOCITY, V_θ, ft./sec.

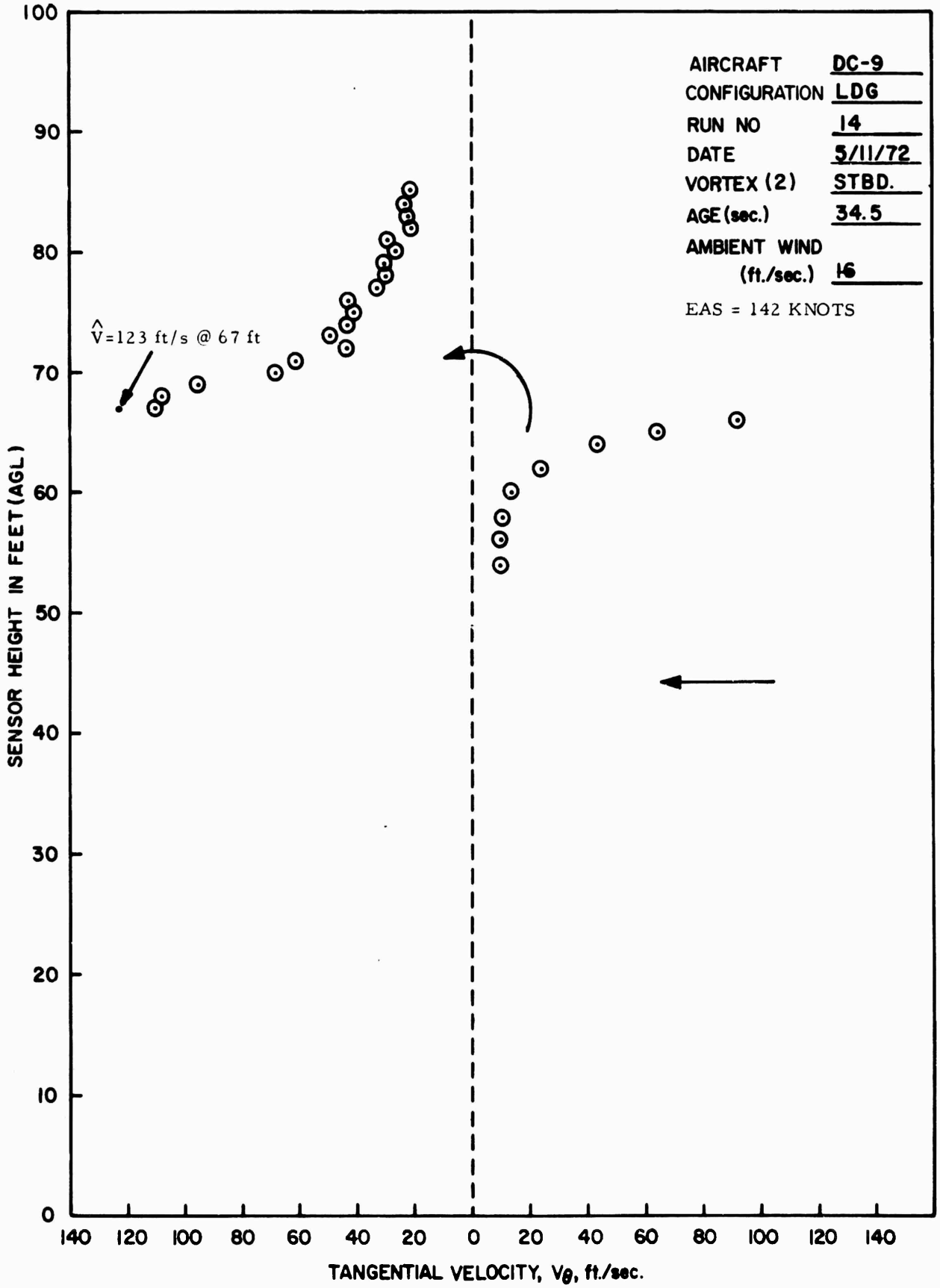
AIRCRAFT DC-9
CONFIGURATION LDG
RUN NO 14
DATE 5/11/72
VORTEX (2) STBD.
AGE (sec.) 34.5
AMBIENT WIND (ft./sec.) 16
EAS = 142 KNOTS
$\hat{V}$=123 ft/s @ 67 ft
SENSOR HEIGHT IN FEET (AGL)
TANGENTIAL VELOCITY, V_θ, ft./sec.
100
90
80
70
60
50
40
30
20
10
0
140 120 100 80 60 40 20 0 20 40 60 80 100 120 140

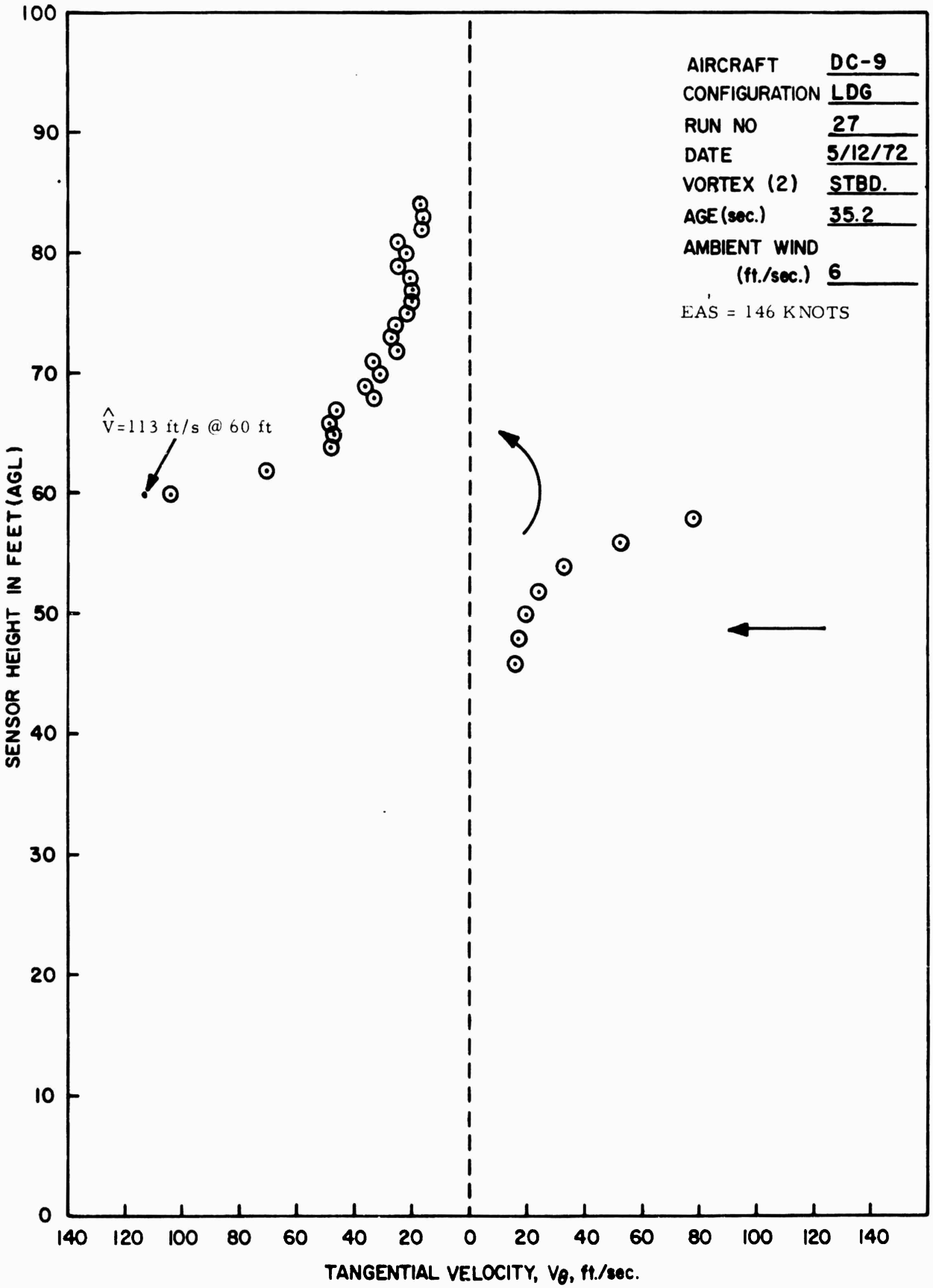
AIRCRAFT DC-9
CONFIGURATION LDG
RUN NO 27
DATE 5/12/72
VORTEX (2) STBD.
AGE (sec.) 35.2
AMBIENT WIND (ft./sec.) 6
EAS = 146 KNOTS
V̂=113 ft/s @ 60 ft
SENSOR HEIGHT IN FEET (AGL)
100
90
80
70
60
50
40
30
20
10
0
140 120 100 80 60 40 20 0 20 40 60 80 100 120 140
TANGENTIAL VELOCITY, Vθ, ft./sec.

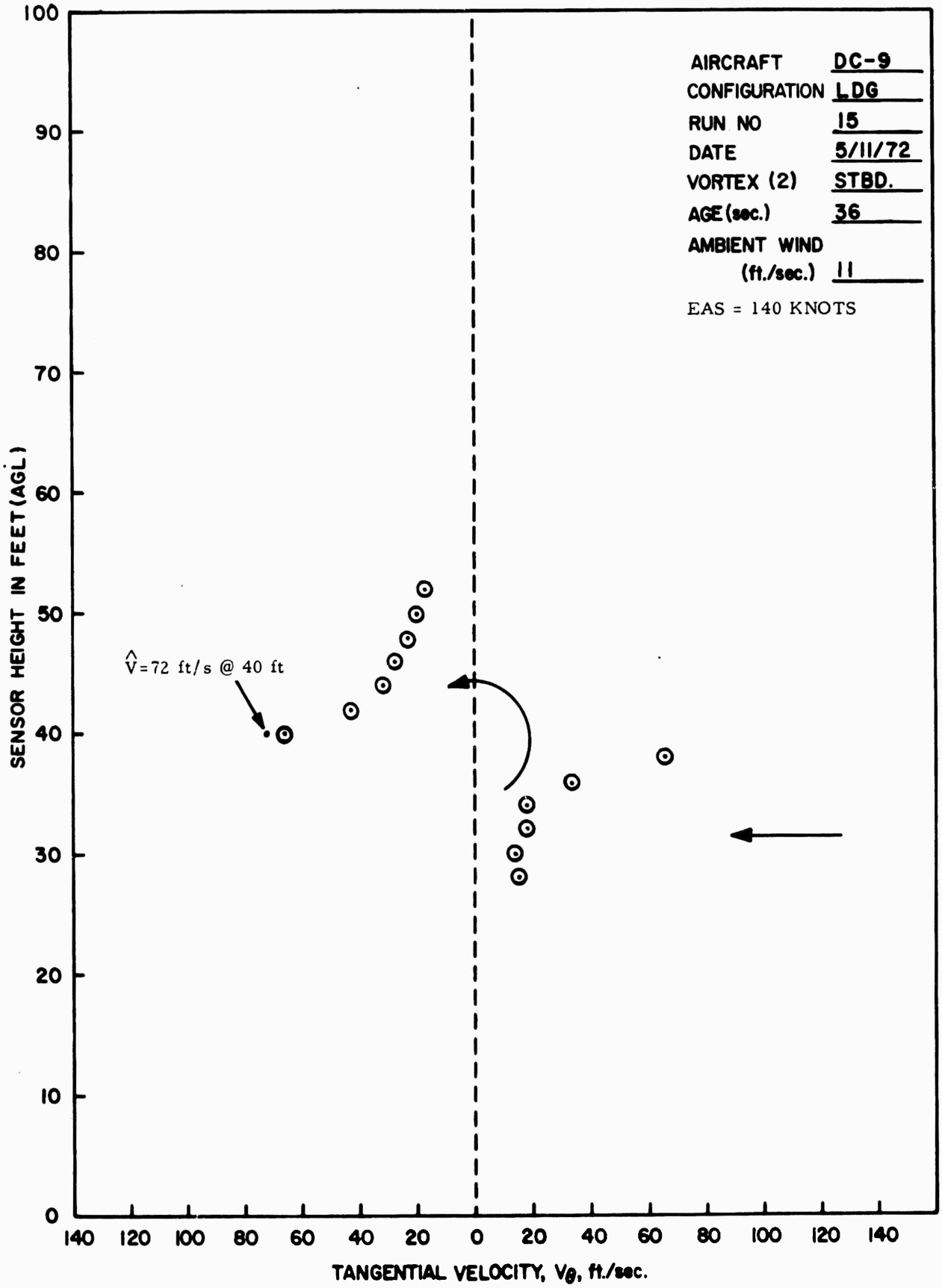
AIRCRAFT DC-9
CONFIGURATION LDG
RUN NO 15
DATE 5/11/72
VORTEX (2) STBD.
AGE (sec.) 36
AMBIENT WIND (ft./sec.) 11
EAS = 140 KNOTS
$\hat{V}$=72 ft/s @ 40 ft
SENSOR HEIGHT IN FEET (AGL)
TANGENTIAL VELOCITY, V_θ, ft./sec.
100
90
80
70
60
50
40
30
20
10
0
140 120 100 80 60 40 20 0 20 40 60 80 100 120 140

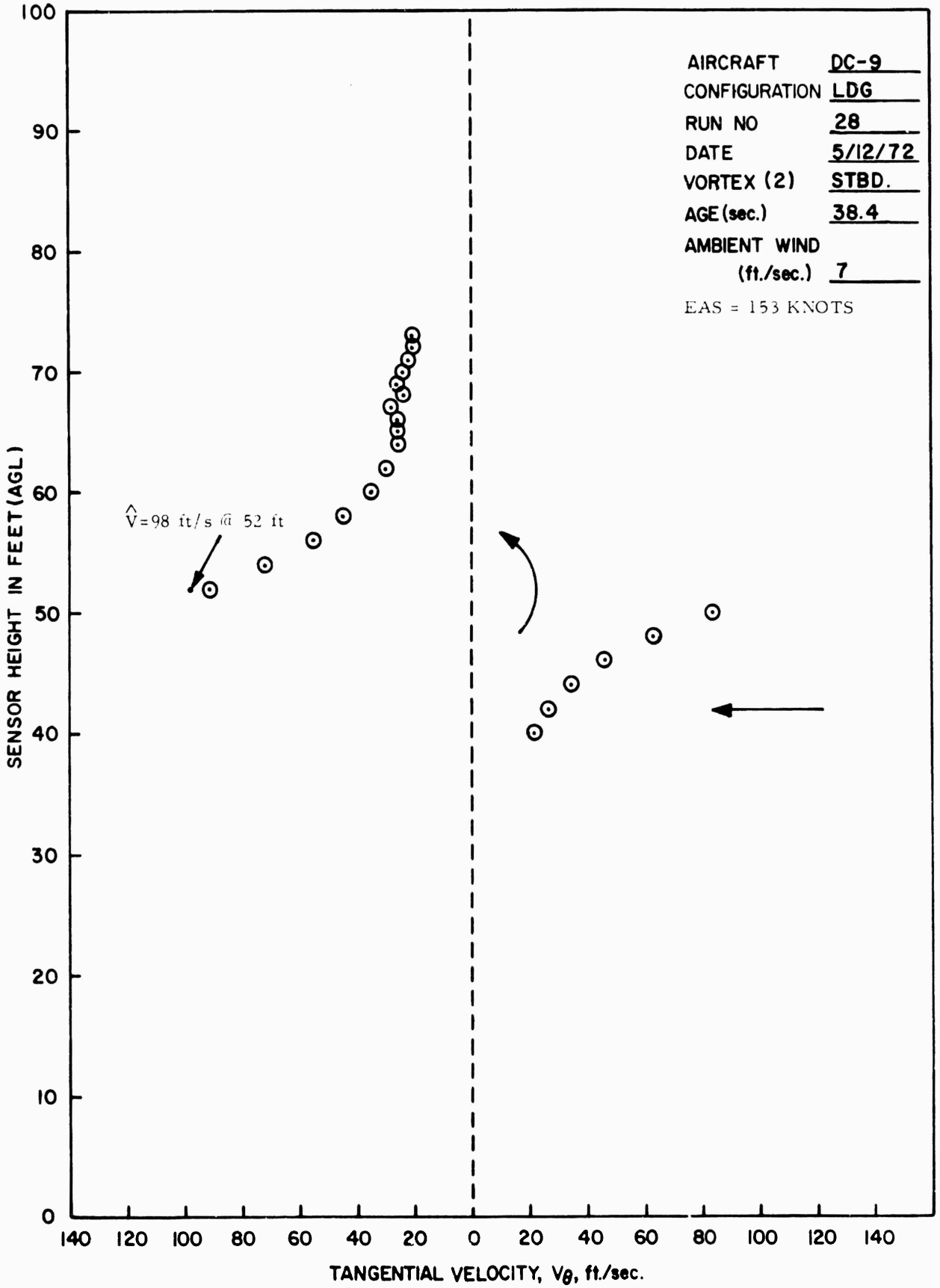
AIRCRAFT DC-9
CONFIGURATION LDG
RUN NO 28
DATE 5/12/72
VORTEX (2) STBD.
AGE (sec.) 38.4
AMBIENT WIND (ft./sec.) 7
EAS = 153 KNOTS
$\hat{V}$=98 ft/s @ 52 ft
SENSOR HEIGHT IN FEET (AGL)
TANGENTIAL VELOCITY, V_θ, ft./sec.
100
90
80
70
60
50
40
30
20
10
0
140 120 100 80 60 40 20 0 20 40 60 80 100 120 140

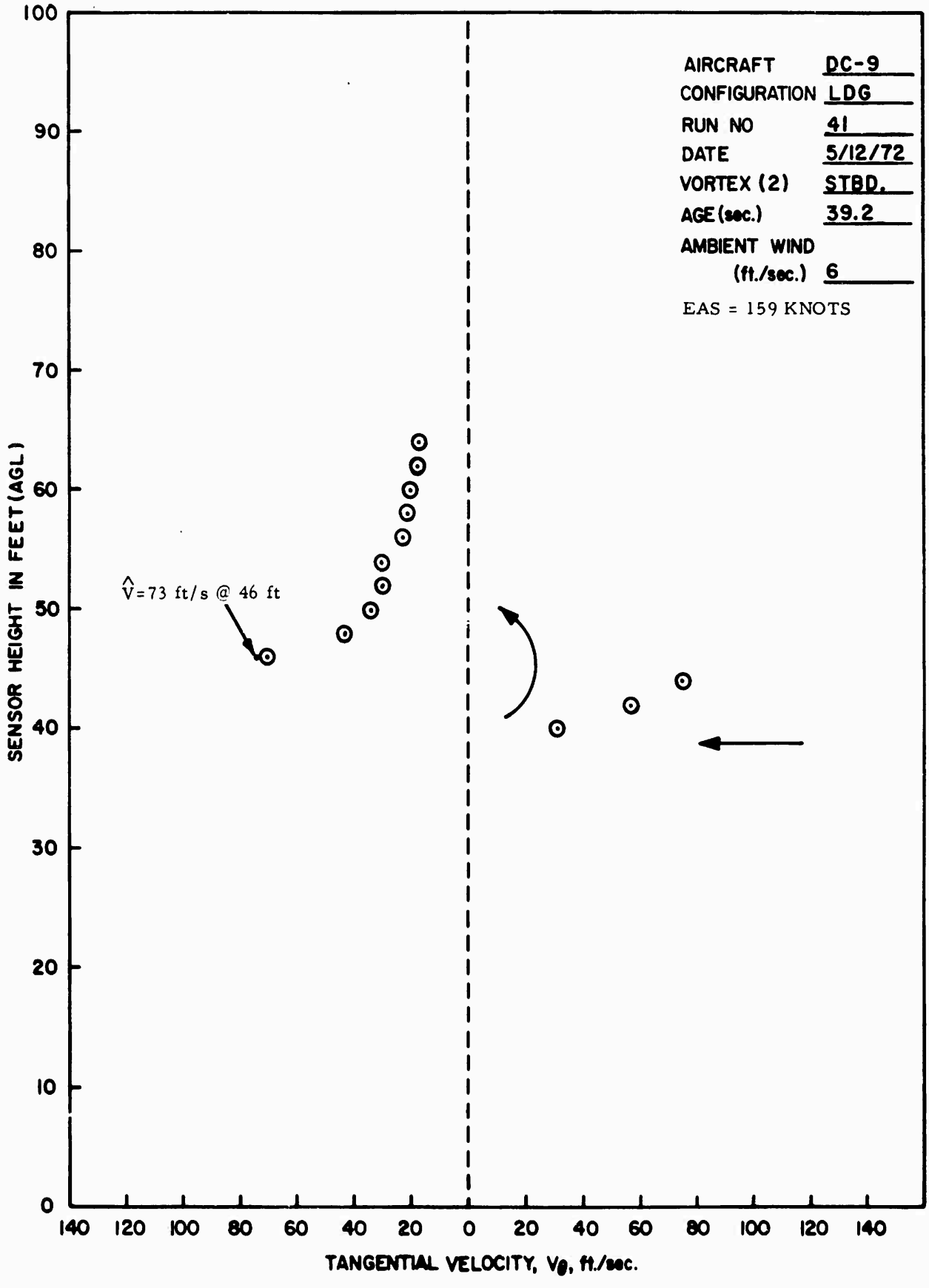
AIRCRAFT DC-9
CONFIGURATION LDG
RUN NO 41
DATE 5/12/72
VORTEX (2) STBD.
AGE (sec.) 39.2
AMBIENT WIND (ft./sec.) 6
EAS = 159 KNOTS
$\hat{V}$=73 ft/s @ 46 ft
SENSOR HEIGHT IN FEET (AGL)
TANGENTIAL VELOCITY, Vθ, ft./sec.
100
90
80
70
60
50
40
30
20
10
0
140 120 100 80 60 40 20 0 20 40 60 80 100 120 140

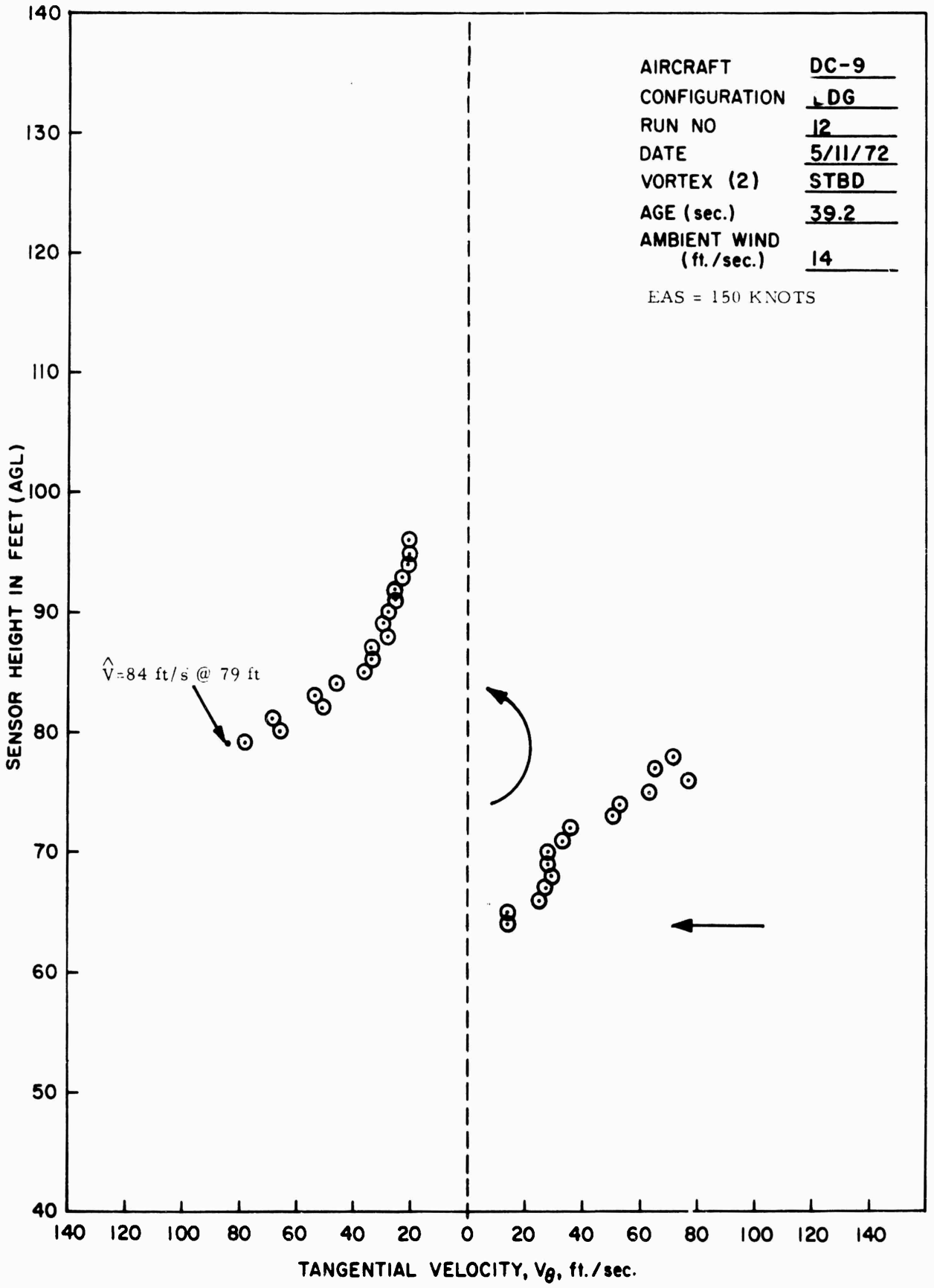
AIRCRAFT DC-9
CONFIGURATION LDG
RUN NO 12
DATE 5/11/72
VORTEX (2) STBD
AGE (sec.) 39.2
AMBIENT WIND (ft./sec.) 14
EAS = 150 KNOTS
$\hat{V}$=84 ft/s @ 79 ft
SENSOR HEIGHT IN FEET (AGL)
TANGENTIAL VELOCITY, V_θ, ft./sec.
140
130
120
110
100
90
80
70
60
50
40
140 120 100 80 60 40 20 0 20 40 60 80 100 120 140

APPENDIX C

SUMMARY FLIGHT TEST DATA

Explanation of superscripts and other notes for tables of appendix C.

1. Airplane centerline offset (feet) abreast of tower.

2. Airplane height (feet above ground level (AGL)) abreast of tower.

[1]and[2] by phototheodolite where available. When phototheodolite not available, offset estimated visually from ground markings (concentric circles centered on tower base) and height determined from airplane radar altimeter.

3. Configuration: TO = Takeoff flap angle = 20°.
L = Landing flap angle = 30°

O/T - Indicates that the vortex passed over the top of the test tower. Particularly in the first nine runs, consideration of safety resulted in test runs being made at a greater altitude than would otherwise have been used.

It will be noted that in several instances, the second vortex struck the tower at a greater height than did the first (runs 23, 25, 33-37, 43, 51, and 59). This is an experimental fact that has been noted in other test series, and is apparently attributable to atmospheric and buoyancy effects which, as has been noted, have a strong influence on vortex descent rates.

FLIGHT TEST DATA - DC9 WAKE TURBULENCE

Run Number	1	2	3	4	5	6	7	8	9	10	11	12
Aircraft Position[1], ft	166	224	338	299	327	306	296	-	318	377	350	488
Aircraft Height AGL[2], ft	201	207	207	205	204	198	206	198	216	216	217	208
Equivalent Airspeed, knots	155	155	160	160	162	165	165	165	160	140	142	150
Gross Weight, lb X 10^{-3}	76.0	75.7	75.2	75.0	75.0	73.5	72.7	72.0	71.9	71.3	70.9	70.1
Configuration[3]	T.O.	T.O.	T.O.	T.O.	T.O.	T.O.	T.O.	T.O.	T.O.	L	L	L
Peak Recorded Absolute Velocity, First Vortex ft/s	-	-	-	-	-	-	-	No Hit	-	73	98	36
Peak Recorded Absolute Velocity, Second Vortex ft/s	71	83	119	92	116	118	75	No Hit	76	123	124	84
Vortex Height on Tower First Vortex, ft	O/T	O/T	O/T	O/T	O/T	O/T	O/T	-	O/T	118	130	123
Vortex Height on Tower Second Vortex, ft	142	142	126	120	119	120	140	-	142	85	98	79
Vortex Age, (First) s	9.0	13.5	20.0	19.5	22.0	18.5	-	-	15.0	21.5	19.5	28.0
Vortex Age, (Second) s	15.0	18.5	26.0	26.5	32.0	24.5	20.5	-	22.0	27.5	25.o	39.2
Mean Descent Rate First Vortex, ft/s	-	-	-	-	-	-	-	-	-	4.56	4.46	3.04
Mean Descent Rate Second Vortex, ft/s	3.93	3.51	3.12	3.21	2.66	3.18	3.22	-	3.36	4.76	4.76	3.29
Mean Lateral Velocity First Vortex, ft/s	14.3	13.8	15.0	13.4	13.2	14.5	-	-	18.7	15.8	16.0	16.1
Mean Lateral Velocity Second Vortex, ft/s	13.5	14.1	14.4	12.6	11.4	14.0	16.2	-	16.1	15.1	15.5	13.4
Crosswind Velocity Component ft/s	12.2	13.2	13.2	11.4	10.9	13.5	13.8	14.5	13.8	14.7	14.6	13.6
Windspeed at 140 ft/s	12.3	13.5	13.4	11.5	11.4	13.6	14.2	14.7	13.8	14.7	14.7	13.7

FLIGHT TEST DATA - DC9 WAKE TURBULENCE

Run Number	13	14	15	16	17	18	19	20	21	22	23	24
Aircraft Position[1], ft	483	477	333	297	317	389	380	452	479	583	555	279
Aircraft Height AGL[2], ft	214	219	214	203	212	220	229	219	214	215	217	210
Equivalent Airspeed, knots	142	142	140	142	148	150	150	154	150	153	153	150
Gross Weight, lb X 10^{-3}	69.6	68.8	78.2	78.0	76.8	76.6	75.1	74.5	74.1	73.9	73.6	72.2
Configuration[3]	L	L	L	L	L	L	L	L	L	L	L	L
Peak Recorded Absolute Velocity, First Vortex ft/s	39	51	79	102	90	59	43	No Hit	No Hit	No Hit	60	133
Peak Recorded Absolute Velocity, Second Vortex ft/s	127	123	72	115	90	35	No Hit	No Hit	No Hit.	No Hit	38	114
Vortex Height on Tower First Vortex, ft	117	123	56	79	80	96	140	O/T	-	-	20	127
Vortex Height on Tower Second Vortex, ft	84	67	40	51	56	50	-	O/T	-	-	60	113
Vortex Age, (First) s	27.0	27.5	28.5	18.5	20.5	29.0	28.5	-	-	-	30	14.5
Vortex Age, (Second) s	34.0	34.5	36.0	23.0	24.0	34.0	-	-	-	-	34.0	18.0
Mean Descent Rate First Vortex, ft/s	3.59	3.49	5.54	6.70	6.44	4.28	3.12	-	-	-	6.57	5.72
Mean Descent Rate Second Vortex, ft/s	3.82	4.41	4.83	6.61	6.50	5.00	-	-	-	-	4.62	5.39
Mean Lateral Velocity First Vortex, ft/s	16.0	16.0	10.4	14.1	13.7	12.1	12.0	-	-	-	17.3	16.7
Mean Lateral Velocity Second Vortex, ft/s	15.3	14.9	10.3	14.5	14.8	12.5	10.0	-	-	-	17.4	17.6
Crosswind Velocity Component ft/s	13.6	16.1	10.9	10.3	13.0	10.3	10.1	12.7	12.2	13.1	16.0	16.1
Windspeed at 140 ft/s	13.8	16.2	11.0	10.7	14.4	11.5	10.1	13.2	13.2	13.2	16.0	16.1

FLIGHT TEST DATA - DC9 WAKE TURBULENCE

Run Number	25	26	27	28	29	30	31	32	33	34	35	36
Aircraft Position[1], ft	322	-	248	260	373	393	503	484	486	504	602	597
Aircraft Height AGL[2], ft	211	-	229	224	237	255	268	255	286	282	312	300
Equivalent Airspeed, knots	148	150	146	153	153	158	156	156	154	153	159	157
Gross Weight, lb X 10^{-3}	71.9	71.5	77.9	77.4	76.9	76.4	75.9	75.3	-	-	-	-
Configuration[3]	L	L	L	L	L	L	L	L	L	L	L	L
Peak Recorded Absolute Velocity, First Vortex ft/s	63	-	114	112	31	26	15	23	21	20	21	21
Peak Recorded Absolute Velocity, Second Vortex ft/s	50	-	113	98	20	-	20	21	18	20	18	19
Vortex Height on Tower First Vortex, ft	99	-	97	102	86	105	95	74	69	46	73	70
Vortex Height on Tower Second Vortex, ft	110	-	59	52	46	-	73	66	90	98	109	89
Vortex Age, (First) s	23.0	-	27.2	27.2	48.0	52.0	72.0	60.0	65.0	66.0	70.0	76.0
Vortex Age, (Second) s	32.0	-	35.2	38.4	67.0	-	98.0	101	82.0	78.0	90.0	95.0
Mean Descent Rate First Vortex, ft/s	4.87	-	4.80	4.49	3.15	2.88	2.40	3.02	3.34	3.58	3.41	3.03
Mean Descent Rate Second Vortex, ft/s	3.16	-	4.83	4.48	2.85	-	1.99	1.87	2.39	2.36	2.26	2.22
Mean Lateral Velocity First Vortex, ft/s	12.4	-	7.8	8.2	7.0	6.8	6.5	7.5	6.9	7.1	8.1	7.4
Mean Lateral Velocity Second Vortex, ft/s	11.2	-	8.1	7.7	6.1	-	5.5	5.1	6.4	6.9	7.1	6.7
Crosswind Velocity Component ft/s	14.1	12.9	5.8	6.7	7.3	6.3	5.3	6.5	5.8	7.6	7.3	5.8
Windspeed at 140 ft/s	14.3	14.9	5.9	7.3	7.3	6.3	5.4	6.6	6.0	7.8	7.3	5.9

FLIGHT TEST DATA - DC9 WAKE TURBULENCE

Run Number	37	38	39	40	41	42	43	44	45	46	47	48
Aircraft Position[1], ft	603	600	281	261	107	139	91	295	227	268	274	375
Aircraft Height AGL[2], ft	297	300	241	242	216	216	219	226	232	229	255	252
Equivalent Airspeed, knots	157	154	160	157	159	158	157	154	155	158	158	157
Gross Weight, lb X 10^{-3}	-	-	71.6	70.8	70.4	70.0	68.8	77.5	77.0	76.6	75.9	75.4
Configuration[3]	L	L	L	L	L	L	L	L	L	L	L	L
Peak Recorded Absolute Velocity, First Vortex ft/s	17	-	20	18	118	120	39	82	30	67	35	38
Peak Recorded Absolute Velocity, Second Vortex ft/s	18	-	16	20	73	-	17	-	51	24	26	-
Vortex Height on Tower First Vortex, ft	94	-	90	110	94	52	60	76	97	66	79	26
Vortex Height on Tower Second Vortex, ft	109	-	67	94	46	-	110		56	32	62	-
Vortex Age, (First) s	91	-	54	34	21.6	29.6	35	41.0	20.0	40.0	39	44
Vortex Age, (Second) s	115	-	86	67	39.2	-	93	-	28.0	54	47	-
Mean Descent Rate First Vortex, ft/s	2.23	-	2.80	3.88	5.65	5.54	4.54	3.66	6.75	4.08	4.51	5.14
Mean Descent Rate Second Vortex, ft/s	1.63	-	2.02	2.21	4.34	-	1.17	-	6.29	3.65	4.11	-
Mean Lateral Velocity First Vortex, ft/s	6.2	-	4.5	6.6	3.2	3.4	1.5	6.3	9.5	5.8	6.1	7.7
Mean Lateral Velocity Second Vortex, ft/s	6.7	-	3.7	4.4	3.7	-	1.4	-	9.4	5.6	6.6	-
Crosswind Velocity Component ft/s	8.2	7.2	5.7	5.3	5.5	3.1	3.5	6.0	6.7	7.4	7.2	7.6
Windspeed at 140 ft/s	8.3	7.3	5.9	6.2	5.9	3.2	7.5	5.1	6.7	7.6	7.6	7.8

FLIGHT TEST DATA - DC9 WAKE TURBULENCE

Run Number	49	50	51	52	53	54	55	56	57	58	59	60	61
Aircraft Position[1], ft	335	359	392	337	368	373	107	167	156	290	367	358	345
Aircraft Height AGL[2], ft	285	257	258	257	271	285	207	209	218	200	207	224	213
Equivalent Airspeed, knots	160	157	157	157	159	160	160	160	164	159	158	160	161
Gross Weight, lb X 10^{-3}	75.0	74.5	74.1	73.5	73.1	71.9	71.4	71.0	70.6	70.2	69.8	69.4	69.0
Configuration[3]	L	L	L	L	L	L	L	L	L	L	L	L	L
Peak Recorded Absolute Velocity, First Vortex ft/s	-	47	44	50	-	-	50	116	94	26	58	87	108
Peak Recorded Absolute Velocity, Second Vortex ft/s	-	48	23	-	-	-	-	94	118	-	29	-	58
Vortex Height on Tower First Vortex, ft	-	81	32	73	-	-	142	133	142	76	74	62	90
Vortex Height on Tower Second Vortex, ft	-	48	64	-	-	-	-	110	117	-	104	-	86
Vortex Age, (First) s	-	34	34	31	-	-	8.0	12.0	11	30	19.2	21.3	18.9
Vortex Age, (Second) s	-	46	52	-	-	-	-	17.6	14.8	-	22	-	21.6
Mean Descent Rate First Vortex, ft/s	-	5.18	6.65	5.94	-	-	8.13	6.50	6.91	4.13	6.93	7.61	6.51
Mean Descent Rate Second Vortex, ft/s	-	4.54	3.73	-	-	-	-	5.63	6.82	-	4.68	-	5.88
Mean Lateral Velocity First Vortex, ft/s	-	9.5	10.4	9.7	-	-	8.7	10.8	10.8	8.4	17.2	15.1	16.3
Mean Lateral Velocity Second Vortex, ft/s	-	8.6	8.3	-	-	-	-	11.6	13.0	-	18.4	-	17.7
Crosswind Velocity Component ft/s	8.5	8.1	8.6	8.6	7.7	9.1	11.5	9.0	-	8.3	12.5	13.7	-
Windspeed at 140 ft/s	8.8	8.1	8.8	8.8	7.8	9.8	11.5	10.2	8.7	8.7	13.1	14.3	14.6

APPENDIX D

DEVELOPMENT OF THE ANALYSIS OF THE TRAJECTORY OF A PARALLEL PAIR OF VORTICES IN GROUND EFFECT

The horizontal and vertical velocity components induced on the vortex "A" by the other member of the pair and by the two image vortices are given by:

$$\dot{y} = \frac{\Gamma y^2}{4\pi z (y^2 + z^2)}$$

$$\dot{z} = \frac{-\Gamma z^2}{4\pi y (y^2 + z^2)}$$

$$\therefore \frac{dz}{dy} + \frac{z^3}{y^3} = 0,$$

so $\frac{1}{y^2} + \frac{1}{z^2} = K$, a constant.

OGE = OUT OF GROUND EFFECT

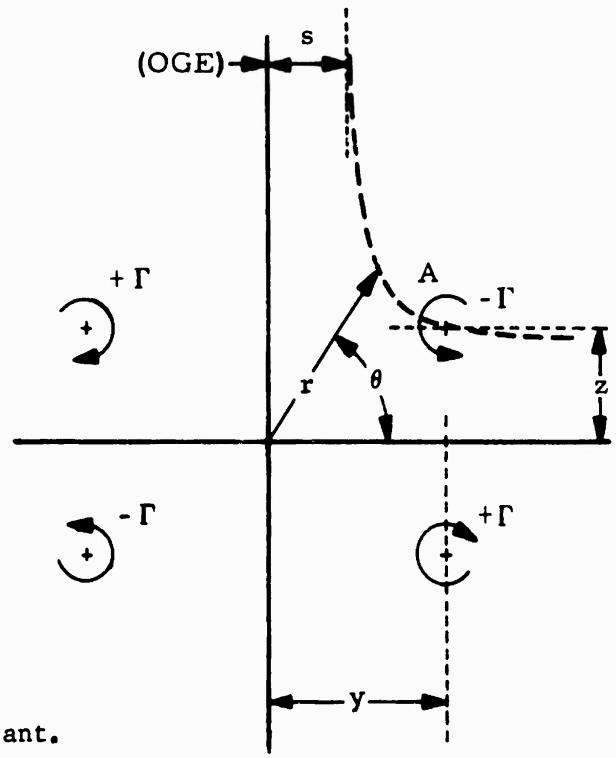

This may be written

$$a^2 (y^2 + z^2) = 4y^2 z^2 \qquad (1)$$

where "a" is to be determined.

Transforming to polar coordinates,

$$y = r \cos\theta$$

and

$$z = r \sin\theta$$

then $$a = r \sin 2\theta \qquad (2)$$

Since we know "a" to be a constant, we may postulate a value of θ and determine the corresponding value of r. Let $\theta = \frac{\pi}{4}$ $(45°)$.

Then $$a = r_{45} \qquad (3)$$

Determine value of r_{45}

The distance between the members of the vortex pair before they descend into ground effect is defined as 2s. For finite z (i.e., in ground effect) the semi-distance between them is

$$y = s + \Delta s$$

From equation (1),

$$r_{45}^2\left[(s + \Delta s)^2 + z^2\right] = 4(s + \Delta s)^2 z^2$$

$$r_{45}^2\left[\frac{(s + \Delta s)^2}{z^2} + 1\right] = 4(s + \Delta s)^2$$

As z approaches infinity, Δs approaches zero,

$$r_{45} = 2s \qquad (4)$$

Equation (1) then becomes

$$s^2(y^2 + z^2) = y^2 z^2 \qquad (5)$$

Summarizing the results obtained so far,

$$\dot{y} = \pm\frac{\Gamma y^2}{4\pi z(y^2 + z^2)} \qquad (6a)$$

$$\dot{z} = \frac{-\Gamma z^2}{4\pi y (y^2 + z^2)} \tag{6b}$$

$$s^2 (y^2 + z^2) = y^2 z^2 \tag{6c}$$

From (6c), $$y^3 = \frac{s^3 z^3}{(z^2 - s^2)^{3/2}} \tag{7a}$$

and $$y^2 + z^2 = \frac{z^4}{z^2 - s^2} \tag{7b}$$

and equations (6a) and (6b) become

$$\dot{y} = \pm \frac{\Gamma s^2}{4\pi z^3} \tag{8a}$$

and $$\dot{z} = \frac{-\Gamma s^2}{4\pi y^3} \tag{8b}$$

or $$\dot{z} = \frac{-\Gamma}{4\pi s} \frac{(z^2 - s^2)^{3/2}}{z^3} \tag{8c}$$

$$\therefore \frac{dt}{dz} = \frac{-4\pi s}{\Gamma} \frac{z^3}{(z^2 - s^2)^{3/2}} \tag{9}$$

The integration of equation (9) to determine the time taken for the vortex to descend from height z_1 down to height z_2 is best accomplished by making the substitution

$$z = s \, \mathrm{Sec}\, \phi ,$$

where $\phi = \mathrm{Arcsec}\ z/s$.

When this is done, the time is given by

$$T = \frac{8\pi s^2}{\Gamma} \cot 2\phi \Big|_{\phi_1}^{\phi_2}$$

This result presupposes an established vortex pair of strength Γ , whose initial separation distance, out of ground effect, is 2s.

The follcwing results may be readily deduced from the above analysis:

Equation (5) shows that when y is very large, $z = s$,

and

$$\therefore \dot{y} = \pm \frac{\Gamma}{4\pi s} \; ; \; \dot{z} = 0$$

When z is very large, equation (5) shows that $y = s$

and

$$\therefore \dot{y} = 0 \; ; \; \dot{z} = \frac{-\Gamma}{4\pi s} \; .$$

APPENDIX E

VORTEX TANGENTIAL VELOCITY DISTRIBUTIONS. COMPOSITE PLOTS

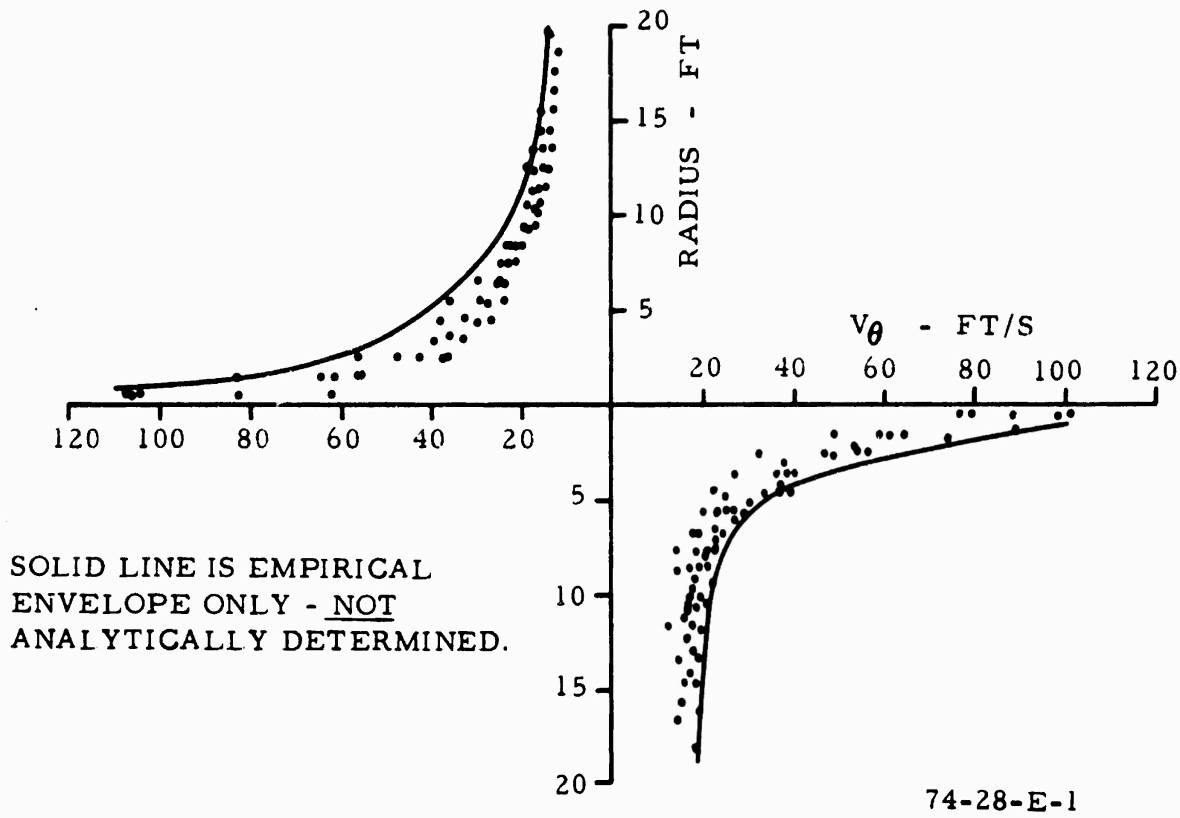

FIGURE E-1. MCDONNELL-DOUGLAS DC9, SERIES 10, VORTEX TANGENTIAL VELOCITY VS. RADIUS. TAKEOFF CONFIGURATION - COMPOSITE PLOT OF UPWIND VORTICES (VORTEX AGE 20.5 - 32 SECONDS)

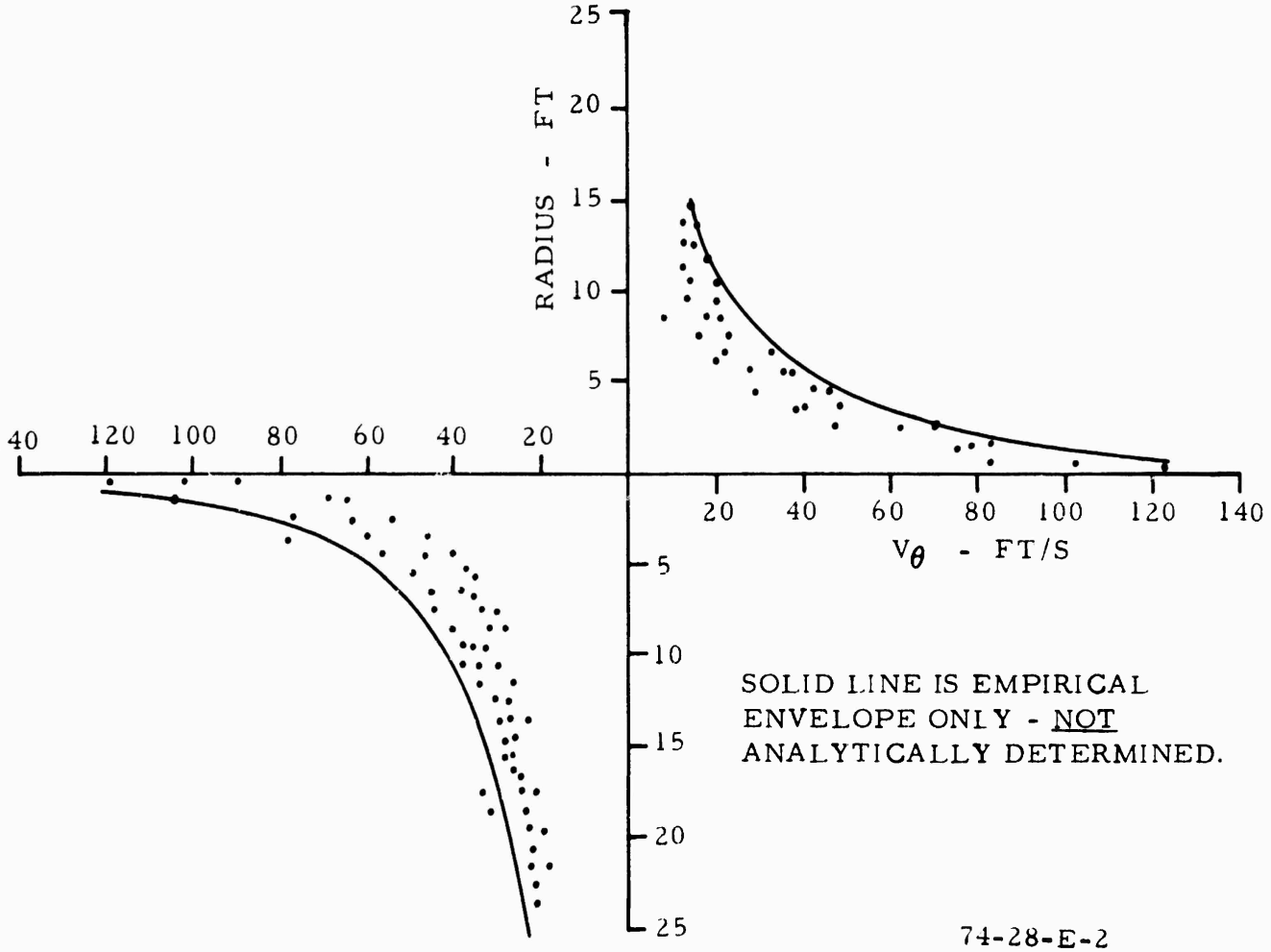

FIGURE E-2. MCDONNELL-DOUGLAS DC9, SERIES 10, VORTEX TANGENTIAL VELOCITY VS. RADIUS. LANDING CONFIGURATION - COMPOSITE PLOT OF DOWNWIND VORTICES. RUN NOS. 16, 24, AND 56. AGE 12 - 18.5 SECONDS

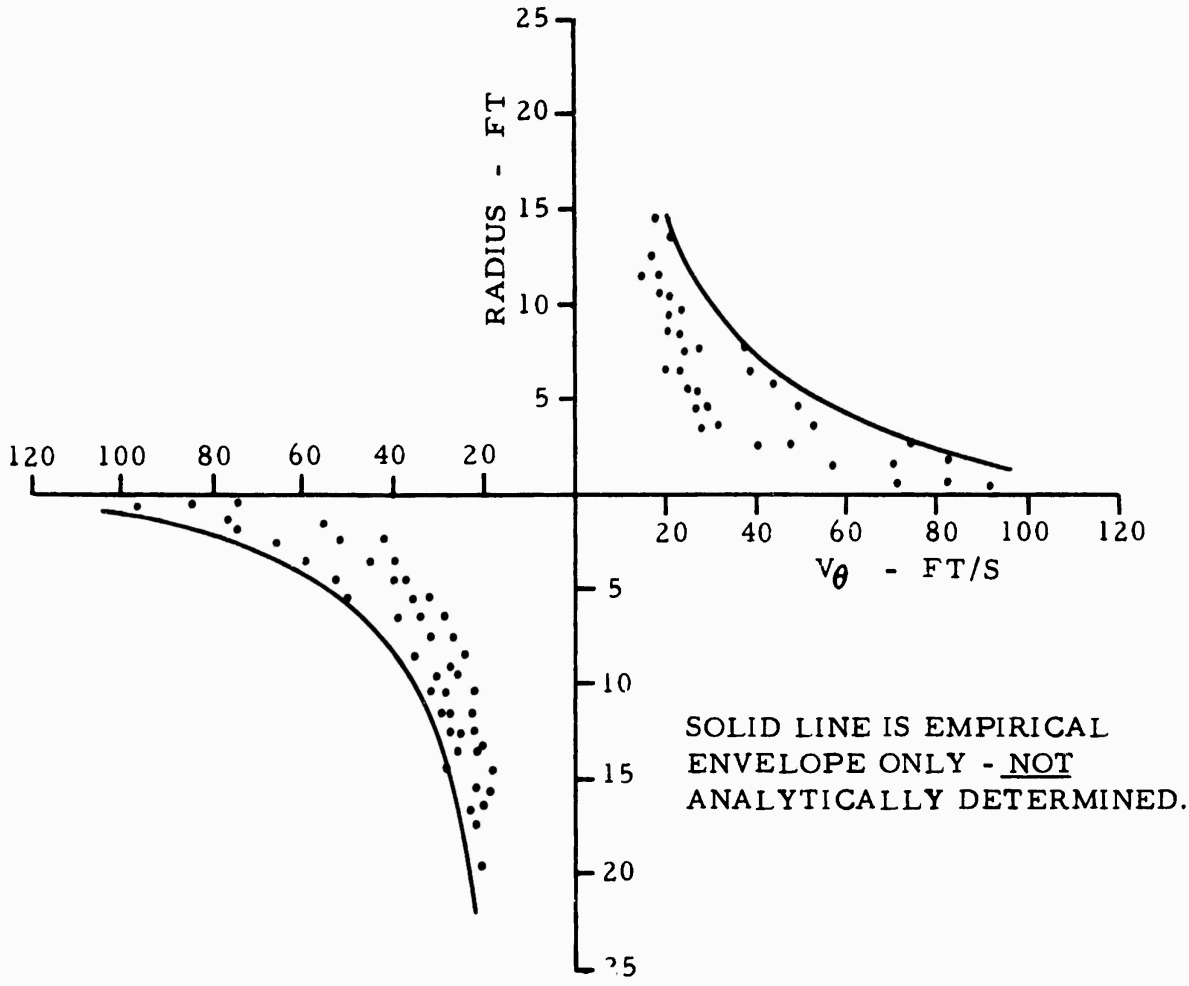

FIGURE E-3. MCDONNELL-DOUGLAS DC9, SERIES 10, VORTEX TANGENTIAL VELOCITY VS. RADIUS. LANDING CONFIGURATION - COMPOSITE PLOT OF DOWNWIND VORTICES. RUN NOS. 11, 17, AND 61. AGE 18.9 - 20.5 SECONDS

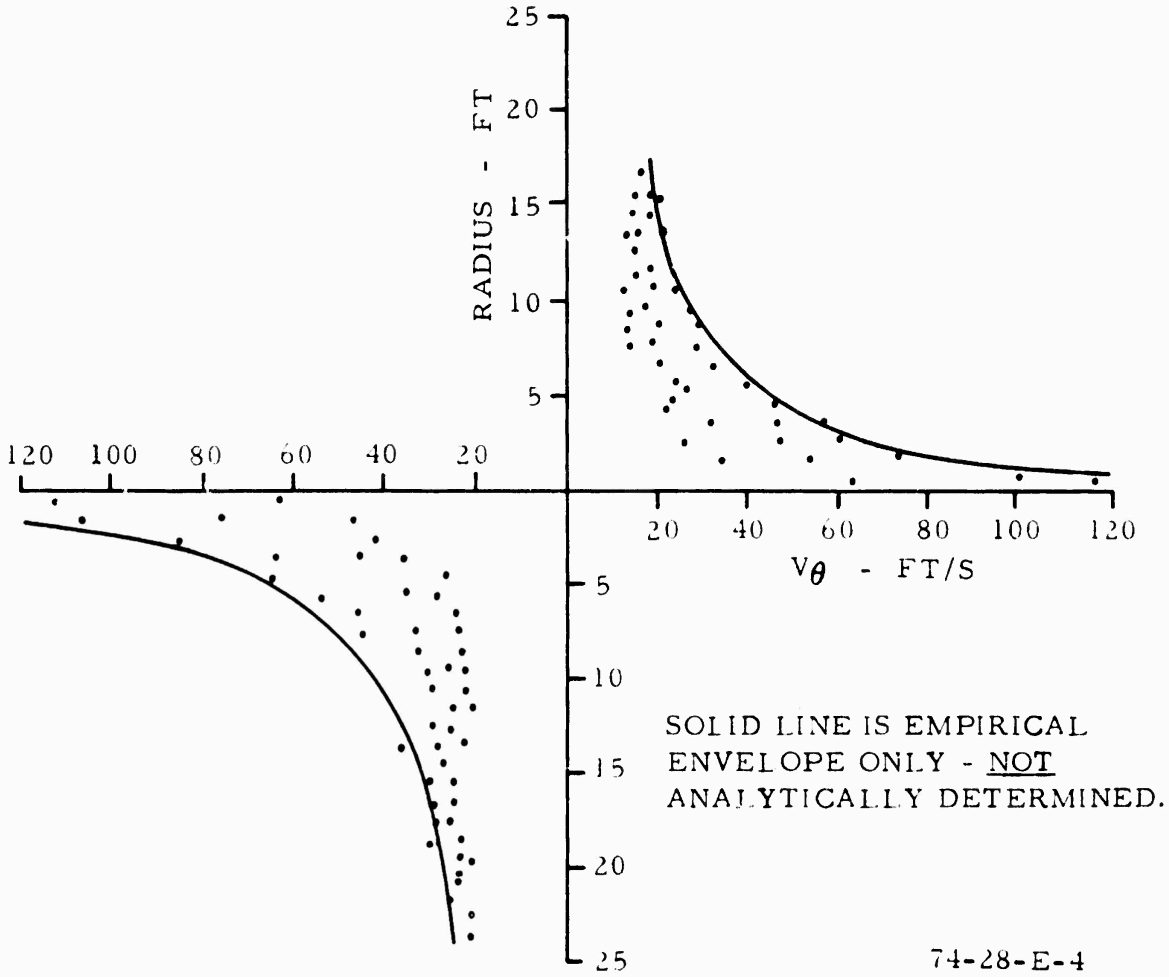

FIGURE E-4. MCDONNELL-DOUGLAS DC9, SERIES 10, VORTEX TANGENTIAL VELOCITY VS. RADIUS. LANDING CONFIGURATION - COMPOSITE PLOT OF DOWNWIND VORTICES. RUN NOS. 10, 41, AND 60. AGE 21.3 - 21.6 SECONDS

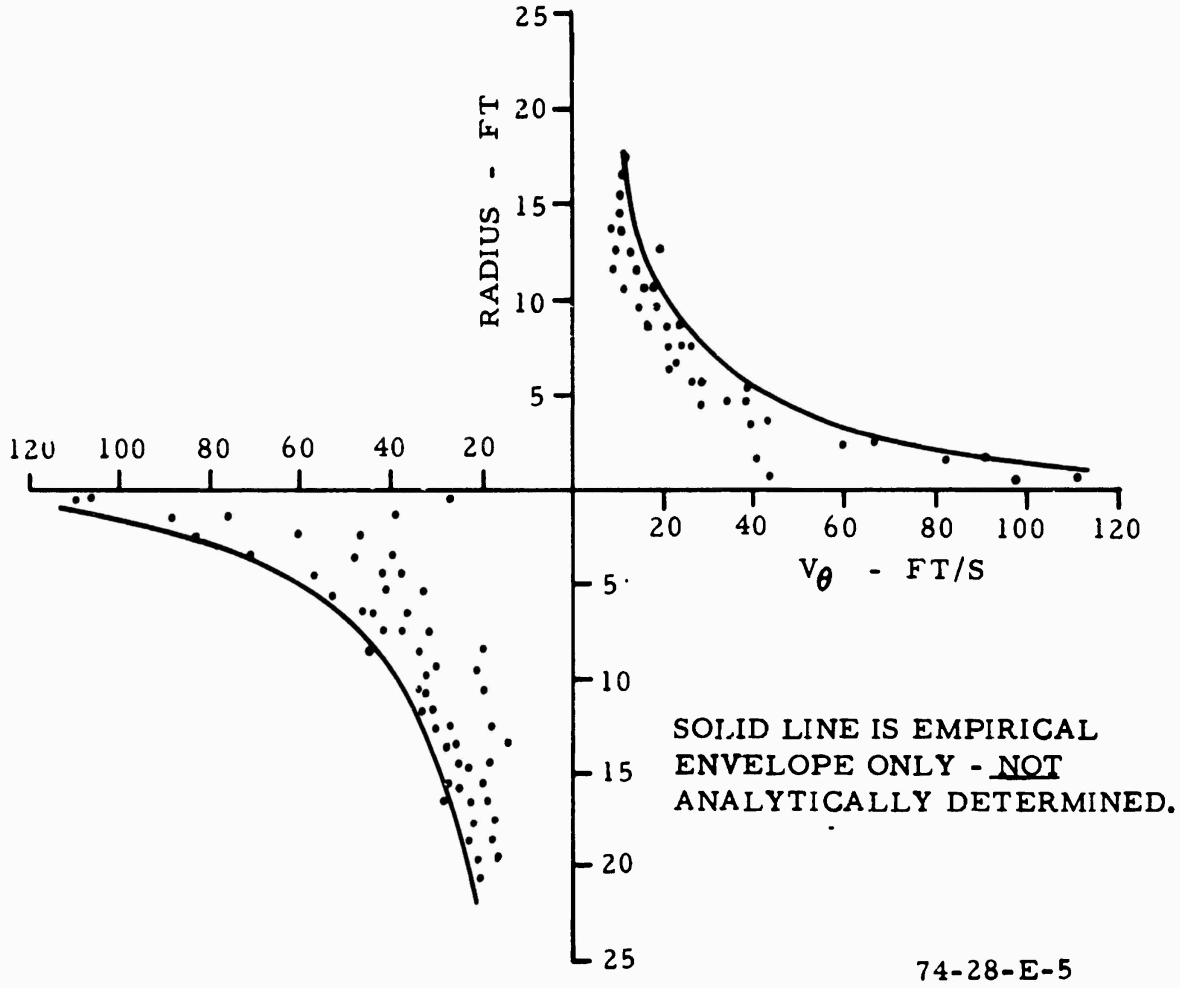

FIGURE E-5. MCDONNELL-DOUGLAS DC9, SERIES 10, VORTEX TANGENTIAL VELOCITY VS. RADIUS. LANDING CONFIGURATION - COMPOSITE PLOT OF DOWNWIND VORTICES. RUN NOS. 25, 27, AND 28. AGE 23 - 27.2 SECONDS

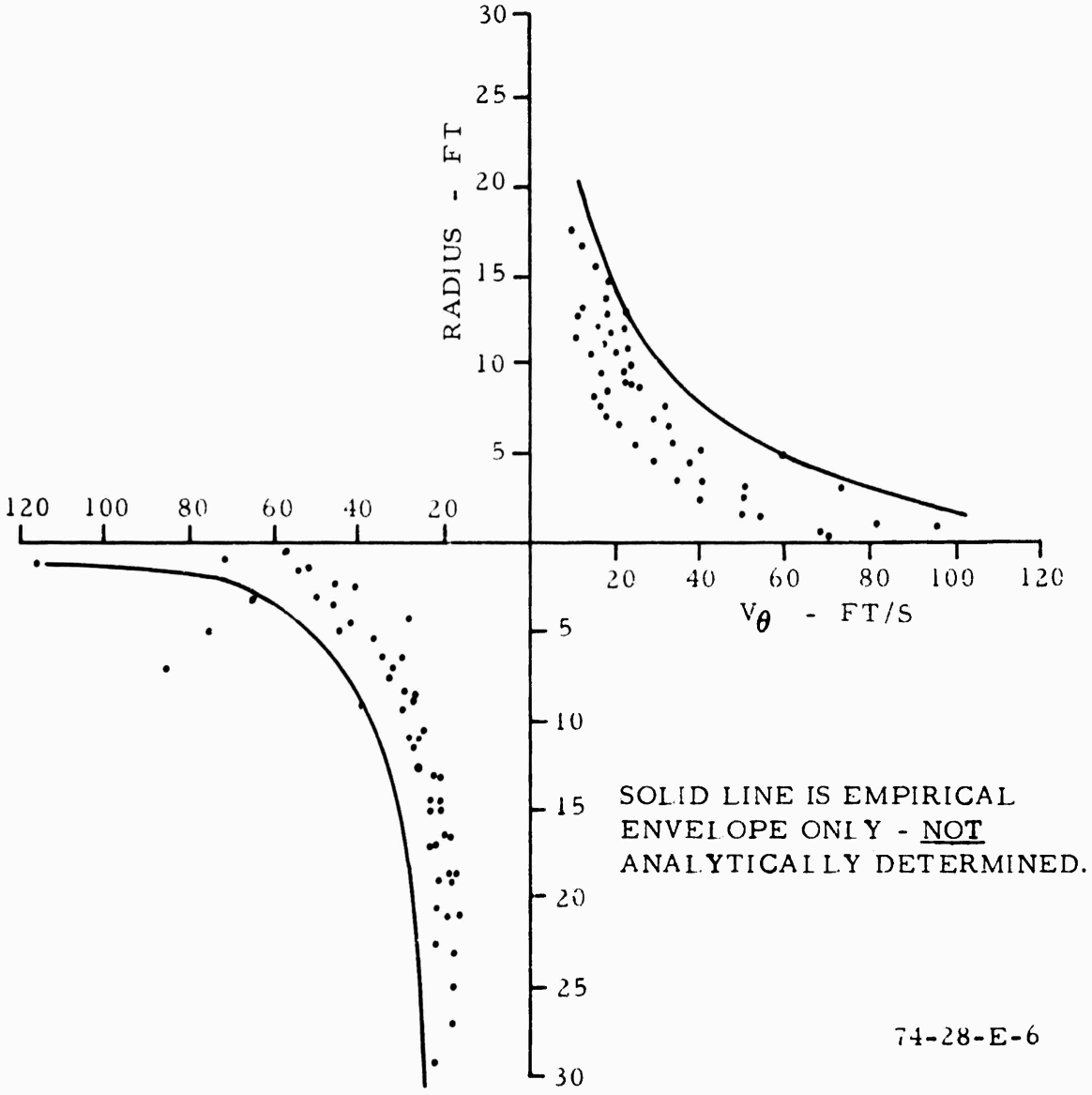

FIGURE E-6. MCDONNELL-DOUGLAS DC9, SERIES 10, VORTEX TANGENTIAL VELOCITY VS. RADIUS. LANDING CONFIGURATION - COMPOSITE PLOT OF DOWNWIND VORTICES. RUN NOS. 15, 42, 44, AND 46. AGE 28.5 - 41 SECONDS

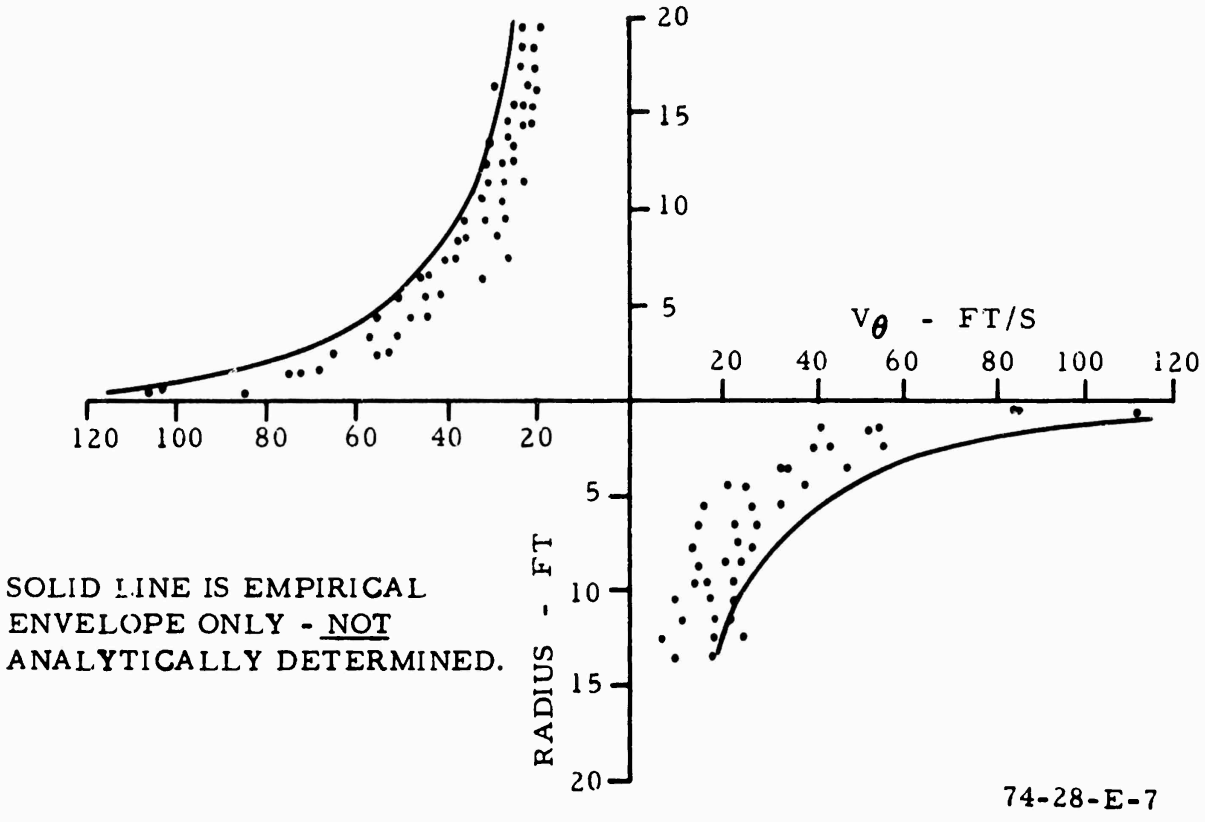

FIGURE E-7. MCDONNELL-DOUGLAS DC9, SERIES 10, VORTEX TANGENTIAL VELOCITY VS. RADIUS. LANDING CONFIGURATION - COMPOSITE PLOT OF UPWIND VORTICES. RUN NOS. 24, 56, AND 57. AGE 14.8 - 18 SECONDS

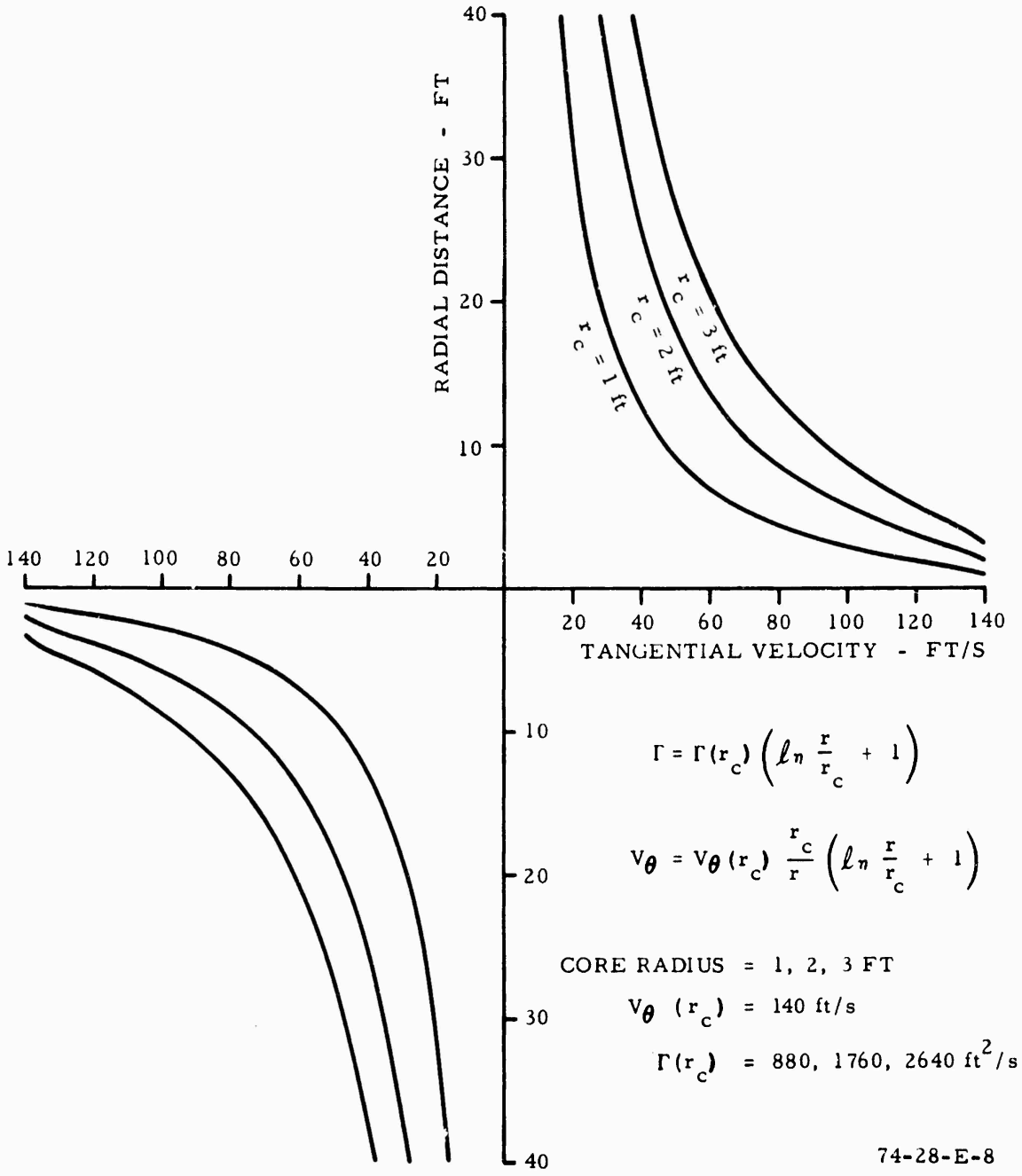

FIGURE E-8. LOGARITHMIC VELOCITY DISTRIBUTION (HOFFMAN-JOUBERT), CORE RADIUS=1, 2, AND 3 FEET

APPENDIX F

WINDSPEED AND DIRECTION AT 140 FEET. AIRPLANE TRACK

DC9 VORTEX FLIGHT TESTS

Run No.	Windspeed at 140 ft - ft/s	Wind Direction at 140 ft - °Mag.	Airplane Track °Mag.	Date	Time
1	12.3	(360)	277	5-11-72	0620
2	13.5	(350)	271	5-11-72	0626
3	13.4	(350)	270	5-11-72	0631
4	11.5	(350)	269	5-11-72	0634
5	11.4	(350)	277	5-11-72	0639
6	13.6	(350)	266	5-11-72	0648
7	14.2	(340)	263	5-11-72	0652
8	(14.7)	(340)	260	5-11-72	0657
9	13.8	(340)	252	5-11-72	0702
10	(14.7)	(350)	257	5-11-72	0707
11	(14.7)	(340)	255	5-11-72	0713
12	13.7	(350)	255	5-11-72	0718
13	13.8	(350)	253	5-11-72	0724
14	(16.2)	341	255	5-11-72	0727
15	11.0	345	249	5-11-72	0823
16	10.7	308	244	5-11-72	0827
17	14.4	288	245	5-11-72	0834
18	11.5	273	244	5-11-72	0840
19	10.1	336	243	5-11-72	0844
20	(13.2)	(350)	244	5-11-72	0848
21	(13.2)	(360)	248	5-11-72	0852
22	(13.2)	349	253	5-11-72	0855
23	16.0	342	249	5-11-72	0858
24	16.1	347	255	5-11-72	0902
25	14.3	335	255	5-11-72	0906
26	14.9	315	(255)	5-11-72	0909
27	13.5	50	311	5-12-72	0547
28	(7.3)	17	310	5-12-72	0551
29	(7.3)	36	312	5-12-72	0554
30	6.2	39	311	5-12-72	0558
31	5.4	27	308	5-12-72	0601
32	6.6	33	312	5-12-72	0605
33	6.0	26	309	5-12-72	0608
34	7.8	24	308	5-12-72	0612
35	(7.3)	(30)	304	5-12-72	0615
36	(5.9)	(30)	308	5-12-72	0618
37	8.3	31	308	5-12-72	0622
38	(7.3)	(30)	(310)	5-12-72	0625
39	5.9	25	311	5-12-72	0629
40	6.2	10	311	5-12-72	0634
41	(5.9)	(20)	310	5-12-72	0638
42	3.2	(20)	306	5-12-72	0642
43	7.5	338	310	5-12-72	0645
44	6.1	338	240	5-12-72	0743
45	6.7	325	232	5-12-72	0747

Run No.	Windspeed at 140 ft - ft/s	Wind Direction at 140 ft - °Mag.	Airplane Track °Mag.	Date	Time
46	7.6	339	235	5-12-72	0751
47	7.6	343	235	5-12-72	0755
48	7.8	311	235	5-12-72	0758
49	(8.8)	(310)	235	5-12-72	0801
50	8.1	325	236	5-12-72	0805
51	8.8	340	238	5-12-72	0808
52	(8.8)	(310)	233	5-12-72	0811
53	7.8	334	235	5-12-72	0815
54	9.8	348	237	5-12-72	0823
55	11.5	326	233	5-12-72	0827
56	10.2	298	236	5-12-72	0830
57	8.7	270	236	5-12-72	0834
58	8.7	311	238	5-12-72	0837
59	13.1	(350)	242	5-12-72	0841
60	14.3	(350)	244	5-12-72	0844
61	14.6	263	238	5-12-72	0847

NOTE: Numbers in parenthesis are spot readings recorded manually, from backup insturmentation at 140-foot level. Readings were taken approximately 5 seconds prior to passage of aircraft past test tower.